

University of Windsor

Scholarship at UWindor

Electronic Theses and Dissertations

Theses, Dissertations, and Major Papers

9-25-2024

Energy Performance and Life-Cycle Cost Optimization of a Controlled Environment Agriculture (CEA) Facility

Gurpreet Khanuja
University of Windsor

Follow this and additional works at: <https://scholar.uwindsor.ca/etd>

Recommended Citation

Khanuja, Gurpreet, "Energy Performance and Life-Cycle Cost Optimization of a Controlled Environment Agriculture (CEA) Facility" (2024). *Electronic Theses and Dissertations*. 9554.
<https://scholar.uwindsor.ca/etd/9554>

This online database contains the full-text of PhD dissertations and Masters' theses of University of Windsor students from 1954 forward. These documents are made available for personal study and research purposes only, in accordance with the Canadian Copyright Act and the Creative Commons license—CC BY-NC-ND (Attribution, Non-Commercial, No Derivative Works). Under this license, works must always be attributed to the copyright holder (original author), cannot be used for any commercial purposes, and may not be altered. Any other use would require the permission of the copyright holder. Students may inquire about withdrawing their dissertation and/or thesis from this database. For additional inquiries, please contact the repository administrator via email (scholarship@uwindsor.ca) or by telephone at 519-253-3000ext. 3208.

**Energy Performance and Life-Cycle Cost Optimization of a Controlled
Environment Agriculture (CEA) Facility**

By

Gurpreet Khanuja

A Thesis

Submitted to the Faculty of Graduate Studies
through the Department of Mechanical, Automotive, and Materials Engineering
in Partial Fulfillment of the Requirements for
the Degree of Master of Applied Science
at the University of Windsor

Windsor, Ontario, Canada

2024

© 2024 Gurpreet Khanuja

**Energy Performance and Life-Cycle Cost Optimization of a Controlled
Environment Agriculture (CEA) Facility**

by

Gurpreet Khanuja

APPROVED BY:

P. Henshaw

Department of Civil and Environmental Engineering

J. Johrendt

Department of Mechanical, Automotive and Materials Engineering

D. S-K. Ting, Co-Advisor

Department of Mechanical, Automotive and Materials Engineering

R. Ruparathna, Co-Advisor

Department of Civil and Environmental Engineering

August 27, 2024

DECLARATION OF CO-AUTHORSHIP / PREVIOUS PUBLICATION

I. Co-Authorship

I hereby declare that this thesis incorporates material that is a result of joint research, as follows:

Chapters 2, 3, and 4 of the thesis present the results of the joint research undertaken in collaboration with Dr. David Ting and Dr. Rajeev Ruparathna. Chapter 4 includes an additional co-author: Paul Bishop. In all cases, the key ideas, primary contributions, data analysis, interpretation, and writing were performed by me, and the contribution of the co-author was primarily through the provision of guidance, discussion, and editing of the manuscript.

I am aware of the University of Windsor Senate Policy on Authorship, and I certify that I have properly acknowledged the contribution of other researchers to my thesis and have obtained written permission from each of the co-author(s) to include the above material(s) in my thesis.

I certify that, with the above qualification, this thesis, and the research to which it refers, is the product of my own work.

II. Previous Publication

This thesis includes three original papers that have been previously published/submitted to journals for publication, as follows:

Thesis Chapter	Publication Title/Full citation	Publication status*
Chapter 2	Khanuja, G., Ruparathna, R., Ting, D. S-K., (2024) "Enhancing solar insolation in agricultural greenhouses by adjusting its orientation and shape," Clean Energy for Low-Income Communities: Technology, Deployment, and Challenges, Chapter 8.	Published

Chapter 3	Khanuja, G., Ruparathna, R., Ting, D. S-K., (2024) “A methodological framework for modeling passive solar greenhouses”	Under Preparation
Chapter 4	Khanuja, G., Bishop, P., Ruparathna, R., Ting, D. S-K., (2024) “Economic and Performance Optimization for Controlled Environment Agriculture: A Regional Vignette for Canada”.	Under Preparation

I certify that I have obtained written permission from the copyright owner(s) to include the above-published material(s) in my thesis. I certify that the above material describes work completed during my registration as a graduate student at the University of Windsor.

III. General

I declare that, to the best of my knowledge, my thesis does not infringe upon anyone’s copyright nor violate any proprietary rights and that any ideas, techniques, quotations, or any other material from the work of other people included in my thesis, published or otherwise, are fully acknowledged in accordance with the standard referencing practices. Furthermore, to the extent that I have included copyrighted material that surpasses the bounds of fair dealing within the meaning of the Canada Copyright Act, I certify that I have obtained written permission from the copyright owner(s) to include such material(s) in my thesis.

I declare that this is a true copy of my thesis, including any final revisions, as approved by my thesis committee and the Graduate Studies office, and that this thesis has not been submitted for a higher degree to any other University or Institution.

ABSTRACT

Conventional greenhouses (CGs) in colder regions consume substantial energy, primarily powered by fossil fuels, leading to detrimental environmental impacts. High energy demand poses a major obstacle to constructing these greenhouses. To enhance their sustainability, this research explores energy-efficient strategies to optimize solar insolation availability by modifying the greenhouse orientation, design, and roof inclination. Additionally, a methodology for greenhouse energy modeling (GEM) was proposed due to the unavailability of standardized guidelines or works of literature. GEM allows for predicting energy requirements and assessing the economic viability of greenhouses in advance. This methodological framework was tested using an experimental Chinese solar greenhouse (CSG) in Elie, Manitoba, revealing that GEM could accurately predict hourly internal air temperatures with an average prediction error of about 1.6%.

The proposed framework was applied to simulate the heating and cooling demand of an Advanced Growing Building (AGB), indicating that it consumes 88% less heating and cooling energy than a CG producing the same crop output. AGB was simulated for different Canadian locations such as Toronto, Vancouver, Edmonton, and Winnipeg along with crops such as lettuce, tomato, and strawberry. The study shows that Vancouver is the most preferred location for growing all three crops, followed by Toronto, Winnipeg, and Edmonton. An optimization study was conducted using the design of experiments (DOE) and modified binary optimization approach, varying parameters individually that influence either heating, cooling demand, or the life-cycle cost (LCC). The results illustrated that cases 6D3A-1, 6K3A-1, and 6L3A-1 are optimal designs that can grow lettuce crops with a heating and cooling demand of 1.6 kW/kg and LCC of 61 cents/kg, which was 27% and 37% less, respectively, than the AGB base case. This research provides valuable insights for researchers and growers to analyze the energy-efficient parameters that significantly impact energy performance, as well as the effects of location and crop type within the greenhouse.

DEDICATION

This dedication is bestowed upon my dear parents.

With heartfelt gratitude for your unwavering support and guidance.

ACKNOWLEDGEMENTS

I wish to express my deepest commendations to my academic supervisor Dr. David S-K. Ting and Dr. Rajeev Ruparathna for accepting me in their research group and for their invaluable guidance and constant assistance during my research journey. They strongly believed in my abilities and always encouraged me to go beyond my boundaries, fostering both my academic and personal growth.

I would like to extend my sincere gratitude to my committee members Dr. Paul Henshaw, and Dr. Jennifer Johrendt for providing their time and valuable knowledge into my research work. A heartfelt thanks to my industrial partner, Paul Bishop for consistently encouraging me to gain in-depth knowledge and challenging me to overcome the complexities of this project.

I would also like to acknowledge the support of all my research group members, especially Seyed Ehsaan Miri, Anup Jwala Poudel, and King Lucas Darko for encouraging me during difficult times.

I am deeply grateful for the guidance of my friend Abhinav Thakurta, who consistently believed in me and stood by me through my struggles. I also want to thank my roommate Bhumi Rami for being there and listening to all my disappointments throughout this journey.

I extend my special thanks to my parents, Harbhajan Singh Khanuja and Reshamjeet Kaur Khanuja, and my brother Karan Singh Khanuja for continuously being my pillars of strength and inspiring me to pursue my master's degree. Your sacrifices, love, and unwavering support have been significant in demonstrating my capabilities and chasing my aspirations.

TABLE OF CONTENTS

DECLARATION OF CO-AUTHORSHIP / PREVIOUS PUBLICATION	iii
ABSTRACT.....	v
DEDICATION.....	vi
ACKNOWLEDGEMENTS.....	vii
LIST OF TABLES.....	xii
LIST OF FIGURES.....	xiv
LIST OF APPENDICES.....	xviii
NOMENCLATURE.....	xix
CHAPTER 1 INTRODUCTION.....	1
1.1 Background.....	1
1.2 Problem Statement.....	3
1.3 Knowledge Gaps.....	4
1.4 Motivation and Scope.....	5
1.5 Objectives.....	5
1.6 Thesis Organization.....	6
1.7 References.....	8
CHAPTER 2 ENHANCING SOLAR INSOLATION IN AGRICULTURAL GREENHOUSES BY ADJUSTING ITS ORIENTATION AND SHAPE.....	11
2.1 Introduction.....	11
2.2 Literature Review.....	14
2.3 Methodology.....	16
2.3.1 Model Development.....	17
2.3.1.1 Greenhouse Orientations.....	17
2.3.1.2 Roof Inclinations.....	18
2.3.1.3 Greenhouse Shapes.....	19

2.3.2 The TRNSYS-18 Model	21
2.4 Results.....	23
2.4.1 Impact of greenhouse orientations on solar radiation availability	23
2.4.2 Impact of roof inclinations on solar radiation availability	25
2.4.3 Impact of greenhouse shapes on solar radiation availability.....	26
2.5 Conclusions.....	27
2.6 References.....	29

CHAPTER 3 A METHODOLOGICAL FRAMEWORK FOR MODELING PASSIVE SOLAR GREENHOUSES

3.1 Introduction.....	32
3.2 Literature Review.....	34
3.3 Guidelines for Simulating a Passive Solar Greenhouse	36
3.3.1 Greenhouse Model	38
3.3.2 Weather and initial data for simulation.....	39
3.3.3 Greenhouse Construction Material	39
3.3.4 Solar radiation distribution and interactions within the greenhouse	40
3.3.5 Evapotranspiration	42
3.3.6 Infiltration	45
3.3.7 Energy-efficiency features	45
3.3.7.1 Thermal and Shade Curtains	46
3.3.7.2 Supplemental Heating and Cooling	46
3.3.7.3 Thermal Storage.....	46
3.3.7.4 Ventilation.....	47
3.4 A Case Study on Chinese Solar Greenhouse (CSG).....	48
3.4.1 Dimensions of CSG	49
3.4.2 Construction material for CSG	50
3.4.3 Energy-efficiency features for CSG.....	50
3.4.4 Monitored parameters inside the CSG	51
3.5 Demonstration of the Framework	51
3.5.1 Greenhouse Model Development.....	52
3.5.2 Weather and initial data for simulation.....	53
3.5.3 Greenhouse Construction Material	55

3.5.4 Solar Radiation Distribution	56
3.5.5 Evapotranspiration	58
3.5.6 Energy-efficiency features	58
3.5.6.1 Thermal Curtain	58
3.5.6.2 Supplemental Heat	59
3.5.6.3 Thermal Storage Wall	59
3.5.6.4 Natural Ventilation.....	59
3.6 Results and Discussion	60
3.7 Conclusion	67
3.8 References.....	69
CHAPTER 4 ECONOMIC AND ENERGY PERFORMANCE OPTIMIZATION FOR CONTROLLED ENVIRONMENT AGRICULTURE: A REGIONAL VIGNETTE FOR CANADA	75
4.1 Introduction.....	75
4.2 Literature Review.....	78
4.3 Methodology	81
4.3.1 Assessment of Base Case Models.....	81
4.3.1.1 Energy Simulation for AGB and CG	84
4.3.1.2 Life-cycle cost analysis (LCCA).....	88
4.3.2 Optimization Methodology	89
4.3.3 Regional Assessment of AGB.....	93
4.4 Results and Discussion	95
4.4.1 Performance Assessment for AGB	96
4.4.2 Performance Assessment for CG	97
4.4.3 Comparison of performance and LCC for AGB and CG.....	98
4.4.4 Comparison of performance and LCC of individual possible scenarios.....	99
4.4.5 Optimal cases from the Optimization	102
4.4.6 Performance of AGB with variation in locations.....	103
4.5 Conclusion	104
4.6 References.....	105
CHAPTER 5 CONCLUSIONS, RECOMMENDATIONS, AND FUTURE WORKS	112

5.1 Contributions	114
5.2 Limitations and Future-works.....	114
APPENDICES	116
Appendix A.....	116
A.1 Details of AGB and CG	116
A.2 Modeling of evapotranspiration	116
A.3 Operational schedule for thermal curtain and shade curtain	118
A.4 Unit cost estimation for materials used in AGB and CG	120
A.5 Envelope geometry considered under optimization	120
A.6 References	121
Appendix B	123
B.1 Study of crops under consideration	123
B.2 Results	124
B.2.1 Performance of AGB with variation in crops.....	124
B.3 Reference.....	126
VITA AUCTORIS	128

LIST OF TABLES

Table 2-1 Summary of published literature.....	15
Table 2-2 Indicates this study's three main energy-efficient parameters with different cases under each parameter.....	16
Table 2-3 Represents different greenhouse shapes and model descriptions including length (L), breadth (B), maximum height, and roof and wall inclination considered for parameter 3.....	20
Table 3-1 Summary of published literature to simulate greenhouses with different approaches.....	35
Table 3-2 List of parameters, symbols, and formulas used for determining ETo using the Stanghellini model.....	43
Table 3-3 Dimensions of CSG in Elie, Manitoba.	49
Table 3-4 Material of construction for CSG in Elie, Manitoba.	50
Table 3-5 Energy-efficiency features considered for CSG in Elie, Manitoba.	50
Table 3-6 Sensor location for measuring monitored parameters inside the CSG in Elie, Manitoba.....	51
Table 3-7 Comparison of mean, total, and RMSE values for different CWEC weather parameters	55
Table 3-8 Thermal properties of different walls, ground, and windows used in TRNSYS software simulations.	56
Table 4-1 Summary of EEMs employed in different studies.....	79
Table 4-2 Summary of optimization study conducted in this field	80
Table 4-3 U-value of the construction material used in AGB and CG.	85

Table 4-4 Important parameters considered during the modeling of AGB and CG.	86
Table 4-5 Variables affecting either the heating and cooling demand or the LCC.	90
Table 4-6 Possible scenarios considered under each variable.....	90
Table 4-7 Unit cost of natural gas and electricity for different locations	95
Table 4-8 Comparison of performance and LCC for possible scenarios relative to AGB	99
Table A-1 Represents the physical details of the AGB and CG	116
Table A-2 List of parameters, symbols, and formulas used for determining ETo using the Stanghellini model.....	117
Table A-3 Schedules 1 and 2 for thermal curtains and shade curtains.	118
Table A-4 Unit cost for different materials for vendor's website.....	120
Table B-1 Crop parameters for different crops	123

LIST OF FIGURES

Figure 1-1 Thesis Organization..... 7

Figure 2-1 An east-west oriented greenhouse model developed in SketchUp software..... 17

Figure 2-2 Different greenhouse orientations considered in this research..... 18

Figure 2-3 Different roof inclinations considered for this study. 19

Figure 2-4 Greenhouse shapes are considered for this study..... 20

Figure 2-5 A complete TRNSYS model developed in TRNSYS-18 software indicates the input-outputs of each component..... 22

Figure 2-6 Graph for comparison of solar radiation availability (in MWh) on different orientations of the greenhouse. 23

Figure 2-7 Comparison of solar radiation availability in W/m^2 on different roofs of a greenhouse where SR = South roof, NR = North roof, WR = West roof, ER = East Roof..... 24

Figure 2-8 Comparison of solar radiation availability in W/m^2 on different walls of a greenhouse where SW = South Wall, WW = West Wall, NW = North Wall and EW = East Wall..... 24

Figure 2-9 Graph for comparison of solar radiation availability for different roof inclinations of the south roof. 25

Figure 2-10 Graph for comparison of solar radiation availability for different roof inclinations of the north roof..... 26

Figure 2-11 Graph for comparison of total solar radiation availability (in MWh) on different shapes of a greenhouse..... 27

Figure 3-1 Heat interactions between greenhouse air and its surroundings. 37

Figure 3-2 Flow chart explaining the main processes involved in greenhouse energy modeling.....	38
Figure 3-3 Experimental mono-slope Chinese solar greenhouse in Elie, Manitoba.	49
Figure 3-4 Experimental Chinese solar greenhouse model designed using SketchUp software	52
Figure 3-5 Schematic layout of simulation studio representing inputs and outputs connection for each component.	53
Figure 3-6 Comparison of the measured weather parameters with the CWEC dataset weather parameters from 28 th March 2017 to 30 th March 2017. (a) Measured ambient temperature versus CWEC ambient temperature; (b) Measured relative humidity versus CWEC relative humidity; (c) Measured wind speed versus CWEC wind speed; (d) Measured solar irradiance versus CWEC solar irradiance.....	54
Figure 3-7 Comparison of measured internal air temperature with the simulated internal air temperature profiles for different values of solar-to-air factor (f_{solair}). Note: The temperature profile for $f_{solair} = 0.6$ and $f_{solair} = 0.8$ was also studied and lies between the temperature profile $f_{solair} = 0.4$ and $f_{solair} = 1$, however, it was not included to maintain clarity in the figure.	62
Figure 3-8 Comparison of measured internal air temperature with the simulated internal air temperature from 28 th Mar 2017 to 30 th Mar 2017.....	63
Figure 3-9 Comparison of measured supplemental heat with the simulated supplemental heat from 28 th Mar 2017 to 30 th Mar 2017.	65
Figure 3-10 Comparison of measured ground temperature with the simulated ground temperature from 28 th Mar 2017 to 30 th Mar 2017.....	66
Figure 3-11 Comparison of measured north wall temperature with the simulated north wall temperature from 28 th Mar 2017 to 30 th Mar 2017.....	67
Figure 4-1 Represents the phases required to execute the research	81

Figure 4-2 AGB model developed using the SketchUp software. (a) Trnsys3d zone -1 consisting of GS with a volume of 11336 m ³ (b) Trnsys3d zone-2 consisting of outer space (OS) with a volume of 9127 m ³	83
Figure 4-3 CG model developed using the SketchUp software with a volume of 20647 m ³	84
Figure 4-4 Represents the interface of the TRNSYS simulation studio indicating the inputs and outputs connection between individual components	85
Figure 4-5 Airflow network for natural ventilation in AGB.....	87
Figure 4-6 Represents the process of complete optimization methodology	93
Figure 4-7 Variation of weather parameters for different locations under study (a) Average ambient temperature (°C) (b) Average solar radiation on horizontal (kJ/hr/m ²)	94
Figure 4-8 Graphs representing the effects of design parameters, process parameters, and energy-conserving parameters on the heating and cooling demand of AGB. (a) Effects of design, infiltration (inf), and evapotranspiration (evt) (b) Effects of natural ventilation (vent), thermal curtain (TC), shade curtain (SC), and combined parameters (TC+SC)	97
Figure 4-9 Graphs representing the effects of design parameters, process parameters, and energy-conserving parameters on the heating and cooling demand of CG.....	97
Figure 4-10 Comparison of performance and LCC for AGB and CG (a) Heating and cooling demand in kWh/kg (b) Life-cycle costs in Cents/kg.....	98
Figure 4-11 Comparison of performance and LCC for different possible scenarios (a) Heating and cooling demand per kilogram w.r.t the base case (b) Life-cycle costs per kilogram w.r.t the base case	101
Figure 4-12 Distribution of all cases considered under optimization study	102

Figure 4-13 Variation in performance and operating costs for AGB in different locations. (a) Heating and cooling demand in MWh (b) Operating cost for 10 years in Canadian Dollars..... 104

Figure A-1 Represents the cross-sectional details for different profiles of AGB 121

Figure B-1 Represents methods to grow different crops under study (a) Lettuce crops grown in beds (Greener Solutions, 2020) (b) Tomato plants with vines grown in trellises (Essential Home and Garden, 2024) (c) Strawberry crops with runners (Asia Farming, 2024) 123

Figure B-2 Variation of performance and operating cost for different crops. Heating and cooling demand in MWh (b) Operating cost for 10 years in Canadian Dollars..... 125

LIST OF APPENDICES

APPENDIX A Comprehensive information to model Advanced Growing Building.....	114
APPENDIX B Performance of AGB for various crops.....	121

NOMENCLATURE

ACH	Air Changes per Hour
AGB	Advanced Growing Building
ASHRAE	American Society of Heating, Refrigerating and Air-Conditioning Engineers
BPS	Building Performance Simulations
CA	Canopy Area
CEA	Controlled Environment Agriculture
CFD	Computational Fluid Dynamics
CG	Conventional Greenhouse
CSGG	Corrugated Galvanized Steel Sheet
COMIS	Conjunction of Multizone Infiltration Specialists
CSG	Chinese Solar Greenhouse
CWEC	Canadian Weather for Energy Calculations
DOE	Design Of Experiment
EEM	Energy-Efficient Measure
EPW	EnergyPlus format
EVT	Evapotranspiration
FAO	Food and Agriculture Organization
FBG	Fiberglass insulation
GEM	Greenhouse Energy Modeling
GHG	Greenhouse Gas Emission
GLSR	Ground Level Solar Radiation
GS	Growing Space
GSS	Galvanized Steel Sheet
HG	Horticultural Glass
HVAC	Heating, Ventilation and Air-Conditioning
IMP	Insulated Metal Panel
IWEC	International Weather for Energy Calculations
LAI	Leaf Area Index
LCC	Life-Cycle Cost
LCCA	Life-Cycle Cost Analysis
LSSVM	Least square support vector machine
MAE	Mean Absolute Error
OECD	Economic Co-operation and Development
OS	Outer Space
PSG	Passive Solar Greenhouse
PC	Polycarbonate
PE	Polyethylene
PV	Photovoltaic
PVC	Polyvinyl Chloride
SC	Shade Curtain
TC	Thermal Curtain

RH	Relative Humidity
RMSE	Root Mean Square Error
rRMSE	Relative Root Mean Square Error
TMY	Typical Meteorological Year
TMY2	Typical Meteorological Year Version 2
TMY3	Typical Meteorological Year Version 3
TRNSYS	TRaNsient SYStem Simulation program
UN	United Nations
VB	Visual Basics
VPD	Vapor Pressure Deficit

CHAPTER 1

INTRODUCTION

Controlled Environment Agriculture (CEA) is defined as a method of growing crops within a carefully regulated environment, enabling precise control over variables such as temperature, humidity, carbon dioxide levels, and supplemental lighting. These factors are crucial for maximizing optimal plant growth (Engler and Krarti, 2021). CEA offers an advanced alternative to conventional greenhouses (CGs), increasing plant growth efficiency and providing clean, green crops year-round. It also ensures biosecurity, disease and pest-free crops, reducing transportation and fossil fuel use (Benke and Tomkins, 2017). Additionally, CEA minimizes input requirements such as water, soil, and space.

1.1 Background

Agriculture is the process of growing crops mainly for food. However, it is the backbone of many developing countries, supporting livelihoods by providing raw materials for food and raising incomes. United Nations (UN) projected that the human population would expand from roughly 8 billion today to 9.7 billion in 2050 and 10.4 billion by 2100 (United Nations DoEaSA, 2013). This suggests the need for more food to cater to the increasing population. To ensure food security in 2050, food production should be increased by 35% (FAO, 2009). Meanwhile, this increasing demand for food tends to create a harmful impact on the arable land as the quality of arable land degrades due to frequent use. Additionally, urbanization driven by population growth also reduces the arable land available for agriculture. The United Nations Food and Agriculture Organization (UN-FAO) revealed that by 2050, arable land per person is projected to decrease to one-third of the amount available in 1970 (UN-FAO, 2016). UN has projected that more than 600 million people worldwide will be facing hunger in 2030 with high food prices continuing to plague many nations (Sustainable Development Goals, 2022). This indicates that conventional agriculture is not sufficient to support the current population demand.

Agriculture is highly sensitive to climate change and extreme weather conditions (Benke and Tomkins, 2017). Both developed and under-developed nations face challenges with conventional agriculture due to adverse weather conditions stemming from their topographical constraints. Excessive heat, cold, or rainfall can severely impact crop

growth, posing significant threats to agricultural yields. Hu *et. al.*, (2024) estimated climate change varies the crop yield by 37%. Simultaneously, agricultural activities produce greenhouse gas (GHG) emissions that contribute to climate change (Hein, 2024). Agriculture is the fifth-largest contributor to GHG emissions, accounting for 10% of Canadian emissions. From 1990 to 2021, these emissions have witnessed an increase from 49 megatons to 69 megatons of CO₂ equivalent (Government of Canada, 2023). Conventional agriculture encounters many drawbacks, requiring a transition to increase sustainability in agriculture, focusing on growing crops while conserving the planet's ability to sustain future generations.

The agricultural industry is embracing scientific advancements to support the production of fresh crops near urban areas, which promotes the health and well-being of individuals (Brown and Jameton, 2000). Sustainable agriculture, particularly in the form of urban agriculture, is gaining popularity. A key component of urban agriculture is CEA, a method of indoor farming that provides a conditioned growing environment inside an energy-efficient greenhouse. CEA provides precise control over environmental parameters such as inside air temperature, relative humidity, CO₂ concentrations, supplemental lighting, and inside air velocity (Engler and Krarti, 2021). CEA has the advantage of providing crops throughout the year at a reasonable cost, quality, and freshness. Additionally, CEA addresses food security for the growing urban population (Despommier, 2011), environmental sustainability, a lower carbon footprint of food production (Coelho *et. al.*, 2018), and chemical-free food with no risks of pests and diseases (Sullivan *et. al.*, 2019). By mitigating issues associated with traditional farming, such as the need for heavy machinery, pesticides, herbicides, and fertilizers, and by requiring significantly less water (Benke and Tomkins, 2017), CEA presents a viable solution for long-term cost savings and reduced environmental impact.

CEA proves to be an emerging agricultural method for crop cultivation, but it also encounters certain limitations. One of the primary challenges is the significant energy requirement needed to maintain optimal conditions for plant growth. This energy is typically provided by electricity or fossil fuels to power heating, cooling, ventilation, and artificial lighting systems within the growing space. This massive energy demand not only

poses environmental concerns but also drives up operating costs for growers, making CEA less cost-effective. Additionally, CEA involves the use of advanced construction materials and sophisticated heating, cooling, ventilation systems, and artificial lighting, which further escalates installation costs.

To address these challenges, researchers have explored energy-efficient methods (EEMs) to reduce CEA's energy consumption and lower GHG emissions. One approach to minimizing heating energy usage is the utilization of solar energy. Studies have shown that solar radiation availability on greenhouse surfaces can be optimized by adjusting the orientation, roof angles, and overall design of the greenhouse (Mobtaker et al., 2016; Sethi, 2009). Research has also shifted to modern solar greenhouses, which are categorized as passive and active solar greenhouses. These greenhouses have the potential to reduce energy demand and GHG emissions. Active solar greenhouses are integrated with solar energy technologies such as photovoltaic and thermal solar collectors, while passive solar greenhouses (PSGs) are designed to maximize solar energy capture (Gorjian *et. al.*, 2021). Further research has been conducted on the Chinese solar greenhouse (CSG), a well-established technology in China that operates without needing supplemental heating. Additionally, studies have investigated the installation of other energy-efficient components such as envelope materials (Gupta and Chandra, 2001; Tong *et. al.*, 2013; Choab *et. al.*, 2021), curtains (Gupta and Chandra, 2001; Rasheed *et. al.*, 2019), and ventilation systems (Tantau *et. al.*, 2011; Vadiie and Martin, 2013; Beaulac *et. al.*, 2024) to reduce the heating and cooling demand. These efforts indicate ongoing research to develop a more energy-efficient and sustainable CEA design that minimizes energy demand, reduces manufacturing costs and decreases GHG emissions.

1.2 Problem Statement

CEA provides an optimal environment for plant growth by carefully controlling variables such as temperature, relative humidity, and air velocity. However, this regulated environment requires energy, typically sourced from electricity or fossil fuels, contributing to about 33% of GHG emissions associated with CEA (Engler and Krarti, 2021). Furthermore, CEA is an energy-intensive technology, with energy costs being the largest or second-largest operating expense, accounting for roughly 15-60% of total costs

(Melancon, 2018). In northern latitudes, the heating expense can account for 70% to 85% of total greenhouse operating costs (Rorabaugh *et. al.*, 2002). A study by Eaves and Eaves (2018) on a greenhouse in Quebec found that installation costs range from approximately \$ 450,000 to \$ 500,000 depending on size and technological advancements while operating costs vary from \$ 200,000 to \$ 250,000. This highlights the substantial capital investment required for CEA due to the advanced infrastructure. Therefore, the success of CEA facilities hinges on reducing both operating and capital costs while also minimizing GHG emissions.

1.3 Knowledge Gaps

The need for this research stems from the following knowledge gaps identified:

- 1) The efficiency of CEA can be enhanced by employing energy-efficient methods, such as adjusting greenhouse orientation, shape, and roof inclination to capture more solar radiation for heating. Solar insolation availability varies from location to location, as well as time of the year, understanding the solar insolation patterns for greenhouses in northern latitudes was crucial as the need for heating is maximum. The available literature on greenhouse orientation and shape was specific to the greenhouse locations near the equator, especially in Asia and Europe (Mobtaker *et. al.*, 2016; Sethi, 2009) where solar distribution patterns differ.

- 2) To estimate the energy requirements and life cycle cost of a greenhouse in advance, greenhouse energy modeling (GEM) can be used. However, a significant challenge in performing GEM was the absence of relevant standards, guidelines, or literature. Existing standards, such as the International Building Code and National Building Code of Canada, do not encompass these facilities. Previous research focused on the methods to model greenhouses with different simulation tools to estimate the heating and cooling requirements or thermal performance of a greenhouse. The modeling strategies provided in the above studies remained specific to the software used, however, they lack a detailed, unified framework for the modeling process.

- 3) Many studies overlook the inclusion of plants inside the greenhouse or assume a constant evapotranspiration rate due to the complexity of modeling the dynamic nature of plants, leading to huge inaccuracies in predicting the energy requirements (Vadiee & Martin, 2013; Semple *et al.*, 2017; Ahamed *et al.*, 2019).
- 4) Some of the existing literature only provides reviews on EEMs (Tong *et al.*, 2013; Ahamed *et al.*, 2018), while others largely focus on implementing single or paired EEMs rather than integrating multiple measures to enhance greenhouse efficiency (Tantau *et al.*, 2011; Rasheed *et al.*, 2019; Beaulac *et al.*, 2024). While these individual EEMs can reduce energy demand, their overall impact is often insufficient to significantly lower total energy consumption. Additionally, many studies have overlooked improvements in greenhouse design, which are crucial for reducing energy demand.

1.4 Motivation and Scope

Analyzing the problems and knowledge gaps associated with CEA reveals that a greenhouse facility should be designed to minimize total energy demand and LCC. Consequently, this research is motivated by the goal of designing and verifying a near-net-zero energy facility for CEA. The scope of this research includes developing a modular, scalable facility for various commercial food crops that can be grown optimally within an energy-efficient environment for different locations in Canada. The scope of this study will be a step toward the United Nations Sustainable Development Goal of “Zero Hunger” by elevating food production at reasonable quality and cost (Sustainable Development Goals, 2022).

1.5 Objectives

The primary objective of this research is to develop a CEA facility design that achieves high energy performance and lower LCC. This is accomplished by meeting the following sub-objectives:-

1. Developing a methodological framework to model a passive solar greenhouse and validating the greenhouse energy model.

2. Designing an Advanced growing building (AGB) by optimizing the energy performance and life-cycle cost (LCC).
3. Evaluating the performance of the AGB model across different locations in Canada (Toronto, Vancouver, Winnipeg, and Edmonton) and for various crops (lettuce, tomato, and strawberries).

1.6 Thesis Organization

This thesis is composed of five primary chapters, as depicted in Figure 1-1. It begins with an introduction and background on CEA, covering the problem statement, knowledge gaps, motivation, scope, and objectives of the study. Chapter 2 presents a preliminary study to analyze the solar insolation patterns in greenhouses with varying designs, orientations, and roof inclinations. Chapter 3 outlines a methodological framework for accurately modeling passive solar greenhouses, which was validated using an experimental greenhouse in Elie, Manitoba. The findings from Chapters 2 and 3 were instrumental in developing the AGB and CG models required for Chapter 4. This chapter focuses on identifying the optimal AGB design with the lowest heating and cooling demands and the lowest LCC per kilogram of crop output. Finally, Chapter 5 discusses the conclusions, limitations, and contributions of this research.

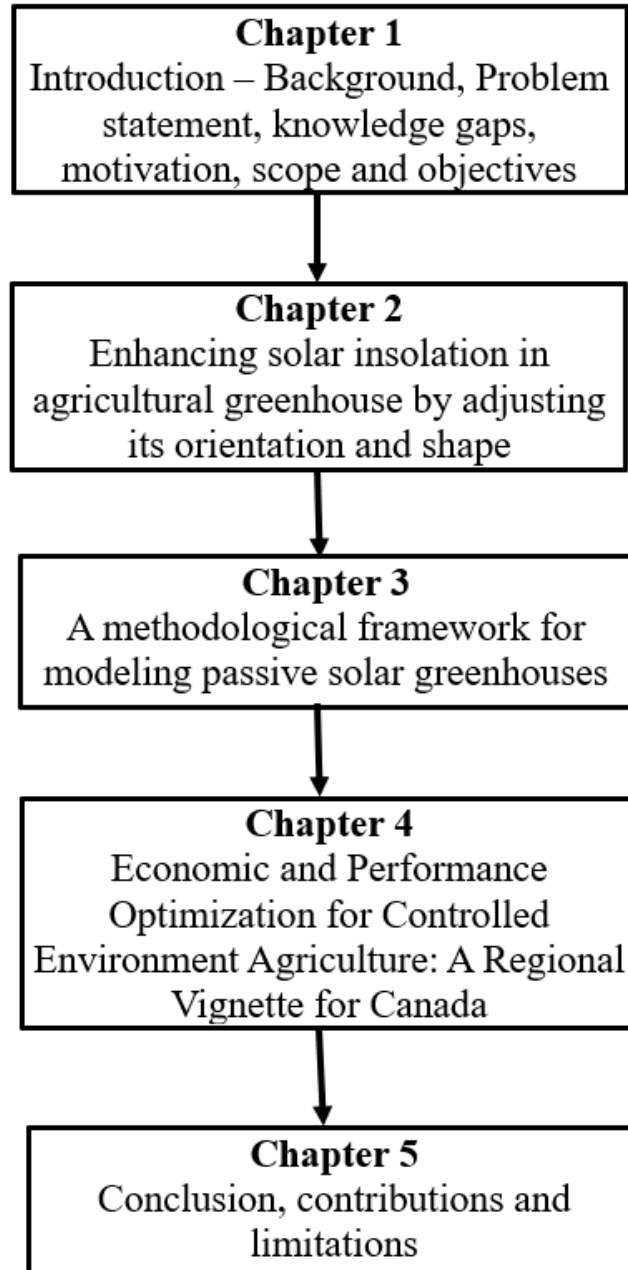


Figure 1-1 Thesis Organization

1.7 References

Ahamed, M. S., Guo, H., Tanino, K., (2018) "Energy saving techniques for reducing the heating cost of conventional greenhouses," *Biosystems Engineering*, Vol 178, pp. 9-33.

Ahamed, M. S., Guo, H., Tanino, K., (2019) "Modeling heating demands in a Chinese-style solar greenhouse using the transient building energy simulation model TRNSYS," *Journal of Building Engineering*, Vol 29, 101114.

Beaulac, A., Lalonde, T., Haillet, D., Monfet, D., (2024) "Energy modeling, calibration, and validation of a small-scale greenhouse using TRNSYS," *Applied Thermal Engineering*, Vol 248 (2024) 123195.

Benke, K., Tomkins, B., (2017) "Future food-production systems: vertical farming and controlled environment agriculture" *Sustainability: Science, Practice, and Policy*, Vol 13:1, pp. 13-26.

Brown, K. H., Jameton, A. L., (2000) "Public health implications of urban agriculture," *Journal of Public Health Policy*, Vol 21 (1), pp. 20–39.

Choab, N., Allouhi, A., Maakoul, A. E., Kousksou, T., Saadeddine, S., Jamil, A., (2021) "Effect of Greenhouse Design Parameters on the Heating and Cooling Requirement of Greenhouses in Moroccan Climatic Conditions," *IEEE Access*, Vol 9, 3047851.

Coelho, F. C., Coelho, E. M., Egerer, M., (2018) "Local food: benefits and failings due to modern agriculture," *Science Agriculture*, Vol 75 (1), pp. 84–94.

Despommier, D., (2011) "The vertical farm: controlled environment agriculture carried out in tall buildings would create greater food safety and security for large urban populations," *Journal of Consumer Protection and Food Safety*, Vol 6 (2), pp. 233–236.

Eaves, J., Eaves, S., (2018) "Comparing the profitability of a greenhouse to a vertical farm in Quebec," *Canadian Journal of Agricultural Economics*, Vol 66, pp. 43-54.

Engler, N., Krarti, M., (2021) "Review of energy efficiency in controlled environment agriculture," *Renewable and Sustainable Energy Reviews*, Vol 141, 110786.

Food and Agriculture Organization, (2009) “How to feed the world in 2050,” UN Food and Agriculture Organization, Rome.

Gorjian, S., Calise, F., Kant, K., Ahamed, M. S., Copertaro, B., Najafi, G., Zhang, X., Aghaei, M., Shamshiri, R., (2021) “A review on opportunities for implementation of solar energy technologies in agricultural greenhouses,” *Journal of Cleaner Production*, Vol. 285, 124807.

Government of Canada, (2023) “Greenhouse gas emissions and agriculture,” (Source: [Greenhouse gas emissions and agriculture - agriculture.canada.ca](https://www.agriculture.canada.ca/greenhouse-gas-emissions-and-agriculture))

Gupta, M. J., Chandra, P., (2001) “Effect of greenhouse design parameters on conservation of energy for greenhouse environmental control,” *Energy*, Vol. 27, pp. 777-794

Hein, T., (2023) “Agriculture in Canada. In *The Canadian Encyclopedia*,” (Retrieved from <https://www.thecanadianencyclopedia.ca/en/article/agriculture-in-canada>)

Hu, T., Zhang, X., Khanal, S., Wilson, R., Leng, G., Toman, E. M., Wang, X., Li, Y., Zhao, K., (2024) “Climate change impacts on crop yields: A review of empirical findings, statistical crop models, and machine learning methods,” *Environmental Modelling and Software*, Vol. 179, 106119.

Melancon, M., (2018) “US (GA): \$5 million to help reduce energy costs of Indoor Farming,” *HortiDaily*, September 11, 2018.

Mobtaker, H. G., Ajabshirchi, Y., Ranjbar, S. F., Matloobi, M., (2016) “Solar energy conservation in a greenhouse: Thermal analysis and experimental validation,” *Renewable Energy*, Vol 96, pp. 509-519.

Rasheed, A., Na, W. H., Lee, J. W., Kim, H. T., Lee, H. W., (2019) “Optimization of greenhouse thermal screens for maximized energy conservation,” *Energies*, Vol. 12, 3592.

Rorabaugh, P. A., Jensen, M. H., Giacomelli, G., (2002) “Introduction to controlled environment agriculture and hydroponics,” *Controlled Environment Agriculture Center, Campus Agriculture Center, University of Arizona*.

Semple, L., Carriveau, R., Ting, D. S-K., (2017) “Assessing heating and cooling demands of closed greenhouse systems in a cold climate,” *International Journal of Energy Research*, Vol 41, Issue 13, pp. 1903-1913.

Sethi, V. P., (2009) “On the selection of shape and orientation of a greenhouse: Thermal modeling and experimental validation,” *Solar Energy*, Vol 83, pp. 21-38.

Sullivan, C. A., Bonnett, G. D., McIntyre, C. L., Hochman, Z., Wasson, A. P., (2019) “Strategies to improve the productivity, product diversity, and profitability of urban agriculture,” *Agricultural Systems*, Vol. 174, pp. 133-144.

Sustainable Development Goals, (2022) “The Sustainable Development Goals Report 2022,” United Nations (Source: [— SDG Indicators \(un.org\)](#))

Tantau, H. J., Meyer, J., Schmidt, U., Bessler, B., (2011) “Low energy greenhouse – A system approach,” *International Symposium on High Technology for Greenhouse Systems: GreenSys2009, Acta Horticulturae*, 893, pp. 75-84.

Tong, G., Christopher, D. M., Li, T., Wang, T., (2013) “Passive solar energy utilization: A review of cross-section building parameter selection for Chinese solar greenhouses,” *Renewable and Sustainable Energy Reviews* 26 (2013), pp. 540-548.

United Nations DoEaSA, (2013) "World population prospects: the 2012 revision. United Nations Food and Agriculture Organization - Population Division" Report No.: 0470670592. (Source: [Home Page | Data Portal \(un.org\)](#))

United Nations Food and Agriculture Organization (FAO), (2016) “Database on Arable Land,” 13 September 2016 (Source: [Vadiee, A., Martin, V., \(2013\) “Energy Analysis and thermo-economic assessment of the closed greenhouse – The largest commercial solar building,” *Applied Energy*, Vol 102 \(2013\), pp. 1256-1266.](http://data.worldbank.org/indicator/AG.LND.ARB.L.HA.PC?end%20&hx003D;2013&hx0026;start%20&hx003D;1961&hx0026;view&hx003D; chart.))</p></div><div data-bbox=)

CHAPTER 2

ENHANCING SOLAR INSOLATION IN AGRICULTURAL GREENHOUSES BY ADJUSTING ITS ORIENTATION AND SHAPE

2.1 Introduction

Agriculture is a primary industry in many countries. It is an essential part of the food supply. The United Nations (UN) recently projected that the human population would expand from roughly 8 billion today to 9.7 billion in 2050 and 10.4 billion by 2100 (United Nations DoEaSA, 2013). As the human population continues to grow rapidly, there is a need to increase the food supply to cater to the increasing demand for food. The Food and Agriculture Organization (FAO) has estimated that to ensure food security in 2050, food production should be increased by 35% (FAO, 2009). This need for rapid expansion of agriculture can have a harmful impact on arable land since the quality of land will degrade due to frequent use. The United Nations Food and Agriculture Organization (UN-FAO) revealed that by 2050, arable land per person is projected to decrease to one-third of the amount available in 1970 (UN-FAO, 2016). Therefore, conventional farming will not be sufficient to support global food demand. Agriculture is ranked as the fifth-largest contributor of greenhouse gas (GHG) emissions. It accounts for 10% of the total Canadian national emissions, with an estimated 69 megatons of CO₂ equivalent being emitted. From 1990 to 2021, these emissions have witnessed an increase from 49 megatons to 69 megatons of CO₂ equivalent (Government of Canada, 2023). Conventional agriculture is also sensitive to climate change (Benke and Tomkins, 2017; Sullivan *et. al.*, 2019). It is estimated that for every 1°C increase in atmospheric temperature, 10% of the arable land where we now grow food crops will be lost (Despommier, 2011).

Numerous developed and underdeveloped nations are struggling with conventional agriculture due to unfavorable weather conditions stemming from their topographical limitations. Thus, the agricultural industry is actively pursuing scientific advancements to facilitate the production of fresh crops close to urban areas which not only promotes the health and well-being of individuals but also supports the cultivation of local foods (Brown and Jameton, 2000; Dixon *et. al.*, 2007). Recently, there has been a resurgence

of interest in urban agriculture in many Organizations for Economic Co-operation and Development (OECD) countries where new advancements, agro-architecture, environmental controls, phenomics, and automation have been employed to grow food in urban areas commercially (Sullivan *et. al.*, 2019). Urban Agriculture has multiple advantages such as providing crops throughout the year at a reasonable cost, quality, and freshness. It also aims to provide food security for the growing urban population (Despommier, 2011), environmental sustainability, and to lower the carbon footprint of food production (Coelho *et. al.*, 2018) and provide chemical-free food with no risks of pests and diseases (Sullivan *et. al.*, 2019). Urban Agriculture has been defined as an “industry that produces, processes and markets food, on land and water dispersed throughout urban and peri-urban areas” (Smit *et. al.*, 2001). Urban agriculture includes both conditioned agriculture as well as unconditioned agriculture in urban areas. One of the major subsets of urban agriculture is controlled environment agriculture (Engler and Krarti, 2021). Controlled Environmental Agriculture (CEA) is a form of indoor farming that provides a regulated environment inside an energy-efficient greenhouse for growing crops. CEA provides conditioned growing spaces that provide control over environmental parameters such as inside air temperature, relative humidity, CO₂ concentrations, supplemental lighting, and inside air velocity (Engler and Krarti, 2021).

A controlled environment greenhouse requires heating during the night and winter months and cooling during the daytime and summer months. This is because the internal temperature of the greenhouse is not favorable for crop cultivation. Moreover, plants require supplemental lighting when natural sunlight is not available. Consequently, maintaining a controlled environment inside the greenhouse constitutes very high operating costs for cold countries like Canada. In a study done for a greenhouse located in Quebec, the cost of installing a greenhouse approximates \$450,000 to \$500,000 depending upon the size and advancements considered in the facility whereas the operating cost varies from \$200,000 to \$250,000 (Eaves and Eaves, 2018). Another study conducted for a greenhouse in Southern California revealed that heating, ventilation, air conditioning (HVAC), and dehumidification systems account for approximately 56% of the total operating cost (Schimelpfenig and Smith, 2021). This cost is further distributed

between heating (33%), ventilation (5%), and cooling (18%) respectively (Schimelpfenig and Smith, 2021; Brosseau and Hemery, 1970). Rorabaugh *et. al.* (2002) demonstrated that the heating cost of northern greenhouses such as in Canada can be from 75 to 85% of the total operating cost. This total cost can vary based on geographical location, facility type, automation, environmental control systems, and crop type (Melancon, 2018). The aforementioned operational cost associated with CEA is widely recognized as a significant hindrance in the agricultural industry and academia. Therefore, this study aims to explore energy-efficient methods for reducing the heating energy demand in these types of greenhouses by enhancing the amount of solar insolation available on different surfaces of a greenhouse. CEA can be successfully employed in low-income communities by using renewable energy for its operation. This will help to produce cheap crops locally and ensure food security. By minimizing the operational energy demand, the total CEA energy demand could be supplied by using renewable energy sources.

High heating costs can be reduced by utilizing clean and freely available solar energy (Mobtaker *et. al.*, 2016). This could be achieved by using a passive solar greenhouse which operates entirely on the stored radiant energy from the sun. The function of a passive solar greenhouse is to store excessive solar energy during the daytime and use this stored energy during the nighttime to maintain a higher interior temperature than the ambient temperature. The interior air temperature of a passive solar greenhouse also depends upon ambient air temperature, amount, and duration of solar radiation intensity, transmitted solar radiation inside the greenhouse, overall heat transfer coefficient, covering material, wind speed, and its direction, and the type of crop grown (Ali, 2008). In high northern latitudes, heating a greenhouse for about eight months of the year is essential to ensure the growth and development of crops growing therein (Ahamed *et. al.*, 2017). Therefore, to have enough amount of heating energy available for almost a year either supplemental heating is required, or energy-efficient methods can be implemented to capture more solar energy. Even though solar energy is abundantly available it is important to understand the availability of solar radiation on a greenhouse throughout the year. A study shows that the thermal contribution of solar energy in Montreal varies from approximately 13 to 54% every month. During the coldest period of the year in this

region, the direct contribution of solar energy for heating purposes fluctuated between 13% in December and January months to roughly 20% in November and February months (Lawand *et. al.*, 1975). Consequently, it is essential to optimize the availability of solar radiation for the year. This includes gaining more solar radiation during the winter months and less solar radiation during the summer months (Gupta and Chandra, 2001). An increase in solar radiation availability inside the greenhouse will also increase the rate of photosynthesis for plants (Mobtaker *et. al.*, 2016; Lawand *et. al.*, 1975). It is anticipated that solar radiation can be varied by changing the greenhouse orientations and greenhouse shapes (Mobtaker *et. al.*, 2016). Solar radiation availability also differs by changing the inclination of walls and roofs. Hence, the main objective of this paper is to analyze the solar radiation availability on different surfaces of a greenhouse. The study analyzes the impact of greenhouse orientation, roof inclinations, and greenhouse shapes on the accessibility of solar insolation. The findings of this study will inform the greenhouse orientation that maximizes the solar radiation for the given location, and solar radiation availability on different walls and roofs of a greenhouse. It will also inform the effect of different roof inclinations and the greenhouse shape which helps in increasing the solar radiation.

2.2 Literature Review

High operating costs will always be a barrier to the success of CEA facilities. Hence, many studies have been conducted to identify energy-efficient measures for reducing the operating costs of a greenhouse. One of the primary constraints that greatly affect the designing process of these CEA facilities revolves around the absence of specific and well-defined codes or standards that can be utilized to effectively design and construct these CEA facilities. However, different researchers tried to study greenhouses having different orientations and shapes. The available works of literature related to energy-efficient parameters were specific to the locations close to the equator, especially in Asia and Europe. Mobtaker *et. al.* (2016) investigated how shapes can impact the energy consumption of a greenhouse in Tabriz, Iran. The result showed that the additional energy requirement to maintain the temperature desirable for the plant's growth was lowest in the east-west orientated single-span greenhouse with a north brick wall. Ali (2008) developed a model for analyzing the effect of different orientations of greenhouses (most

suitable for all year-round applications) on solar radiation availability. An east-west orientation received more solar radiation in January month and less solar radiation in July month with small differences in received solar radiation during the two months. Gupta and Chandra (2001) studied the energy-efficient greenhouse under cold climatic conditions in Northern India. Simulation results indicated that an arch-shaped greenhouse required 2.6 % and 4.2 % less heating as compared to gable and quonset shapes. An east-west orientated arch greenhouse required 2% less heating as compared to a north-south orientated one.

Lawand *et. al.* (1975) designed and tested a greenhouse for colder regions. The greenhouse was orientated on an east-west axis, the south-facing roof being transparent, and the inclined north-facing wall being insulated with a reflective cover on the interior face. The study was conducted at Laval University for one winter which showed a reduction in heating requirement by 30 – 40% compared to a standard, double layered plastic covered greenhouse. Sethi (2008) studied the effect of different greenhouse shapes on the hourly transmitted total solar radiation (i.e., beam, diffused, and ground reflected) for both east-west orientation and north-south orientation in Ludhiana, India. Results showed that uneven span shape greenhouse receives the maximum and quonset shape receives the minimum solar radiation during each month of the year at all latitudes. East-west orientation is best suited for year-round at all latitudes. Ahamed *et. al.* (2018) conducted a study on greenhouses located in Canadian Prairies. The design parameters include the shape, orientation, angle of the roof, and width of the span. The simulation results proved that the uneven-span greenhouse receives the highest solar radiation whereas the quonset shape receives the lowest solar radiation. Also, it shows that for northern latitudes, an east-west oriented greenhouse is more energy-efficient from a heating and cooling point of view. Table 2-1 summarizes the details of the literature studies conducted earlier.

Table 2-1 Summary of published literature.

Author's Name	Location	Greenhouse Orientation	Roof Inclination	Greenhouse Shapes	Main Focus
Lawand <i>et. al.</i> (1975)	Canada	X	-	-	Calculating the heating requirement of the greenhouse

Gupta and Chandra (2001)	India	X	-	X	Calculating the heating requirement in the energy-efficient greenhouse
Ali (2008)	-	X	-	-	Analyzing the effect of different orientations on solar radiation availability
Sethi (2008)	India	X	-	X	Computing the transmitted total solar radiation (beam, diffused and ground reflected)
Mobtaker <i>et. al.</i> (2016)	Iran	X	-	X	Calculating the additional energy requirement
Ahamed <i>et. al.</i> (2018)	Canada	X	-	X	Calculating heating requirements for different greenhouses

2.3 Methodology

This paper focused on enhancing the solar radiation availability on a greenhouse by changing the greenhouse orientation, roof inclination, and greenhouse shapes. This work does not focus on solar radiation entering the greenhouse. Therefore, the transmissivity of different surfaces was not considered. Numerous cases were considered under each energy-efficient parameter defined in Table 2-2. These cases are described in more detail in their respective sections.

Table 2-2 Indicates this study's three main energy-efficient parameters with different cases under each parameter.

Parameter – 1	Parameter – 2	Parameter – 3
Greenhouse Orientation	Roof Inclination	Greenhouse Shape
1. East-West Orientation	1. 15° roof inclination	1. Even Shape
2. 60° North of East	2. 30° roof inclination	2. Uneven shape
3. 45° North of East	3. 45° roof inclination	3. Vinery shape
4. 30° North of East	4. 60° roof inclination	4. Semi-circular shape
5. North-South Orientation		5. Elliptical or arch shape
6. 30° North of West		6. Single span

7.	45° North of West	7. Quonset shape
8.	60° North of West	

2.3.1 Model Development

Different greenhouse models were designed in SketchUp software and then imported to TRNSYS-18 (version 18.00.0008) for further simulation. TRNSYS is an energy simulation software used to simulate the behavior of a transient system. SketchUp software is a plug-in feature to TRNSYS software to import 3-D drawings of buildings in TRNBuild. TRNSYS-18 automatically reads the data of 3-D drawings from SketchUp software. SketchUp is a popular software for drafting building models and enables the creation of detailed greenhouse models. The greenhouse models designed for this study have a ground surface area of 2000 m² (L = 50 m & B = 40 m), a side wall height of 5 m, and the maximum vertical height of the greenhouse as 16.5 m. To obtain comparable results for all the greenhouse models being evaluated, the main dimensions such as length, breadth, side wall height, and maximum height of the greenhouses were kept constant across all models. The basic design of a greenhouse is presented in Figure 2-1.

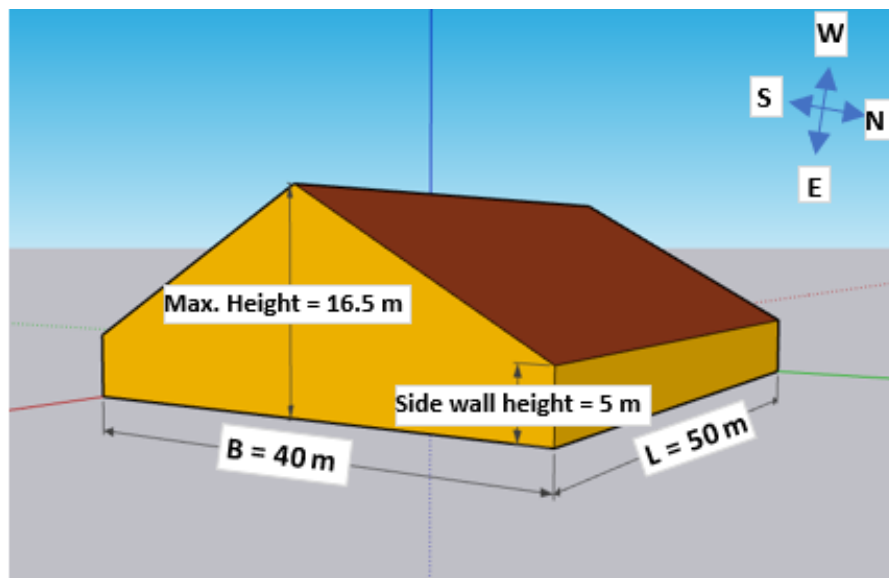


Figure 2-1 An east-west oriented greenhouse model developed in SketchUp software

2.3.1.1 Greenhouse Orientations

Previous studies presented two main orientations *i.e.*, the east-west orientation and the north-south orientation (Mobtaker *et. al.*, 2016; Sethi 2008; Ahamed *et. al.*, 2018). However, no study was executed for other orientations other than these orientations. Therefore, the axis of the even-span greenhouse (as shown in Figure 2-1) was oriented at

distinct angles of 15° increments from east to west to understand the pattern and effect of solar radiation availability on these greenhouses. Figure 2-2 indicates the different greenhouse orientations considered for this study.

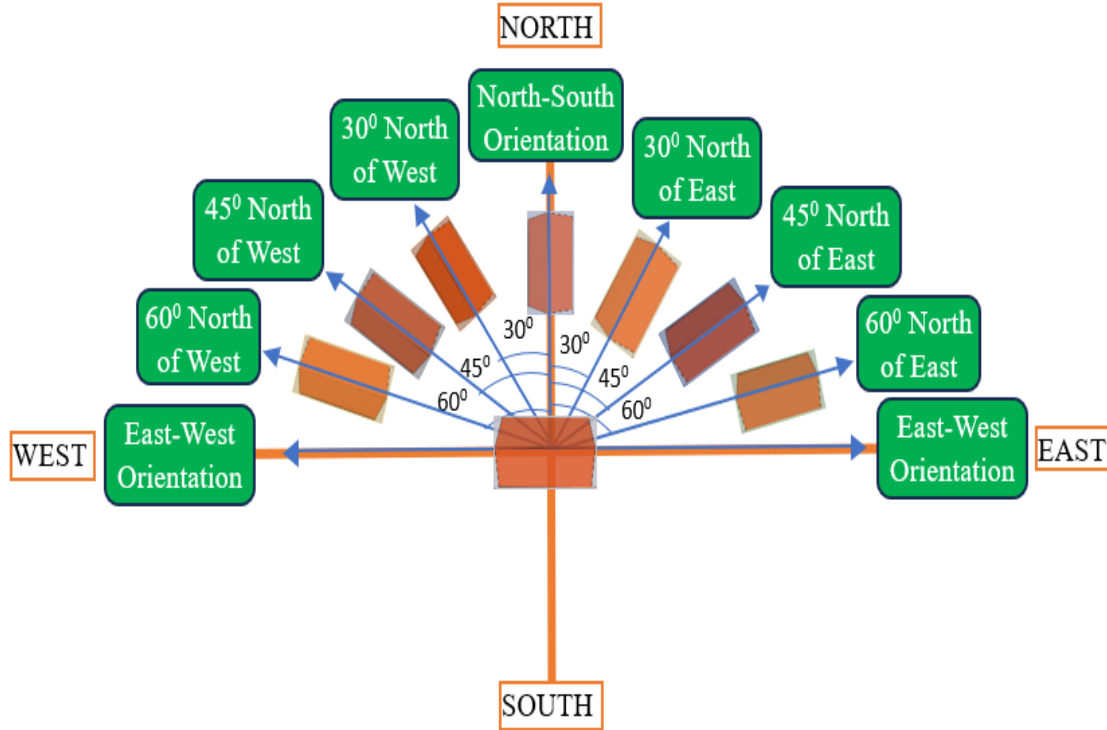


Figure 2-2 Different greenhouse orientations considered in this research.

2.3.1.2 Roof Inclinations

The impact of roof inclination on an even span greenhouse from 15° to 60° with an augmentation of 15° was studied. This was the minimum difference in inclination to see the observable changes in solar radiation availability by changing the roof inclinations. Roof inclinations beyond 60° were not considered because the maximum height of the greenhouse increased drastically. Figure 2.1 shows the main dimensions such as length (L), breadth (B), side wall height, and maximum height of the greenhouse model. For these models, the maximum height changes as the roof inclination changes. The dimensions of the greenhouse models considered for roof inclinations are defined above in Figure 2-3.

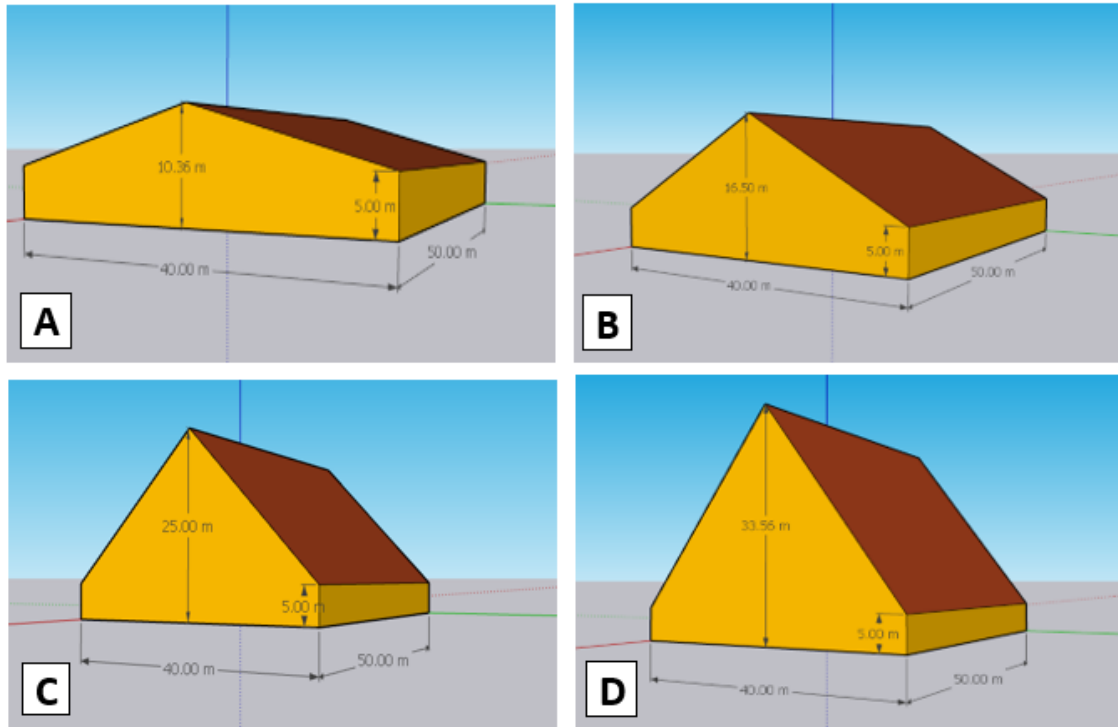


Figure 2-3 Different roof inclinations considered for this study.
 A) 15° roof inclination B) 30° roof inclination C) 45° roof inclination D) 60° roof inclination.

2.3.1.3 Greenhouse Shapes

The commonly identified greenhouse shapes based on previous literature reviews include even span, uneven span, vinery, semi-circular, elliptical or arch shape, single span, and quonset shape (Mobtaker *et. al.*, 2016; Gupta and Chandra, 2001; Sethi, 2008; Ahamed *et. al.*, 2018). The ground surface area and the maximum height were fixed for all the greenhouse shapes to compare the solar radiation availability. The inclination of different walls and roofs was decided based on the results obtained for the different roof inclinations and to meet the maximum height of 16.5 m for all the greenhouses.

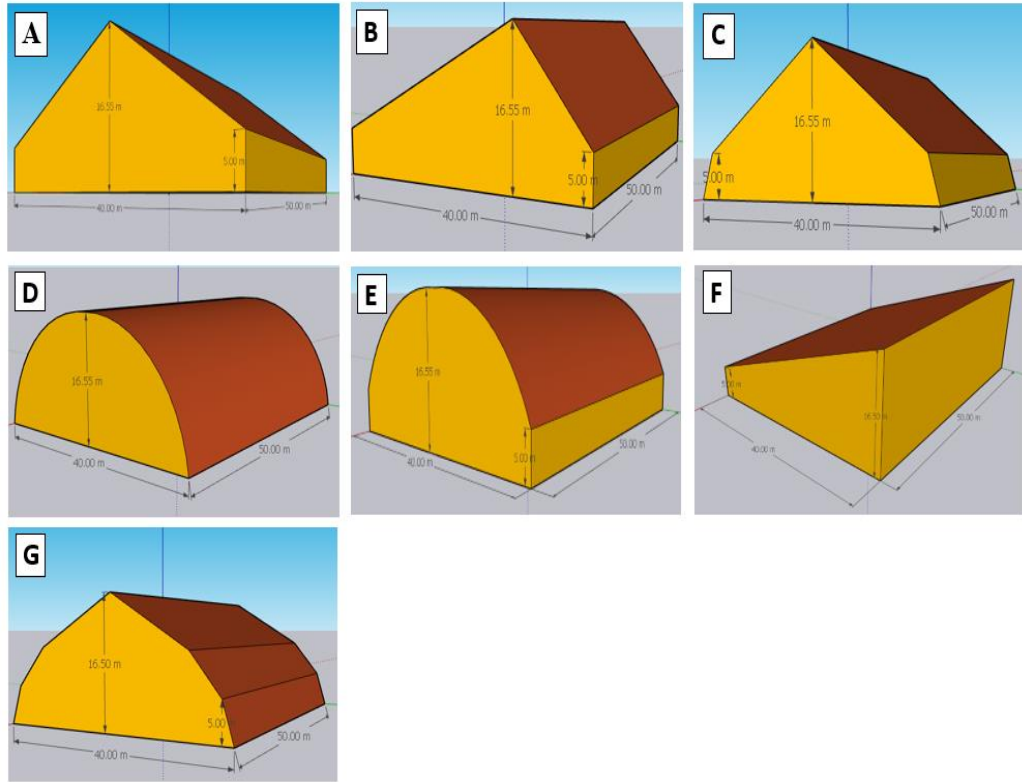


Figure 2-4 Greenhouse shapes are considered for this study.

A) Even Span B) Uneven Span C) Vinery Shape D) Semi-circular
 E) Elliptical or arch F) Single Span G) Quonset shape

The greenhouse model design for different greenhouse shapes is shown in Figure 2-4. Greenhouse models for different greenhouse shapes are explained in Table 2-3. It includes the dimensions of a greenhouse, maximum height, and inclination of different roofs and walls as applicable.

Table 2-3 Represents different greenhouse shapes and model descriptions including length (*L*), breadth (*B*), maximum height, and roof and wall inclination considered for parameter 3.

Cases	Greenhouse shapes	Model Description
Case A	Even Span	$L = 50 \text{ m}$ & $B = 40 \text{ m}$; Max. Height = 16.5 m Roof Inclination = 30°
Case B	Uneven span	$L = 50 \text{ m}$ & $B = 40 \text{ m}$; Max. Height = 16.5 m South Roof Inclination = 22° ; North Roof Inclination = 45°
Case C	Vinery shape	$L = 50 \text{ m}$ & $B = 40 \text{ m}$; Max. Height = 16.5 m Wall Inclination = 70° ; Roof Inclination = 32°
Case D	Semi-circular shape	$L = 50 \text{ m}$ & $B = 40 \text{ m}$; Max. Height = 16.5 m

Case E	Elliptical or arch-shape	L = 50 m & B = 40 m; Max. Height = 16.5 m
Case F	Single Span	L = 50 m & B = 40 m; Max. Height = 16.5 m Roof Inclination = 16 ⁰
Case G	Quonset Shape	L = 50 m & B = 40 m; Max. Height = 16.5 m Roof Inclination 1 = 70 ⁰ ; Roof Inclination 2 = 45 ⁰ ; Roof Inclination 3 = 26 ⁰

2.3.2 The TRNSYS-18 Model

The basic simulation model of TRNSYS-18 is shown in Figure 2-5. Once the greenhouse models were developed in the SketchUp software, these files were saved as a .idf file. With the help of the simulation studio of TRNSYS, the above .idf file was then loaded into the simulation studio for simulations. The description of the greenhouse model was stored in the building component. The building component is a type-56 for multi-zone building modeling which models the thermal behavior of a building. To use this component, a pre-processing program known as TRNBuild was to be executed which reads in and processes a file containing the building description. TRNBuild generates an information file describing the outputs and required inputs of type-56 (TRNSYS-18 Multizone Building, 2021). This building component gets weather input such as total solar radiation, direct solar radiation, dry bulb temperature, slope, and the azimuth of surfaces, etc. from the weather component (Type-15).

The weather file selected for this analysis was the typical meteorological year (.tmy) file for the city of Toronto, Ontario (TRNSYS-18 Weather data, 2017). TMY files contain the generated values from a data bank for a specific location of at least 12 years (Typical Meteorological Year, 2024). The output from the weather component gives solar radiation flux available on the different surfaces of the greenhouse models in $\text{kJ hr}^{-1}\text{m}^{-2}$. A radiation unit converter was added between a weather component and a building component. The function of this converter was to interpolate radiation data, calculate the angle of incidence, total, and beam solar radiation input related to the position of the sun, and estimate insolation on several surfaces either fixed or variable orientation. Type-77 component models the vertical temperature distribution of the ground with details like mean surface temperature for the year and thermal properties of the soil which also affects

the inside temperature of the building. Type-55 is an integrator that was used to integrate the total solar radiation available for a year. Different output components were used for this analysis. Type-25c is a printer to print the numerical results on an Excel file for further analysis whereas the solar plotters, and T_plotters are online plotters to plot the graphs obtained from the results. The basic calculation that was used to calculate the total solar radiation on different surfaces of a greenhouse is as follows: -

Total solar radiation in MWh for a year =

$$[(IT_1 * A_1) + (IT_2 * A_2) + (IT_3 * A_3) + \dots + (IT_n * A_n)] * 10^{-6} \dots\dots\dots(2-1)$$

Where,

IT_1 = Solar radiation on surface 1 of the greenhouse (W/m^2)

A_1 = Area of surface 1 of the greenhouse (m^2)

IT_2 = Solar radiation on the surface 2 of the greenhouse (W/m^2)

A_2 = Area of surface 2 of the greenhouse (m^2)

IT_n = Solar radiation on the n^{th} surface of the greenhouse (W/m^2)

A_n = Area of the n^{th} surface of the greenhouse (m^2)

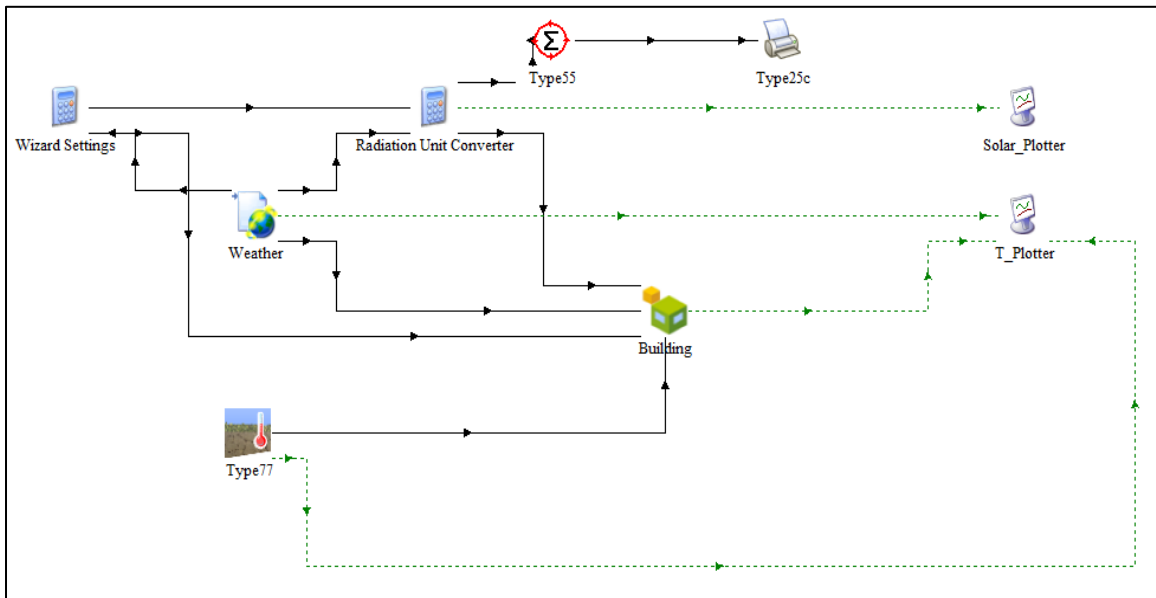


Figure 2-5 A complete TRNSYS model developed in TRNSYS-18 software indicates the input-outputs of each component.

2.4 Results

The results obtained from the TRNSYS file were arranged based on the numerous cases considered. This study was important to apprehend the pattern of solar radiation on different walls and roofs of a greenhouse during different months of the year. The result for each parameter is explained in the following subsections.

2.4.1 Impact of greenhouse orientations on solar radiation availability

The results shown in Figure 2-6 indicate that solar radiation can be increased by orienting the greenhouse at 30° North of East for the location of Toronto, Ontario. For this location, the least solar radiation is received by the east-west orientation. However, the variation in solar radiation availability among the greenhouse orientations is insignificant. The percentage difference between the maximum solar radiation availability and the minimum solar radiation availability for different greenhouse orientations is only 0.6%. This implies that the greenhouse orientations barely alter the solar radiation availability. However, based on the literature review, an east-west-oriented greenhouse was the preferred orientation for the location in India (Gupta and Chandra, 2001; Sethi, 2008). This may be due to the changes in the location and solar radiation patterns for that location. Therefore, other factors such as space availability, radiation on different walls, *etc.* should also be studied to finalize the orientation of a greenhouse. Hence, analysis was done to check the solar radiation availability on different walls and roofs of a greenhouse.

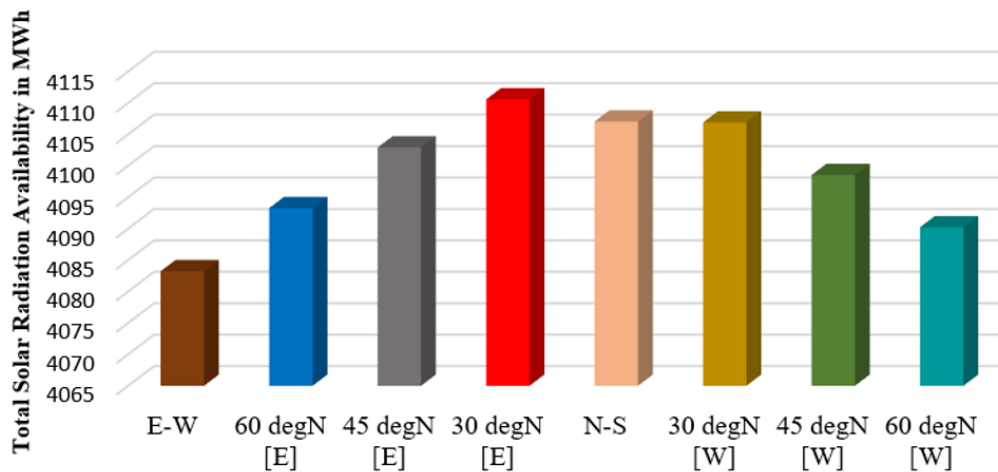


Figure 2-6 Graph for comparison of solar radiation availability (in MWh) on different orientations of the greenhouse.

The graphs shown in Figures 2-7 and 2-8 explain the solar radiation availability on the different roofs and walls of a greenhouse. The result shows that the south roof receives the maximum solar radiation throughout the year. This is almost 50% more solar radiation as compared to the east roof and the west roof during the winter months. The results also show that the north roof receives the least solar radiation throughout the year. This may be useful in obtaining the objective of optimizing solar radiation availability during the winter months when a large amount of heating is required to maintain the inside air temperature. Also, the south wall receives 70% more solar radiation as compared to other walls during the winter months.

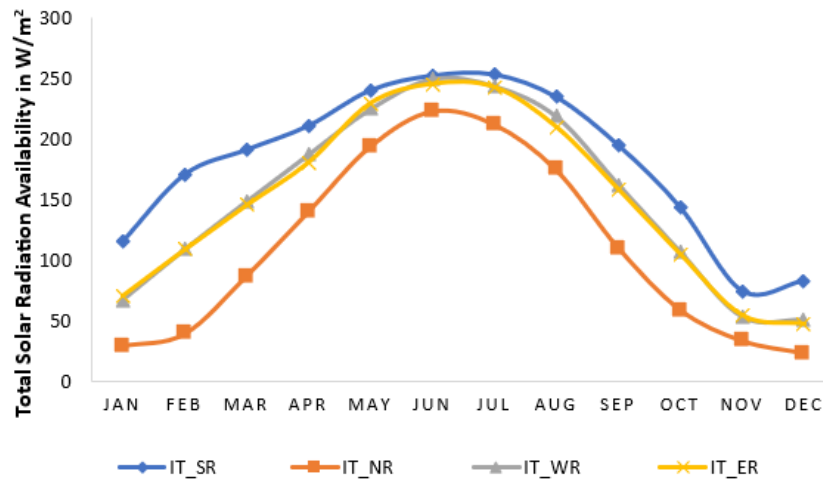


Figure 2-7 Comparison of solar radiation availability in W/m^2 on different roofs of a greenhouse where SR = South roof, NR = North roof, WR = West roof, ER = East Roof.

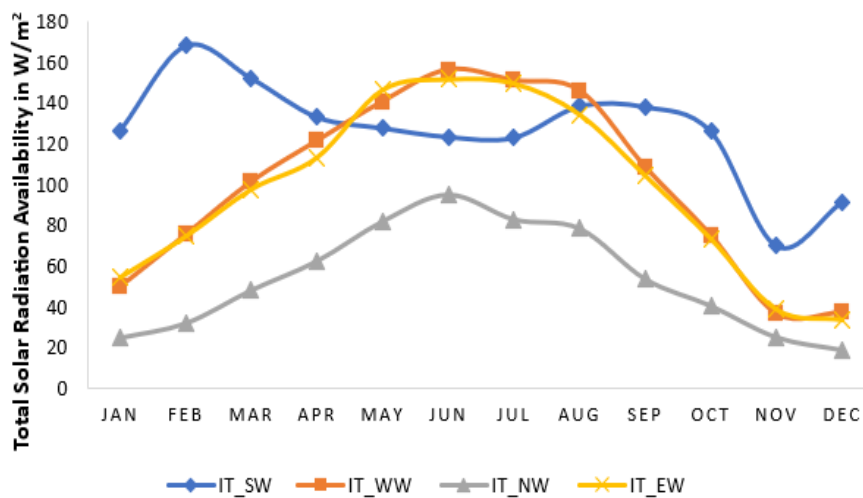


Figure 2-8 Comparison of solar radiation availability in W/m^2 on different walls of a greenhouse where SW = South Wall, WW = West Wall, NW = North Wall and EW = East Wall

2.4.2 Impact of roof inclinations on solar radiation availability

Figures 2-9 and 2-10 show the solar radiation pattern for different inclinations of the south roof and north roof. Solar radiation availability during the winter months is maximum when the south roof inclination is 60° and the north roof inclination is 15° . For the south roof, the solar radiation availability increases during the winter months and decreases during the summer months as the roof inclination changes from 15° to 60° . However, for the north roof, the maximum solar radiation availability is seen for 15° roof inclination throughout the year. Since the prime objective of this study is to optimize solar radiation availability during the winter month, the focus will be on south roof inclination rather than north roof inclination. This is because the south roof receives 2 to 3 times more solar radiation flux compared to the north roof during the winter months. Hence, it can be concluded that the solar radiation flux on the south roof can be increased by approximately 40% by increasing the south roof inclination from 15° to 60° . This indicates that roof inclination is an important parameter for increasing solar radiation availability.

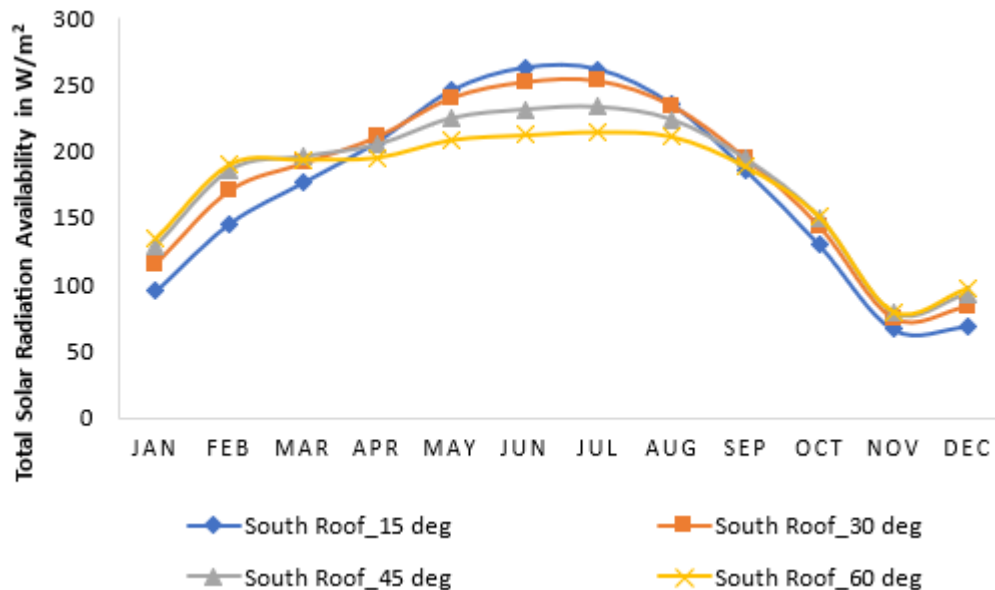


Figure 2-9 Graph for comparison of solar radiation availability for different roof inclinations of the south roof.

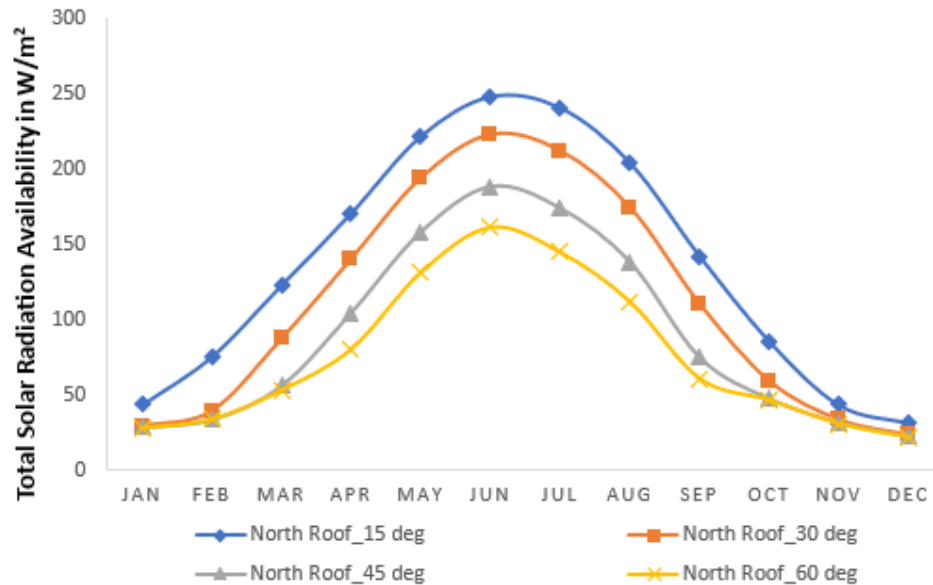


Figure 2-10 Graph for comparison of solar radiation availability for different roof inclinations of the north roof.

2.4.3 Impact of greenhouse shapes on solar radiation availability

Figure 2-11 shows the variation of total solar radiation availability on the different shapes of a greenhouse. For the selected location, a single-span greenhouse receives the maximum solar radiation of about 4574 MWh/year and a semi-circular greenhouse receives the least solar radiation of about 3916 MWh/year. This is because a single-span greenhouse has the highest available south roof area through of which it can capture more solar radiation. The solar radiation percentage difference between the maximum and minimum solar radiation availability for different greenhouse shapes is approximately 17%. Mobtaker *et. al.*, (2016) also investigated the different shapes of greenhouses for the climatic conditions of Tabriz, Iran. The result showed that the additional energy requirement to maintain a desirable temperature for the plant's growth was lowest in an east-west oriented single-span greenhouse. This is because an east-west oriented single-span greenhouse receives the highest solar radiation. As indicated in Figure 2-11, this shape reduces the additional energy requirement to maintain the optimum temperature for plant growth. Also, as per the Ahamed *et. al.*, (2018) study, an uneven-span greenhouse receives maximum solar radiation, because they did not consider a single-

span greenhouse in their study. According to the current results, an uneven-span greenhouse receives the second highest solar radiation after a single-span greenhouse.

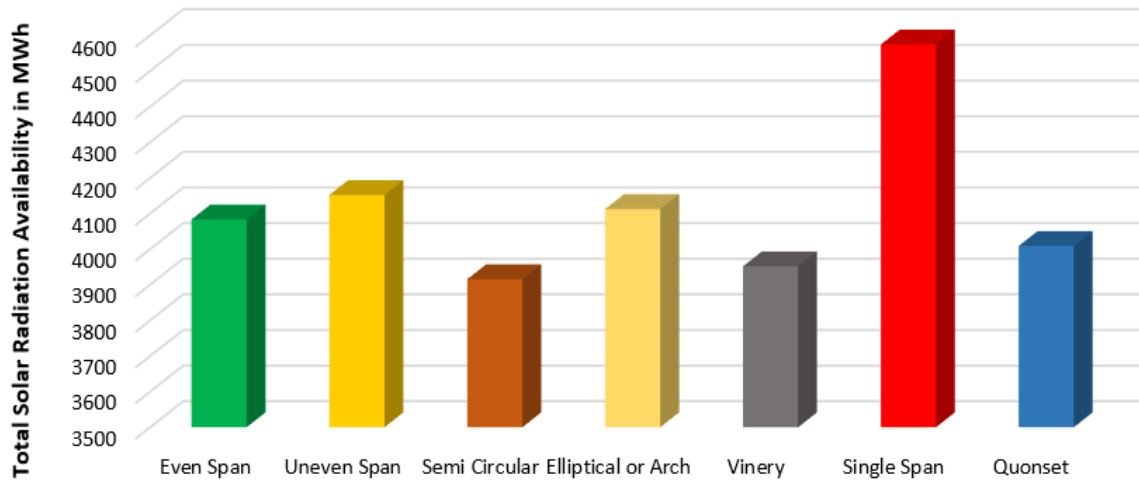


Figure 2-11 Graph for comparison of total solar radiation availability (in MWh) on different shapes of a greenhouse

2.5 Conclusions

Based on the results, it is apparent that the solar radiation availability on the greenhouse can be varied by changing the greenhouse orientations, roof inclinations, and greenhouse shapes. Some parameters have a major impact on solar insolation availability such as greenhouse shapes and roof inclinations. However, some parameters do not have much effect on the solar insolation falling on the greenhouse such as greenhouse orientation. Therefore, these parameters can be executed in pairs or together to meet the requirements for a greenhouse. However, the following conclusions can be drawn from the above set of results, for the greenhouse located in the city of Toronto, Ontario:

- 1) 30° North of East is the best orientation to increase solar radiation availability. But it is also important to consider other parameters like solar radiation availability on different walls, and space availability.
- 2) The orientation of the greenhouse does not have much impact on the variation of solar radiation availability. The solar radiation percentage difference between the maximum and minimum solar radiation availability for different greenhouse orientations is only 0.6%.

- 3) The south roof receives the maximum solar radiation flux all during the year. This percentage is almost 50% more solar radiation as compared to the east and west roofs.
- 4) Similarly, the south wall receives the maximum solar radiation during the winter months. This percentage is approximately 70% more than the other walls.
- 5) The north wall and the north roof always receive the least solar radiation throughout the year.
- 6) Roof inclination plays a major role in optimizing solar radiation availability. The solar radiation availability on the south roof is maximum during the winter month when the roof inclination is 60° and minimum for the roof inclination of 15° . This increment is approximately equal to 40% more solar radiation as compared to 15° roof inclination.
- 7) The solar radiation percentage difference between the maximum and minimum solar radiation availability for different greenhouse shapes is approximately 17%.

The study of greenhouse orientations, roof inclinations, and greenhouse shape was vital to understanding how these parameters affect solar radiation availability. The studies mentioned above are limited to countries close to the equator, especially those located in Asia and Europe. Therefore, a modification was required to analyze locations having cold climatic conditions such as Canada. Most of the existing literature discusses the inside air conditions, heating, and cooling requirements. To make these greenhouses in cold climates more sustainable, it is important to optimize the solar insolation falling on the roofs and walls of the greenhouse. Future work will be required to extend the findings of this research and will include the investigation of the interior environment of a greenhouse by using combinations of these parameters. A study of this nature should consider analyzing the greenhouse's interactions with the external environmental conditions, soil conditions inside a greenhouse, inputs from the weather file, location parameters, and evapotranspiration from plants and soil. Furthermore, a detailed analysis is required to calculate the amount of solar radiation transmitted inside a greenhouse surface that will regulate the inside air temperature of a greenhouse. This will require the identification of the thermal properties of the construction material. Therefore, a more

complex study is required to understand the dynamic model of a greenhouse to ensure that this will lead to a reduction in the heating costs of a greenhouse.

2.6 References

Ahamed, M. S., Guo, H., Tanino, K., (2017) "A quasi-steady state model for predicting the heating requirements of conventional greenhouses in cold regions," *Information processing in agriculture*, Vol 5, pp. 33-46.

Ahamed, M. S., Guo, H., Tanino, K., (2018) "Energy-efficient design of greenhouse for Canadian Prairies using a heating simulation model" *International Journal of Energy Research*, Vol. 42, pp. 2263-2272.

Ali, S. A., (2008) "Modeling of solar radiation available at different orientations of a greenhouse," *Agriculture Engineering Department*.

Benke, K., Tomkins, B., (2017) "Future food-production systems: vertical farming and controlled environment agriculture," *Sustainability: Science, Practice and Policy*, Vol 13:1, pp. 13-26.

Brosseau, F., Hemery, G., (1970) "Certains aspects économiques de la production de tomates en serres chaudes". *Semaine du Cultivateur*. St. Hyacinthe, Gouvernement du Québec, ministère de l'Agriculture et de la Colonisation, pp 146-159.

Brown, K. H., Jameton, A. L., (2000) "Public health implications of urban agriculture," *Journal of Public Health Policy*, Vol 21 (1), pp. 20–39.

Coelho, F. C., Coelho, E. M., Egerer, M., (2018) "Local food: benefits and failings due to modern agriculture," *Science Agriculture*, Vol 75 (1), pp. 84–94.

Despommier, D., (2011) "The vertical farm: controlled environment agriculture carried out in tall buildings would create greater food safety and security for large urban populations," *Journal of Consumer Protection and Food Safety*, Vol 6 (2), pp. 233–236.

Dixon, J., Omwega, A. M., Friel, S., Burns, C., Donati, K., Carlisle, R., (2007) "The health equity dimensions of urban food systems," *Journal of Urban Health: Bulletin of the New York Academy of Medicine*, Vol 84, pp. 118–129.

Eaves, J., Eaves, S., (2018) "Comparing the profitability of a greenhouse to a vertical farm in Quebec," Canadian Journal of Agricultural Economics, Vol 66, pp. 43-54.

Engler, N., Krarti, M., (2021) "Review of energy efficiency in controlled environment agriculture," Journal of Renewable and Sustainability Energy Reviews, Vol 141, 110786.

Food and Agriculture Organization, (2009) "How to feed the world in 2050," UN Food and Agriculture Organization, Rome.

Government of Canada, (2023) "Greenhouse gas emissions and agriculture," (Source: [Greenhouse gas emissions and agriculture - agriculture.canada.ca](https://agriculture.canada.ca))

Gupta, M. J., Chandra, P., (2001) "Effect of greenhouse design parameters on conservation of energy for greenhouse environmental control," Energy, Vol. 27, pp. 777-794.

Lawand, T. A., Alward, R., Saulnier, B., Brunet, E., (1975) "The development and testing of environmentally designed greenhouse for colder regions," Solar Energy, Vol 17, pp 307-312.

Melancon, M., (2018) "US (GA): \$5 million to help reduce energy costs of Indoor Farming," HortiDaily, September 11, 2018.

Mobtaker, H. G., Ajabshirchi, Y., Ranjbar, S. F., Matloobi, M., (2016) "Solar energy conservation in a greenhouse: Thermal analysis and experimental validation," Renewable Energy, Vol 96, pp. 509-519.

Rorabaugh, P., Jensen, M., Giacomelli, G., (2002) "Introduction to Controlled Environment Agriculture and Hydroponics," Controlled Environment Agriculture Center, Campus Agriculture Center, University of Arizona.

Schimelpfenig, G., Smith, D., (2021) "Controlled Environment Agriculture market characterization report, supply chains, energy sources, use, and barriers to efficiency," Resource Innovation Institute and United States Department of Agriculture.

Sethi, V. P., (2008) "On the selection of shape and orientation of a greenhouse: Thermal modeling and experimental validation," Solar Energy, Vol. 83, pp. 21-38.

Smit, J., Ratta, A., Nasr, J., (2001) "Urban Agriculture: Food, Jobs, and Sustainable Cities," The Urban Agriculture Network, Inc, Washington DC, USA.

Sullivan, C. A., Bonnett, G. D., McIntyre, C. L., Hochman, Z., Wasson, A. P., (2019) "Strategies to improve the productivity, product diversity, and profitability of urban agriculture," Agricultural Systems, Vol. 174, pp. 133-144.

TRNSYS-18, (2017) "TRaNsient System Simulation program – Weather Data," Volume 8, Solar Energy Laboratory, University of Wisconsin-Madison

TRNSYS-18, (2021) "TRaNsient System Simulation program – Multizone Building Modeling with Type56 and TRNBuild" Volume 5, Solar Energy Laboratory, University of Wisconsin-Madison.

Typical Meteorological Year, (2024) "Wikipedia The free encyclopedia for a typical meteorological year," (Source: [Typical meteorological year - Wikipedia](#))

United Nations DoEaSA, (2013) "World population prospects: the 2012 revision. United Nations Food and Agriculture Organization - Population Division" Report No.: 0470670592. (Source: [Home Page | Data Portal \(un.org\)](#))

United Nations Food and Agriculture Organization (FAO), (2016) "Database on Arable Land," 13 September 2016 (Source: <http://data.worldbank.org/indicator/AG.LND.ARB.L.HA.PC?end%20&hx003D;2013&hx0026;start%20&hx003D;1961&hx0026;view&hx003D;chart>)

CHAPTER 3
A METHODOLOGICAL FRAMEWORK FOR MODELING PASSIVE SOLAR
GREENHOUSES

3.1 Introduction

Conventional greenhouses are known for their extensive energy consumption, primarily relying on electricity or fossil fuels, contributing significantly to greenhouse gas emissions (Gorjian *et. al.*, 2021). The energy from electricity and natural gas accounts for about 28% of global greenhouse gas emissions (Greer *et. al.*, 2024). This massive energy demand not only poses environmental threats but also leads to higher operating costs for growers, thereby reducing the cost-effectiveness of conventional greenhouses. Energy consumption costs represent approximately 50% of greenhouse production expenses, making them the second largest operating cost (Acosta-Silva *et. al.*, 2019; Golzar *et. al.*, 2018). In northern latitudes, the heating expense can account for 70% to 85% of total greenhouse operating costs (Rorabaugh *et. al.*, 2002). This underscores the necessity for enhancing the energy efficiency of greenhouses to substantially decrease energy demands. Researchers have explored energy-efficient approaches, such as using renewable energy, to enhance greenhouse sustainability. Solar energy offers an economical solution for greenhouse heating (Beshada *et. al.*, 2006), leading to a transition from traditional greenhouses to modern solar greenhouses (Wang *et. al.*, 2017). Modern solar greenhouses, classified as passive and active, have the potential to reduce energy demand and greenhouse gas emissions. Active solar greenhouses are integrated with solar energy technologies such as photovoltaic and thermal solar collectors, while passive solar greenhouses (PSGs) are designed to increase solar energy capture (Gorjian *et. al.*, 2021).

PSGs are specifically designed to enhance solar energy capture and minimize energy losses. Studies have been conducted to enhance the solar capturing efficiency of the greenhouse by modifying the greenhouse design and orientation (Mobtaker *et. al.*, 2016; Sethi, 2009). As a result, PSGs are oriented to ensure that the maximum possible surface area is exposed to the sun. The south side of a PSG typically consists of a thin, and transparent surface that transmits solar radiation to enter during the daytime. A thermal curtain is employed on the south side at night to minimize heat loss. Despite this, a

significant amount of heat, approximately 54% to 68% during winter, still escapes to the external environment through the south roof (Xu *et al.*, 2017; Zhao *et al.*, 2019). The north wall and north roof provide heat storage, thermal insulation, and structural stability. The north wall absorbs solar radiation for passive heat storage during the day and then releases the stored heat through conduction and convection to warm the greenhouse air (Liu *et al.*, 2022). Hence, solar energy interactions were modeled within greenhouses to estimate energy consumption and analyze the reduction in energy costs.

The high energy demand of greenhouses, particularly in cold regions, is a prime concern for determining their feasibility, enabling growers to make informed decisions about their establishment. Building performance simulations (BPS) are essential because they generate valuable data to enhance the efficiency of the greenhouse without the significant time and expense associated with conducting real-life experiments (Beaulac *et al.*, 2024). Previous research by Vadiie & Martin (2013), Dong *et al.*, (2021), Ahamed *et al.*, (2018), and Choab *et al.*, (2021) performed BPS to estimate the heating and cooling needs of greenhouses under different climatic conditions. Many studies eliminated the effect of plants inside the greenhouse or assumed constant evapotranspiration rates (Vadiie & Martin, 2013; Semple *et al.*, 2017), as well as ventilation, supplemental heating, or cooling (Guo *et al.*, 1994; Yu *et al.*, 2016; Imafidon *et al.*, 2023) which significantly alters the greenhouse's energy requirements. Moreover, a major obstacle in performing greenhouse energy modeling was the absence of specific guidelines or standards. Existing standards, such as the International Building Code, National Building Code, or the National Energy Code, are used for designing and constructing different buildings but do not encompass greenhouse facilities. These facilities do not meet the criteria outlined in these codes and standards. Thus, this study aims to provide a methodological framework to perform energy modeling in greenhouses. While the greenhouse energy modeling process may vary slightly based on the simulation tool used, the fundamental framework to model the dynamic interactions within the greenhouse remains consistent. This framework was applied to simulate the actual operational and environmental conditions of an experimental mono-slope solar greenhouse in Elie, Manitoba. The simulation results were then compared with measured data to identify the accuracy of the greenhouse energy

model. This approach offers a comprehensive understanding of the energy modeling process to accurately replicate real experimental conditions in a greenhouse.

3.2 Literature Review

The absence of standardized guidelines for greenhouse modeling has resulted in a gap where no study certainly outlines critical considerations for modeling a greenhouse. Consequently, many studies simulated the thermal performance of greenhouses and predicted their heating and cooling requirements using MATLAB, CFD, FORTRAN, TRNSYS, and EnergyPlus. Table 3-1 summarizes the literature reviewed for this study, illustrating different modeling approaches used over the years. Some studies focused on analyzing the indoor air temperature including temperatures of the north wall, back roof, and soil. It includes different greenhouse models such as a mathematical model TEMP developed by Guo *et. al.* (1994), a computational fluid dynamics (CFD) study by Tong *et. al.* (2007), and the thermal environment simulation model using MATLAB and Visual Basic (VB) by Meng *et. al.* (2009). A greenhouse simulation model using a finite difference numerical approach was studied by Ma *et. al.* (2010) to predict and evaluate the thermal environment of solar greenhouses. This model has limitations for use outside China. Vadiee & Martin (2013) utilized TRNSYS software to study closed greenhouses with thermal seasonal storage to calculate their heating and cooling load. Yu *et. al.* (2016) developed a predictive model based on a least square support vector machine (LSSVM) to predict the occurrence of temperatures several hours before to reduce financial losses. Dong (2018) modified the original greenhouse model, developed by Chengwei Ma in China (Ma, 2015), to create the SOGREEN model suitable for the cold climate in Saskatchewan. The model was validated using field data from a solar greenhouse in Elie, Manitoba. The average error of 1.9 °C for indoor air temperature and 7% for relative humidity was observed in the model.

Another simulation model, CSGHEAT, developed by Ahamed *et. al.* (2018), estimated hourly heating requirements for a CSG with a relative root mean square error (rRMSE) of 11.5%. Ahamed *et. al.* (2019) used TRNSYS software to calculate the heating requirements and compared these results with the CSGHEAT model's results. The findings

indicate that the monthly average difference in the heating simulation load between the two models was about 5% when excluding thermal blankets and plants from the simulation. Choab *et. al.* (2021) used TRNSYS software to investigate key design parameters affecting a greenhouse's thermal behavior along with heating and cooling energy needs. Evapotranspiration affected the greenhouse's thermal behavior, yielding a relative error of 1.66% for the annual heating demand. Imafidon *et. al.* (2023) utilized TRNSYS with a detailed radiation model to simulate a net-zero passive solar greenhouse in Alberta, Canada. The study investigated the effects of ground parameters and the solar-to-air fraction on the simulation results. The drawbacks drawn from the above studies involve the exclusion of parameters such as evapotranspiration, ventilation, supplemental heating, and cooling (Guo *et al.*, 1994; Meng *et. al.*, 2009; Yu *et. al.*, 2016; Ahamed *et. al.*, 2018; Imafidon *et. al.*, 2023) leading to inaccuracies in estimating the energy demands whereas others involved complex estimation because of the simulation software (Tong *et. al.*, 2007; Yu *et. al.*, 2016; Ahamed *et. al.*, 2019).

Table 3-1 Summary of published literature to simulate greenhouses with different approaches.

Author	Modeling Strategies	Studied Parameters
Guo <i>et. al.</i> (1994)	Mathematical model – TEMP using FORTRAN programming	<ul style="list-style-type: none"> • Indoor air temperature. • Surface temperature.
Tong <i>et. al.</i> (2007)	Computational Fluid Dynamics (CFD)	<ul style="list-style-type: none"> • Indoor air temperature
Meng <i>et. al.</i> (2009)	MATLAB and Visual Basics (VB)	<ul style="list-style-type: none"> • Indoor air temperature • Surface temperature • Soil temperature • Back roof temperature
Ma <i>et. al.</i> (2010)	Simulation model using finite difference numerical method	<ul style="list-style-type: none"> • Compare the thermal performance of different solar greenhouses.
Vadiee & Martin (2013)	TRNSYS software	<ul style="list-style-type: none"> • Heating and cooling load.
Yu <i>et. al.</i> (2016)	Prediction model using least-square support vector machine (LSSVM)	<ul style="list-style-type: none"> • Temperature variation in the CSG
Dong <i>et. al.</i> (2018)	Simulation model - SOGREEN using finite difference numerical method	<ul style="list-style-type: none"> • Energy consumption

Ahamed <i>et. al.</i> (2018)	CSGHEAT model using MATLAB	<ul style="list-style-type: none"> • Ground temperature. • North wall temperature • Hourly heating requirements
Ahamed <i>et. al.</i> (2019)	TRNSYS Software	<ul style="list-style-type: none"> • Heating requirements
Choab <i>et. al.</i> (2021)	TRNSYS Software	<ul style="list-style-type: none"> • Heating and cooling energy needs
Imafidon <i>et. al.</i> (2023)	TRNSYS Software	<ul style="list-style-type: none"> • Effects of ground parameters • Solar-to-air fraction

Most research focused on the methods to model greenhouses with different simulation tools to estimate the heating and cooling requirements or thermal performance of a greenhouse. The modeling strategies provided in the above studies remained specific to the software used, however, they lack a detailed, unified framework for the modeling process.

3.3 Guidelines for Simulating a Passive Solar Greenhouse

The challenges encountered during the greenhouse energy modeling include complex greenhouse interactions because of the greenhouse locations, shapes, orientation, construction materials, crops, and weather conditions (Chen *et. al.*, 2016; Sethi *et. al.*, 2013). The energy modeling employed to simulate greenhouse heating and cooling requirements was developed using a heat balance approach for greenhouse air. All heat gains to the greenhouse air were considered positive, while all heat losses were considered negative. Thus, the greenhouse heating and cooling demand can be expressed as the difference between all heat gains and heat losses. Figure 3-1 depicts the greenhouse volume indicating the heat interactions between the greenhouse air and its surroundings. The greenhouse air temperature is primarily influenced by the heat gain from solar radiation entering the greenhouse through glazing (\dot{Q}_{solair}). A portion of this heat is added to the greenhouse air, while another fraction is absorbed by the greenhouse surfaces. Furthermore, heat is gained and lost via conduction, convection, and radiation between the internal and external air and the different greenhouse surfaces (\dot{Q}_{surf}). Heat loss from the greenhouse air also occurs due to infiltration (\dot{Q}_{inf}) and ventilation (\dot{Q}_{vent}).

Environmental control systems such as motors and lights, may be installed in the greenhouse and contribute additional heat to the air ($\dot{Q}_{g,c}$). Additionally, evapotranspiration heat flux (\dot{Q}_{evt}) creates a cooling effect, thereby reducing the greenhouse temperature.

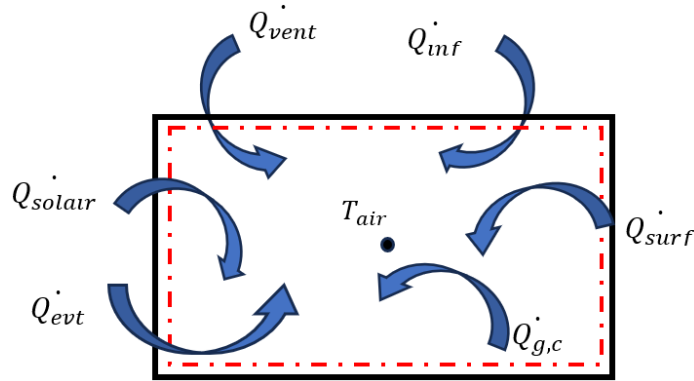


Figure 3-1 Heat interactions between greenhouse air and its surroundings.

Note. This figure is re-created from the TRNSYS-18 Multizone Building manual. From “TRNSYS-18, (2021) “TRaNsient System Simulation program – Multizone Building Modeling with Type56 and TRNBuild” Volume 5, Solar Energy Laboratory, University of Wisconsin-Madison”

Sensible heat flux to the volume of the greenhouse air is presented by \dot{Q}_i in kJ/hr and is given by equation (3-1) (TRNSYS-18 Multizone Building, 2021).

$$\dot{Q}_i = \dot{Q}_{surf} + \dot{Q}_{inf} + \dot{Q}_{vent} + \dot{Q}_{g,c} + \dot{Q}_{solair} + \dot{Q}_{evt} \dots\dots\dots (3-1)$$

where,

\dot{Q}_{surf} is the convective heat gain from surfaces in kJ/hr.

\dot{Q}_{inf} is the infiltration gain in kJ/hr.

\dot{Q}_{vent} is the ventilation gain in kJ/hr.

$\dot{Q}_{g,c}$ is the internal convective gain (by people, equipment, and illumination) in kJ/hr.

\dot{Q}_{solair} is the fraction of solar radiation entering the greenhouse through external windows in kJ/hr.

\dot{Q}_{evt} is the evapotranspiration heat loss due to the plants in kJ/hr.

A negative Q_i indicates that greenhouse heat losses outweigh heat gains, which means heating is required in the greenhouse, whereas positive Q_i signifies more heat gains in

comparison to heat loss, requiring cooling inside the greenhouse.

Based on the heat interactions, the greenhouse energy modeling process was proposed to include the below important considerations:

(3.3.1) Greenhouse model; (3.3.2) Weather and initial data for simulation; (3.3.3) Greenhouse construction material; (3.3.4) Solar radiation distribution and interactions within the greenhouse; (3.3.5) Evapotranspiration; (3.3.6) Infiltration; (3.3.7) Energy-efficiency features such as thermal and shade curtains, supplemental heating and cooling, thermal storage, and ventilation.

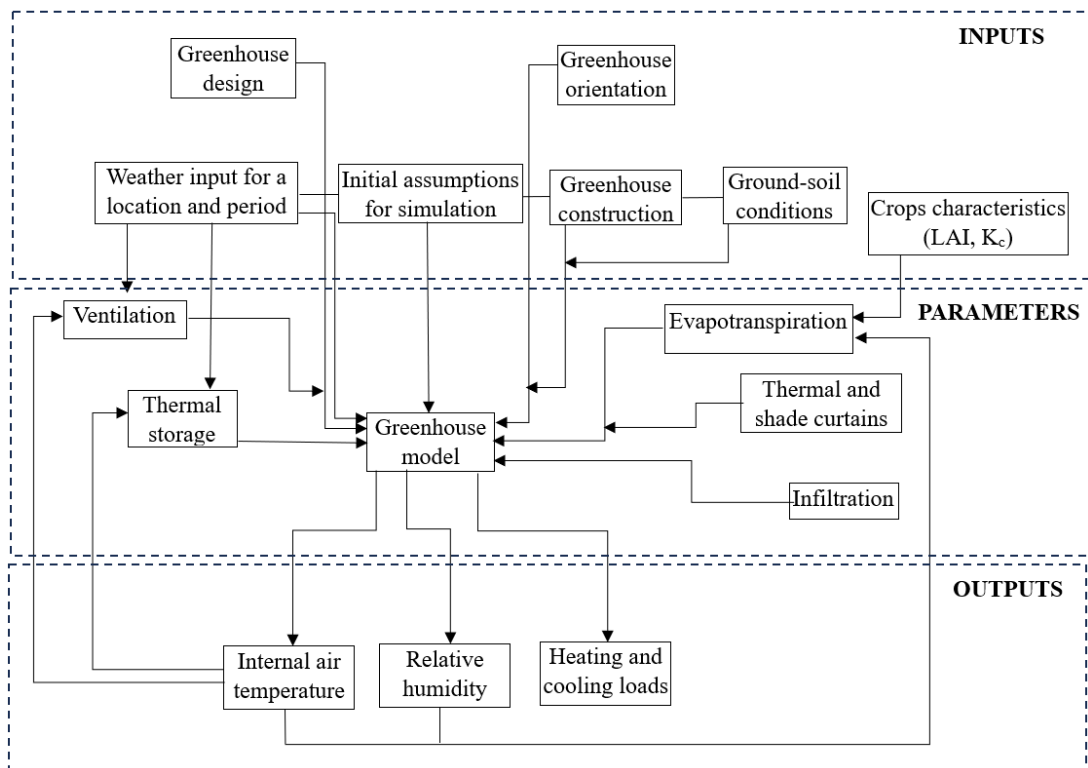


Figure 3-2 Flow chart explaining the main processes involved in greenhouse energy modeling.

The flow chart explaining the general framework for greenhouse energy modeling is illustrated in Figure 3-2. The specific steps and parameters may vary depending on the unique characteristics and requirements of each greenhouse.

3.3.1 Greenhouse Model

The first step in the energy modeling process is to develop the greenhouse model, which provides the physical presence of the greenhouse. The greenhouse model can be created

either by providing the geometric details of the greenhouse manually or using design software depending upon the simulation software being used. The greenhouse model should define comprehensive information about the greenhouse such as its orientation, design, dimensions, volume, inclination, and orientation for each surface. The shape and inclination of the surfaces are the significant cross-sectional parameters that affect the reflection and transmission of solar radiation inside the greenhouse (Tong *et. al.*, 2013). Hence, greenhouse design and orientation are key factors that influence the thermal behavior and energy demand of a greenhouse.

3.3.2 Weather and initial data for simulation

Hourly weather inputs specific to a location and time of year are important for simulating the thermal environment, as greenhouses interact directly with external weather conditions. The greenhouse air temperature depends on ambient air temperature, solar radiation intensity, wind velocity, and wind direction (Sethi & Sharma., 2007). These weather parameters are connected as inputs to the greenhouse model. The weather file must contain hourly weather outputs such as solar radiation, dry bulb temperature, relative humidity, wind velocity, wind direction, solar zenith angle, solar azimuth angle, and other relevant parameters. Energy modeling may also require an initial estimation of parameters like temperature and relative humidity to calculate the hourly greenhouse outputs. These estimations can be assumed to be the average measured internal air temperature and relative humidity obtained from sensors installed in the greenhouse. If measured parameters are unavailable, average temperature and relative humidity values can be taken from the weather file.

3.3.3 Greenhouse Construction Material

The thermal performance of a greenhouse is significantly influenced by its construction materials as it varies the absorbed, transmitted, and reflected solar radiation entering the greenhouse. The modeling of a greenhouse includes thermal properties of materials such as density, heat capacity, conductivity, absorptance, and emissivity. In addition, the g-value, U-value, and transmittance value are also necessary for glazing materials as they significantly impact a greenhouse's heating and cooling requirements. The thermal properties of the materials can be referenced from the ASHRAE handbook under the non-

residential heating and cooling chapter (ASHRAE Handbook, 2013). The details of the construction material can be added to the greenhouse model while developing the model or to the simulation interface depending on the simulation software used.

3.3.4 Solar radiation distribution and interactions within the greenhouse

The solar radiation that falls on the surfaces comprises beam solar radiation and diffuse solar radiation. The amount of solar radiation available inside the greenhouse depends upon the transmissivity and orientation of glazing surfaces (Ahamed *et. al.*, 2017). Solar radiation heat gain \dot{Q}_{solair} entering the greenhouse from the glazing is given by equation (3-2) (Ahamed *et. al.*, 2018) and equation (3-3) (Liu & Jordan, 1963).

$$\dot{Q}_{\text{solair}} = \sum_{i=1}^{i=n} \tau_{g,i} A_{g,i} I_{g,i} \dots \dots \dots (3 - 2)$$

$$I_{g,i} = I_b \frac{\cos\theta_{g,i}}{\cos\theta_z} + \left[I_d \left(\frac{1 + \cos\beta}{2} \right) + (I_b + I_d)\rho_r \left(\frac{1 - \cos\beta}{2} \right) \right] \dots \dots \dots (3 - 3)$$

where,

$\tau_{g,i}$ is the solar transmissivity of glazing ‘i’

$A_{g,i}$ is the glazing area ‘i’ in m²

$I_{g,i}$ is the total solar radiation through inclined glazing ‘i’ in kJ/hr m²

I_b, I_d is the beam and diffuse radiation on a horizontal surface in kJ/hr m²

$\theta_{g,i}$ is the angle of incidence for glazing ‘i’ in degrees

θ_z is the zenith angle of the sun in degrees

β is the angle of the inclined surface with the horizontal in degrees

ρ_r is the reflectivity of outdoor ground

The glazing area and its inclination can be estimated using the greenhouse model. Beam and diffuse solar radiation on a horizontal surface, zenith angle, angle of incidence, and reflectivity of outdoor ground can be collected from the weather data. The transmittance is influenced by the angle of incidence and decreases as the angle of incidence increases. The transmittance of a material varies from 0 to 1 and can be identified for different materials

from the ASHRAE Handbook (ASHRAE Handbook, 2013). The transmitted solar radiation is then absorbed by the internal air, inside surfaces, and plants. This results in various heat interactions within the greenhouse including the net radiative heat transfer with all surfaces inside and outside the greenhouse, convection heat flux from the inside surfaces to the greenhouse air, the convection heat flux from the outside surface to the ambient environment, the conduction heat flux from the walls at the inside surfaces and the conduction heat flux into the wall at the outside surfaces (TRNSYS-18 Multizone Building, 2021). The convective heat gain \dot{Q}_{surf} within the greenhouse can be expressed by equations (3-4), (3-5), and (3-6) (Ahamed *et. al*, 2018): -

$$\dot{Q}_{surf} = Q_t + Q_r \dots\dots\dots (3-4)$$

$$Q_t = (A_g U_g + \sum A_w U_w) \cdot (T_{air} - T_{outside}) \dots\dots\dots (3-5)$$

$$Q_r = \sigma \epsilon_g A_g F_g (T_{air}^4 - T_{glazing}^4) + \sigma \epsilon_i \tau_1 A_f F_{sk} (T_{air}^4 - T_{sk}^4) \dots\dots\dots (3-6)$$

where,

Q_t is the conduction and convection heat transfer in kJ/hr

Q_r is the radiative heat transfer in kJ/hr

A_g is the glazing area in m^2

U_g is the combined conduction and convection heat transfer coefficient for the glazing in $\text{kJ/hr } m^2 \text{ } ^\circ\text{C}$

A_w is the area of each wall or roof in m^2

U_w is the combined conduction and convection heat transfer coefficient for each wall and roof in $\text{kJ/hr } m^2 \text{ } ^\circ\text{C}$

T_{air} is the internal air temperature in $^\circ\text{C}$

$T_{outside}$ is the ambient air temperature in $^\circ\text{C}$

$T_{glazing}$ is the glazing temperature in $^\circ\text{C}$

σ is the Stefan – Boltzmann constant in $\text{kJ/hr } m^2 \text{ } ^\circ\text{C}^4$

ϵ_g, ϵ_i is the emissivity of the glazing and indoor components

F_g, F_{sk} is the glazing view factor and sky view factor

τ_1 is the transmissivity of glazing to longwave radiation

A_f is the floor area in m^2

T_{sk} is the sky temperature in $^{\circ}C$

The values of U_g and U_w can be calculated using the relation given by Tiwari (2003). The emissivity and transmissivity to longwave radiation of a surface can be selected for different materials from the ASHRAE Handbook (ASHRAE Handbook, 2013). T_{sky} and $T_{outside}$ can be estimated from the weather data, whereas T_{air} and $T_{glazing}$ will be received from the greenhouse model simulation. The view factor between the greenhouse and the sky can be considered as 1 as the greenhouse is completely enclosed by the sky (Vadiee, 2011) whereas the view factor for the glazing can be calculated using the relation given by Liu & Jordan (1961). Greenhouses also experience internal convective gain from heat exchange through environmental control systems such as artificial lighting, radiators, motors, equipment, etc. present inside the greenhouse. A thermal analysis study indicates that environmental control systems could reduce 13-56% of the total heating requirements over the year (Ahamed *et. al.*, 2017). This highlights the significant role of environmental control systems in adding heat and regulating the thermal environment of the internal air. The contributions of these systems to the greenhouse's thermal environment are crucial for accurate energy modeling.

3.3.5 Evapotranspiration

Evapotranspiration (EVT) is the combined process of evaporation and plant transpiration within a greenhouse. Many studies overlook the inclusion of plants inside the greenhouse or assume a constant evapotranspiration rate due to the complexity of modeling the dynamic nature of plants, leading to huge inaccuracies in predicting the energy requirements (Ahamed *et. al.*, 2019). Plants have a thermal capacity to absorb solar radiation, transferring less heat to the internal air. A major challenge in modeling plant growth from the initial stage, crop development, mid-season, to late season (Gong *et. al.*, 2020), results in altering the crop's leaf area index (LAI). Since it is difficult to simulate the changing LAI throughout the year, an average LAI is often used for energy modeling. LAI is defined as the ratio of total leaf area (m^2) to ground area (m^2). The crops grow to their maximum extent during the mid-season; therefore, most studies assume the LAI and crop coefficient for the mid-season. The reference crop evapotranspiration (ET_o) is

estimated using the Stanghellini model suitable for closed greenhouses where the wind speeds are typically less than 1 m/s (Pamungkas *et.al.*, 2014) and is given by equation (3-7).

$$ET_o = 2 \times LAI \times \frac{1}{\lambda} \times \frac{s \times (R_n - G) + K_t \frac{VPD \times \rho \times C_p}{r_a}}{s + \gamma \left(1 + \frac{r_c}{r_a}\right)} \dots\dots\dots (3 - 7)$$

The reference crop evapotranspiration (ET_o) represents the evapotranspiration from a standard vegetated surface under specific conditions. To calculate the actual evapotranspiration rate (ET_{actual}) within the greenhouse, the crop coefficient (K_c) is multiplied by the reference evapotranspiration rate given by equation (3-8). The crop coefficient for mid-season conditions is around 1.10 ± 0.04 (Pamungkas *et.al.*, 2014). Table 3-2 provides the symbols, relationships, and units for each parameter used in the Stanghellini model.

$$ET_{actual} = K_c \times ET_o \dots\dots\dots (3 - 8)$$

Table 3-2 List of parameters, symbols, and formulas used for determining ET_o using the Stanghellini model.

Parameters	Symbol	Formula	Units	References
Saturation vapor pressure	e_s	$e_s = 0.61078 \times \exp\left(\frac{17.269 T}{237.3 + T}\right)$	kPa	Pamungkas <i>et. al.</i> , (2014)
Actual vapor pressure	e_a	$e_a = \frac{e_s \times RH}{100}$		
Vapor pressure deficit	VPD	$VPD = e_s - e_a$		
Slope of the saturation vapor pressure curve	s	$s = 0.04145 \times \exp^{(0.06088.T)}$	kPa/°C	
Atmospheric pressure	P	$P = 101.325$	kPa	-
Latent heat of vaporization	λ	$\lambda = 2.26$	MJ/kg	-
Specific heat of air	C_p	$C_p = 0.001013$	MJ/kg °C	Pamungkas <i>et. al.</i> , (2014)
Psychrometric constant	γ	$\gamma = \frac{C_p P}{\epsilon \lambda}$	kPa/°C	Donatelli <i>et. al.</i> , (2005)

Atmospheric density	ρ	$\rho = 1.204$	kg/m^3	-
Leaf Temperature	T_o	$T_o = 2.52 + (0.84 \times T) + (-0.54 \times \text{VPD})$	$^{\circ}\text{C}$	Pamungkas <i>et. al.</i> , (2014)
Canopy resistance	r_c	$r_c = \frac{100}{0.5 \times \text{LAI}}$	s/m	
Aerodynamics resistance	r_a	$r_a = \frac{665}{1 + 0.54 \times U}$		Donatelli <i>et. al.</i> , (2005)
Net radiation	R_n	$R_n = R_{ns} - R_{nl}$	MJ/m ² /hr	Pamungkas <i>et. al.</i> , (2014)
Net shortwave radiation	R_{ns}	$R_{ns} = (0.07 \times \text{GLSR})/1000/\text{CA}$		
Net outgoing longwave radiation	R_{nl}	$R_{nl} = \frac{(0.16)(3600) \rho \times C_p \times (T - T_o)}{r_R}$		
Radiative resistance	r_R	$r_R = \frac{\rho \times C_p}{4 \times \sigma(T + 273.16)^3}$	s/m	
Emissivity	ϵ	$\epsilon = 0.622$	-	
Specific gas constant	R	$R = 287$	J/kg K	
Stefan-Boltzmann constant	σ	$\sigma = 5.669 \times 10^{-14}$	MJ/ K ⁴ m ² s	

The soil heat flux (G) is considered negligible for greenhouses due to the absence of any open area (Pamungkas *et. al.*, 2014). Hourly inputs such as temperature (T), relative humidity (RH), ground-level solar radiation (GLSR), and inside air velocity (U), along with leaf area index (LAI) and crop coefficient (k_c) are necessary inputs to model the hourly evapotranspiration rate. Finally, the evapotranspiration convective heat flux \dot{Q}_{EVT} from the plants is given by the equation (3-9) (Choab *et. al.*, 2021):

$$\dot{Q}_{\text{evt}} = \text{ET}_{\text{actual}} \cdot \lambda \cdot \text{CA} \dots\dots\dots (3-9)$$

where,

$\text{ET}_{\text{actual}}$ is the actual evapotranspiration rate in kg/m² hr.

λ is the latent heat of vaporization in kJ/kg.

CA is the canopy area in m².

3.3.6 Infiltration

Infiltration is defined as the unintentional air movement between the interior of the building and the outdoor environment from opening or holes in the greenhouse envelope. This may occur due to the pressure differential between the internal and the external environment. A study identified the infiltration rates of a newly constructed conventional greenhouse and a PSG ranging from 5.63 to 5.92 ACH (Red River College, 2015). This indicates that infiltration tends to reduce greenhouse efficiency by allowing cooler outside air to enter through openings, thereby increasing the heat loads and decreasing the cooling loads. Depending on factors like air tightness, wind speed, and temperature gradient between the inside and outside air, infiltration accounts for about 20% of total heat loss from a greenhouse (Jolliet *et. al.*, 1991), indicating the necessity to model infiltration. The total infiltration gain \dot{Q}_{inf} can be found by equation (3-10) (Ahamed *et. al.*, 2018).

$$\dot{Q}_{inf} = \dot{V} \rho C_p (T_{outside} - T_{air}) \dots\dots\dots (3-10)$$

where,

\dot{V} is the air exchange rate through infiltration in m³/hr

ρ is the air density in kg/m³

C_p is the specific heat capacity of air in kJ/kg °C

$T_{outside}$ is the outside ambient air temperature in °C

T_{air} is the internal air temperature in °C

3.3.7 Energy-efficiency features

Energy-efficient parameters are implemented within the greenhouse to create an optimal environment for plant growth. Furthermore, the integration of various energy-saving techniques such as thermal curtains, shade curtains, supplemental heating and cooling, thermal storage, and ventilation are among the most prevalent strategies employed. Implementation of additional energy-efficient strategies depends upon the level of advancements and innovations present within the greenhouse environment. Guidelines for modeling the following energy efficiency features are as follows:

3.3.7.1 Thermal and Shade Curtains

Thermal and shade curtains are often installed on greenhouse glazing to provide resistance to heat flow (Santolini *et. al.*, 2022). Thermal curtains are used at night while shade curtains are used during the day to optimize the energy demand of a greenhouse. Three key parameters are essential for modeling these curtains:

- additional thermal resistance depending on the curtain materials, such as fabric, metals, or plastic,
- location relative to the glazing,
- balanced operation schedule.

3.3.7.2 Supplemental Heating and Cooling

Excessive heat losses at night or heat gained during the day pose a potential threat to the crops, due to which supplemental heating or cooling is required to maintain the greenhouse air temperature. The energy modeling for the supplemental systems involves:

- the source capacity,
- set-point temperature,
- operational schedule.

When the greenhouse's air temperature goes above the upper set-point or below the lower set-point, either supplemental cooling or heating is activated to maintain optimal temperature inside the greenhouse. Sometimes, the upper set point temperature is maintained by natural ventilation i.e. opening of vents to allow cooler air to enter the greenhouse. However, ventilation does not provide precise control over temperature limits which may disturb the thermal environment of the greenhouse.

3.3.7.3 Thermal Storage

Thermal storage is installed in greenhouses to capture the surplus heat during the day and release this heat to the greenhouse air to maintain optimal temperature at night with minimal or no supplemental heating. Thermal storage walls, phase change material, rock bed storage, water barrels, and more are commonly used thermal storage systems in a greenhouse (Nauta *et. al.*, 2022). To model the thermal storage systems, below parameters must be included:

- the physical dimension of the storage (height, width, and thickness),
- the thermal properties (conductivity, specific capacitance, absorptance, and

emittance),

- Inputs like greenhouse air temperature, total, and beam radiation reaching the surface of the thermal storage, angle of incidence, and inside air velocity are required to calculate heat absorbed by the thermal storage.

This stored energy flows to the greenhouse space acting as a heat gain to the greenhouse air at night.

3.3.7.4 Ventilation

Ventilation classified into natural and forced ventilation is essential to control high temperature, moisture levels, and CO₂ levels inside the greenhouse for good crop production. Natural ventilation supplies fresh air inside the greenhouse without the use of any mechanical systems. It depends on the external wind pressures and the inside and outside temperatures. On the other hand, forced ventilation uses fan assemblies to bring the outside air inside the greenhouse through controlled openings. Cooler air from outside enters the greenhouse to reduce the cooling demand and creates a more uniform distribution of heat, which prevents the accumulation of hot air near the plants. Natural ventilation has a limitation during the summer months when the temperature gradient between inside and outside air is not significant, and the need for ventilation is the greatest.

Ventilation requires the below parameters to be modeled:

- sizing of fan assemblies in case of forced ventilation,
- location and size of inlets and outlets,
- operation schedule for the ventilation system.
- opening percentage to the ventilation vents.

The ventilation gain \dot{Q}_{vent} is given by equation (3-11) (TRNSYS-18 Multizone Building, 2021).

$$\dot{Q}_{vent} = \dot{V} \rho C_p (T_{vent} - T_{air}) \dots\dots\dots (3-11)$$

where,

\dot{V} is the air exchange rate through ventilation in m³/hr

ρ is the air density in kg/m³

C_p is the specific heat capacity of air in kJ/kg °C

T_{vent} is the ventilation air temperature in °C

T_{air} is the internal air temperature in °C

Once the modeling of individual components and the connections between them are accomplished, the simulation should be executed. The outputs after the simulation should be compared with the recorded values to observe the accuracy and the performance of modeling to be quantitatively evaluated using statistical measurements such as root mean square error (RMSE), average predicted or percent error, and mean absolute error (MAE). These parameters were calculated using equations (3-12), (3-13), and (3-14).

$$\text{RMSE} = \sqrt{\frac{\sum(y_m - y_s)^2}{n}} \dots\dots\dots (3 - 12)$$

$$\text{Average Prediction Error} = \frac{(y_{\text{am}} - y_{\text{as}})}{y_{\text{am}}} \times 100 \dots\dots\dots (3 - 13)$$

$$\text{MAE} = \frac{\sum|y_m - y_s|}{n} \dots\dots\dots (3 - 14)$$

where y_m and y_{am} are the measured and average measured data, y_s and y_{as} are the simulated and average simulated data, and n is the number of data points.

3.4 A Case Study on Chinese Solar Greenhouse (CSG)

A commercial mono-slope solar greenhouse is located in Elie, Manitoba (49° 55' N and 97° 28' W) with a local elevation of 239 meters. The measured dataset used for validation covers the period from 28th March 2017 to 30th March 2017 (Ahamed *et. al.*, 2018). Various sources were consulted to gather information on the greenhouse's specifications. The structure of the experimental CSG in Elie, Manitoba is illustrated in Figure 3-3.



Figure 3-3 Experimental mono-slope Chinese solar greenhouse in Elie, Manitoba.

Note. The image was reprinted from a thesis for Master of Science. From “Dong, S., (2018) “Thermal environment modeling of the mono-slope solar greenhouse for cold regions,” [Thesis for Master of Science, University of Saskatchewan].

3.4.1 Dimensions of CSG

The CSG was east-west oriented where young tomato plants with a 14 cm height were grown in wet soil. The ground had soil with no cover (Dong, 2018). Table 3-3 provides the dimensions of the CSG.

Table 3-3 Dimensions of CSG in Elie, Manitoba.

Parameters	Values	References
Length	30 m	Ahamed <i>et. al.</i> , 2019
Breadth	7 m	
Footprint Area	210 m ²	
North wall height	2.1 m	Ahamed <i>et. al.</i> , 2018
Ridge height	3.5 m	Dong <i>et. al.</i> , 2021
Angle of glazing near the ground (up to 1 m height)	60°	Ahamed <i>et. al.</i> , 2019
Angle of glazing for the rest of the section	26°	
Angle for north roof	34°	

3.4.2 Construction material for CSG

The materials used for constructing this experimental greenhouse are detailed in Table 3-4. The construction of the north wall included fiberglass insulation strategically installed to minimize heat transfer, along with sand, chosen for its high specific heat storage capacity to store heat (Dong, 2018).

Table 3-4 Material of construction for CSG in Elie, Manitoba.

Surfaces	Material of construction	Thickness	References
South glazing	Single-layer Polyethylene film	0.152 mm	Dong <i>et. al.</i> , 2021
North wall	Corrugated galvanized sheet steel (External)	2 mm	Dong, 2018
	Fiberglass insulation	152 mm	
	Plywood	13 mm	
	Sand	152 mm	
	Corrugated galvanized sheet steel (Internal)	2 mm	
North Roof, East and West Wall	Corrugated galvanized sheet steel (External)	2 mm	Dong, 2018; Dong <i>et. al.</i> , 2021
	Fiberglass insulation	152 mm	
	Plywood	13 mm	
	Plastic film (Internal)	2 mm	
Floor/ Soil	Clay	100 mm	Ahamed <i>et. al.</i> , 2019

3.4.3 Energy-efficiency features for CSG

The CSG incorporated energy-efficient parameters to regulate the indoor air temperature, ensuring optimal conditions for tomato plant growth, especially during nighttime. Table 3-5 outlines the energy-efficient parameters integrated into the CSG.

Table 3-5 Energy-efficiency features considered for CSG in Elie, Manitoba.

Energy-efficient parameters	Material	Values	Schedule	Reference
Thermal blanket	Cotton	1.2 m ² K/W	18:00 – 9:00	Beshada <i>et. al.</i> , 2006
Electric heater	-	3.6 kW	18:00 – 8:30	Dong, 2018
		1.876 kW	8:30 – 9:00	
Ventilation through ridge roof	-	0.156 m ³ /s	8:00-11:00	
		0.521 m ³ /s	11:00-13:00	

		0.573 m ³ /s	13:00-14:30	
		0.156 m ³ /s	14:30-17:00	
Thermal storage	Sand	-	-	Beshada <i>et. al.</i> , 2006

3.4.4 Monitored parameters inside the CSG

The hourly weather data for this location including ambient air temperature, relative humidity, wind speed, and global solar radiation, were recorded every 10 minutes using a portable weather station positioned near the greenhouse (Ahamed *et. al.*, 2018). Indoor air temperature, soil temperature, and north wall temperature were also recorded every 10 minutes (Beshada *et. al.*, 2006). Table 3-6 specifies the location of the sensors used to measure these parameters within the CSG.

Table 3-6 Sensor location for measuring monitored parameters inside the CSG in Elie, Manitoba.

Sensors	Location	Reference
Indoor temperature sensor	122 cm above ground level	Dong, 2018
Relative humidity sensor		
Soil temperature sensor – 2 quantities	5 cm under the ground surface	
	214 cm away from the north wall	
Wall Temperature sensor – 2 quantities	76 cm above the bottom of the north wall surface	

3.5 Demonstration of the Framework

TRNSYS was selected to simulate the above greenhouse due to its wide accessibility, and user-friendly simulation platform known for its accuracy and low computational times. It can produce diverse outputs including temperatures, relative humidity, and heating and cooling loads. TRNSYS also offers various extensions, such as SketchUp software, TRNBuild, TRNFlow, and various sub-models to account for factors like ventilation, infiltration, thermal curtains, evapotranspiration, thermal storage, and more. Based on the energy modeling framework mentioned in section 3.3, the validation process was divided into six categories: (3.5.1) Greenhouse model development (3.5.2) Weather and initial data for simulation; (3.5.3) Greenhouse construction material; (3.5.4) Solar radiation distribution; (3.5.5) Evapotranspiration; (3.5.6) Energy-efficiency features including thermal curtain, supplemental heat, thermal storage wall, and natural ventilation.

3.5.1 Greenhouse Model Development

The experimental greenhouse model was developed using Google SketchUp because TRNSYS software can automatically read the geometric information provided by this software. Google SketchUp employs a plug-in known as Trnsys3d, which efficiently generates geometric designs for building models. It is crucial to create Trnsys3d zones within the SketchUp model, as they facilitate the simulation of dynamic energy flow (Hiller & Kendel, 2023). Utilizing the tools available within the SketchUp module, the experimental greenhouse model was constructed inside the Trnsys3d zone. Trnsys3d enables the creation of fenestration objects directly within the SketchUp software. Consequently, the glazing for this CSG was developed in SketchUp accounting for approximately 98% of the total wall and roof area. Figure 3-4 depicts the greenhouse model created using SketchUp software, highlighting the glazing on the south side.

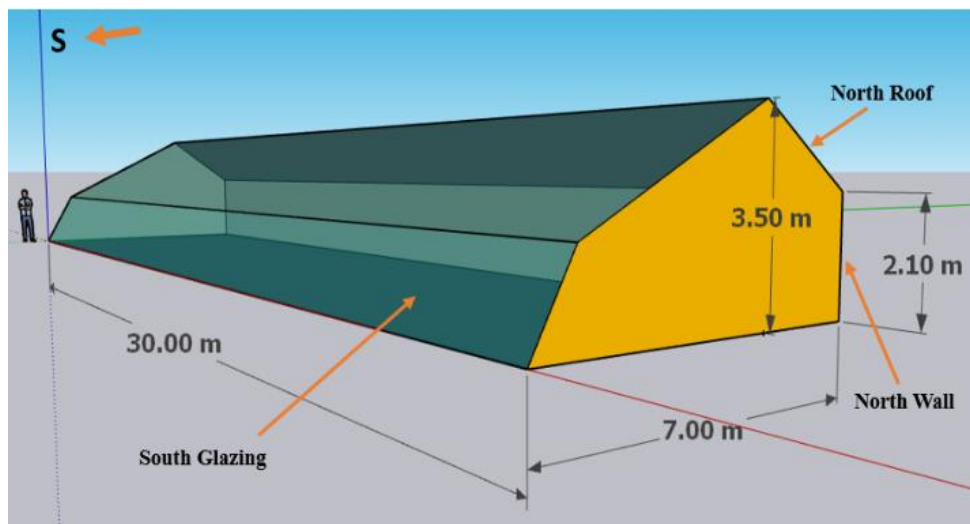


Figure 3-4 Experimental Chinese solar greenhouse model designed using SketchUp software

The greenhouse model from SketchUp was transferred to an integrated tool known as TRNSYS simulation studio, which was used from the project design to the simulation. The interface of the simulation studio consists of many interrelated components that transfer inputs and outputs from one another. A schematic layout as shown in Figure 3-5, was developed for the TRNSYS simulation, encompassing components such as weather data, radiation unit converter, multi-zone building components, evapotranspiration, thermal storage wall, plotters, integrator, and printer.

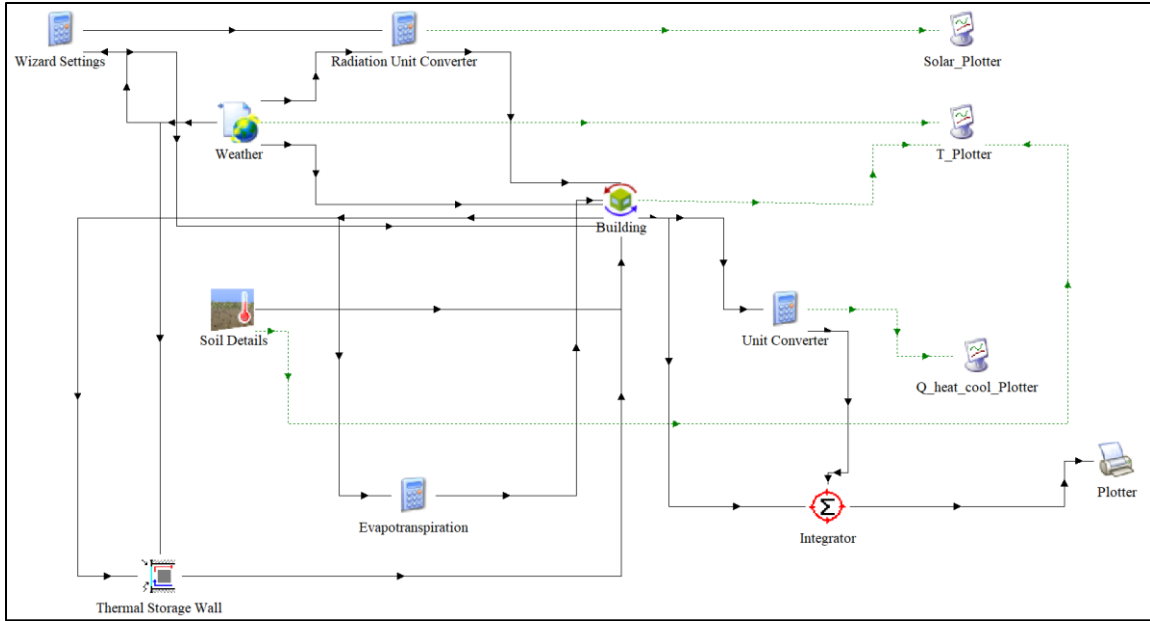


Figure 3-5 Schematic layout of simulation studio representing inputs and outputs connection for each component.

3.5.2 Weather and initial data for simulation

The weather component in TRNSYS software can read standard weather data formats or user-supplied data files. However, the limitation of this study was that the user-defined weather data for Elie, Manitoba for the year 2017, available from the Government of Canada website (Government of Canada) had missing/unobserved weather parameters. Therefore, in the absence of user-defined weather inputs a standard weather data format was used. Type-15 weather component in TRNSYS processes the standard files and includes modes for TRNSYS TMY, TMY2, TMY3, EPW, IWEC, CWEC, Meteonorm, and German TRY (TRNSYS-18 Weather data, 2017). These files contain generated values from a data bank for a specific location of a minimum of 12 years (Typical Meteorological Year, 2024). The process of identifying an accurate standard weather file for the experimental CSG in Elie, Manitoba for March 2017 involved locating the nearest weather station to this greenhouse. The Winnipeg Richardson International Airport station was identified, and all the weather data available for this location was collected (Environment Canada; Climate.OneBuilding). The datasets under consideration represent the average values observed across multiple years which involved the TMY dataset covering the period from 2007 to 2021, and the CWEC dataset spanning from 2000 to 2017. To ensure the most accurate weather data was used for the simulation, both datasets were compared with

the measured values. However, the comparison for only the CWEC dataset was shown because it matched closely for all the weather parameters. The weather parameters such as measured ambient temperature and CWEC ambient temperature, measured relative humidity and the CWEC relative humidity, measured wind speed and the CWEC wind speed, and measured solar irradiance and CWEC solar irradiance were compared as shown in Figure 3-6.

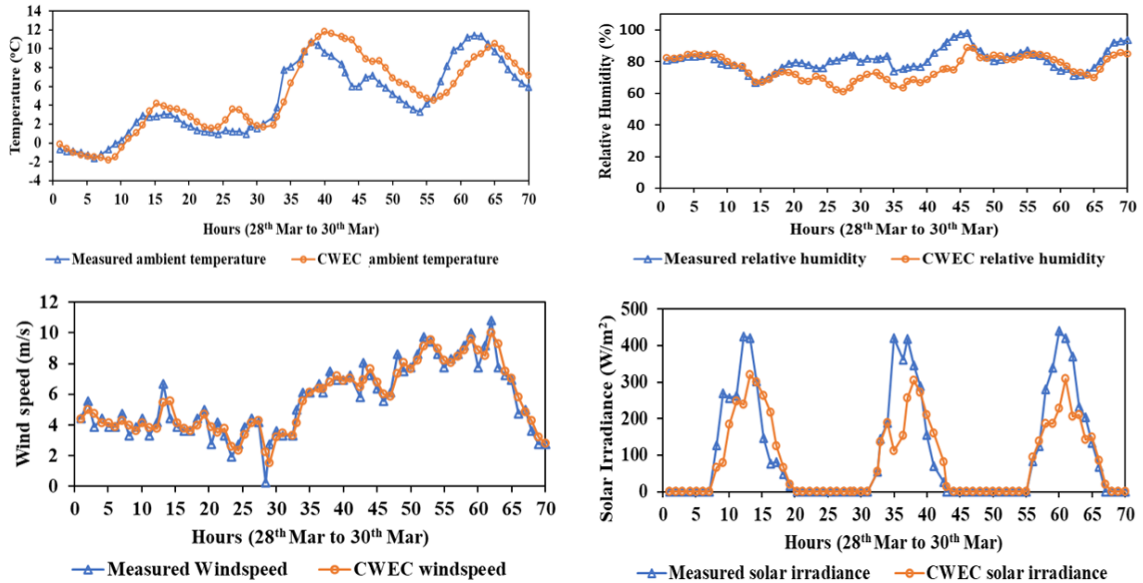


Figure 3-6 Comparison of the measured weather parameters with the CWEC dataset weather parameters from 28th March 2017 to 30th March 2017. (a) Measured ambient temperature versus CWEC ambient temperature; (b) Measured relative humidity versus CWEC relative humidity; (c) Measured wind speed versus CWEC wind speed; (d) Measured solar irradiance versus CWEC solar irradiance.

The temperature profile showed some deviations during certain hours within the considered time as indicated in Figure 3-6a. Figures 3-6b and 3-6c indicate minimal differences in the recorded values. However, significant discrepancies were observed for solar radiation (Figure 3-6d). This was because these were average values over the years rather than specific values for the year 2017. Table 3-7 illustrates the RMSE, mean value, and total value for ambient temperature, relative humidity, wind speed, and solar irradiance. After analyzing these four weather parameters, it was concluded that the CWEC dataset (2000-2017) was the most accurate weather file for the year 2017.

Table 3-7 Comparison of mean, total, and RMSE values for different CWEC weather parameters

Weather Parameters	RMSE	Mean Value	Total Value
Measured Ambient Temperature	-	4.5 °C	-
CWEC Ambient Temperature	1.3 °C	5 °C	-
Measured Relative Humidity	-	81.5 %	-
CWEC Relative Humidity	8.7 %	76.1 %	-
Measured Wind Speed	-	5.540 m/s	-
CWEC Wind Speed	0.6 m/s	5.548 m/s	-
Measured Solar Irradiance	-	-	7606 W/m ²
CWEC Solar Irradiance	77 W/m ²	-	6022 W/m ²

Finally, the selected CWEC dataset was in EnergyPlus format (.epw) which was compatible with the Type 15-3 weather component. TRNSYS also requires the initial values of temperature and relative humidity for simulation within the type-56 component. These initial values were assumed to be average values of the measured inside temperature and measured inside relative humidity, which were 19.7 °C and 70% respectively.

3.5.3 Greenhouse Construction Material

In TRNSYS software, type-56, or the multi-zone building component was used to model the materials on walls and glazing on the south side. Type-56 consists of a separate pre-possessing program known as TRNBuild. TRNBuild reads and processes the file containing the building description developed by the SketchUp software and generates an information file describing the outputs and required inputs for type 56 (TRNSYS-18 Multizone Building, 2021). The layers of material were created using the thermal properties of materials (conductivity, density, and specific heat) in TRNBuild, and then combined with respective thicknesses to form opaque walls, roofs, or floors. The south glazing of the experimental greenhouse was made up of a single polyethylene layer for which the optical and thermal properties were defined using the Lawrence Berkeley National Lab Window program. A DOE-2 file was then created and added to the TRNBuild. Table 3-8 represents the thermal properties of different materials used in the TRNSYS software for thermal simulation.

Table 3-8 Thermal properties of different walls, ground, and windows used in TRNSYS software simulations.

Materials	CGSS	Fiberglass	Plywood	Sand	Plastic film	Polyethylene film	Soil
Thickness (mm)	2	152	13	152	2	0.18	100
Density (kg/m ³)	7830	14	460	2240	900	-	1100
Conductivity (kJ/hr m K)	163.08	0.14	0.334	3.31	19.8	-	1.98
Specific heat (kJ/kg K)	0.5	0.8	1.88	0.84	1.9	-	1
Solar Radiation Transmissivity	-	-	-	-	-	0.88	-
U- value (W/m ² K)	-	-	-	-	-	5.56	2.84
g- value	-	-	-	-	-	0.89	-
Visible light transmittance	-	-	-	-	-	0.91	-
References	Dong, 2018					Ahamed <i>et. al.</i> , 2019	

This component creates greenhouse inputs and defines the desired outputs from the simulation. Inputs such as weather output, soil detail, thermal curtain, ventilation, and others were connected with the greenhouse parameters, providing information every hour. This component calls for regime types, including information regarding infiltration, ventilation, heating, cooling, and gain/loss in the greenhouse, which are elaborated in the subsequent sections. The outputs from the greenhouse were connected to the unit converter to convert them into the desired units, which were then sent to the integrator (Type-55) to integrate them over an hour and finally print the output values from the printer (Type-25 c).

3.5.4 Solar Radiation Distribution

This section models the solar distribution on the different surfaces and internal air of the greenhouse. A radiation unit converter was used to convert the total solar radiation and beam radiation from kJ/hr.m² to W/m², as well as to calculate the azimuth angle and angle of incidence for different surfaces. This converter receives inputs from the weather file,

converts and calculates the respective values, and then provides outputs to the multi-zone building component. In TRNSYS, beam solar radiation was modeled using a detailed approach that uses shading and insolation matrices to distribute the primary direct solar radiation entering the greenhouse. These matrices were based on three-dimensional data of the building and shading surfaces, generated by an auxiliary program known as TRNSHD (Hiller *et. al.*, 2000). Additionally, shortwave diffuse radiation and longwave radiation exchange including multi-reflection were distributed using a view factor matrix, which was generated by another auxiliary program known as TRNVFM (TRNSYS-18 Multizone Building, 2021). However, for TRNSYS to run these models in a detailed mode, the zone must be a convex and closed volume which means that every surface within the zone must be in the line of sight with all other zone surfaces (no obstructed views) (TRNSYS-18 Multizone Building, 2021).

TRNSYS also accounts for a factor in calculating the amount of solar heat added to the greenhouse air. Solar-to-air factor (f_{solair}) represents the fraction of solar heat entering the greenhouse air volume through the glazing that is immediately transferred as a convective gain to the internal air (TRNSYS-18 Multizone Building, 2021). This factor was important for TRNSYS simulation as it significantly affects energy demand. The fraction may vary from 0 to 1. A study by Imafidon *et. al.*, (2023) indicated that increasing this factor from 0 to 1, reduced the deviation in the daily temperature variation between the simulated and measured data. Many studies use TRNSYS for energy simulation, however, no study focused on the estimation of this factor. Therefore, it was crucial to understand the correct range of f_{solair} so that it could be accurately used for the simulation. The solar-to-air factor depends on the quantity of internal items with very low thermal capacity, such as furniture because the presence of such materials will lead this fraction closer to 1, indicating more heat is added to the internal air. However, the experimental greenhouse consists of plants and thermal storage, both with high thermal capacity to absorb more heat. This suggests that the value of f_{solair} would not be close to 1 for this type of experimental greenhouse. Consequently, to identify the correct range of f_{solair} , it was varied in the interval of 0.2 to determine the values that most closely match the recorded data.

3.5.5 Evapotranspiration

Evapotranspiration (EVT) was complicated to be modeled because of the dynamic nature of plants. Since the CSG was closed, the hourly evapotranspiration rate was estimated using the Stanghellini model. TRNSYS software modeled evapotranspiration using a sub-component that takes hourly inputs like inside air temperature, relative humidity, incoming shortwave solar radiation on the ground, and inside air velocity from the type-56 component to calculate the parameters used in equation (3-7) using Table 3-2. The values for LAI and wind velocity were considered from the study by Ahamed *et. al.*, (2018). The LAI of tomato crops was considered as $1 \text{ m}^2/\text{m}^2$ because the plants were young during the measuring period. Finally, the evapotranspiration heat loss was calculated using equation (3-8) and provided input to the type-56 component. Since evapotranspiration results in heat loss from the greenhouse environment, it was integrated as a loss into the “Gain/loss type” manager to account for the heat loss. At last, the evapotranspiration loss was added to the simulation under airnode regime data.

3.5.6 Energy-efficiency features

Energy-efficient parameters relevant to the experimental greenhouse were considered for the energy modeling. These include the installation of a thermal curtain, supplemental heating, a thermal storage wall, and natural ventilation.

3.5.6.1 Thermal Curtain

The resistance of the thermal curtain, its location, and the operational schedule were modeled within the type-56 component under the “Window Type” manager. Since the thermal curtain was employed externally in the experimental greenhouse, an additional external thermal resistance of $0.334 \text{ h m}^2 \text{ K/kJ}$ (as mentioned in Table 3-5) was added manually to the south glazing. A daily schedule was defined for the thermal curtain based on the schedule mentioned in Table 3-5 using the “Schedule Type” manager within the TRNBuild. The value was set to ‘1’ when the thermal curtain was completely employed, and ‘0’ when not employed. TRNSYS reads the inputs for this thermal curtain when it was selected in the airnode regime data, and the value for the shade factor was assigned from the schedule.

3.5.6.2 Supplemental Heat

The supplemental heating provided by an electric heater of capacity 3.6 kW was modeled using the “Heating Type” manager under the regime types. The set-point temperature control was set at 18 °C (Dong *et. al.*, 2021). Additionally, an operational schedule was defined for an electric heater in the TRNBuild using the “Schedule Type” manager. The schedule was based on the literature provided in Table 3-5. The value was set to ‘1’ when the electric heater was working at full capacity, ‘0.5’ when working at half capacity, and ‘0’ when the electric heater was off. This schedule came into action when the schedule was integrated into the “Heating Type” manager for limited sensible heating power, where the schedule was multiplied by the heater’s capacity of 12960 kJ/hr. Finally, the heating feature was set to “ON” under the airnode regime data.

3.5.6.3 Thermal Storage Wall

The thermal wall storage was modeled on the north wall by adding the physical dimensions (height, width, and thickness), and the thermal properties (conductivity, specific capacitance, absorptance, and emittance). The thermal storage wall was modeled using a type-36 d component, connected to the weather and type-56 components. The weather data provided inputs such as ambient temperature, wind velocity, and angle of incidence, while the type-56 component supplied the hourly greenhouse air temperature, total, and beam radiation reaching the north wall surface. The type-36 d component calculates the energy flowing to the room and provides input to the type-56 component, acting as a heat gain to the greenhouse air. Consequently, a gain was created in the “Gain/loss type” manager to account for the heat gain from the north wall. Finally, the thermal storage wall gain was added to the simulation under airnode regime data. The heat storage in the side wall and the north roof of the CSGs was assumed negligible since their construction does not consist of sand for heat storage.

3.5.6.4 Natural Ventilation

An extension, known as TRNFlow was required to model natural ventilation. TRNFlow uses COMIS to model the airflow between the greenhouse and the environment (TRNFlow Manual, 2009). Cooling was not considered in the experimental greenhouse because the temperature was controlled through natural ventilation by opening a vent near the ridge (Ahamed *et. al.*, 2018). Dong (2018) made assumptions about the ventilation rates based

on indoor temperature fluctuation and CO₂ needs, as indicated in Table 5. However, the assumed ventilation rates indicated forced ventilation as it had a fixed schedule of operation, whereas natural ventilation varies every hour depending upon the temperature gradient and wind pressure. This posed a major challenge in modeling natural ventilation without any specific details. The first challenge was to identify the size of vents, which were assumed based on the recommendation provided by the American Society of Agricultural and Biological Engineers standards that the combined roof vent area should equal the combined sidewall vent area and each should be at least 15 to 20 percent of the floor area. For northern climates, 15% may suffice, but warmer climates require greater amounts (Bartok, 2015). As a good practice, a screen was installed on the vent to prevent insects from entering the greenhouse. Based on the minimum mesh size to exclude pests and screen availability, the screen size percentage was considered as 41% (The Mesh company). This resulted in an actual opening area for natural ventilation of 13 m². A large opening of 13 m by 1 m was created in TRNFlow. The vent was located near the ridge on the north roof. In TRNSYS it was necessary to define the airflow link, which was considered from the external environment to the greenhouse air volume (TRNFlow Manual, 2009). The opening factor was defined based on the assumption by Dong (2018), with a maximum opening factor of 1 during the peak ventilation rate of 0.573 m³/s, 0.9 during the ventilation rate of 0.521 m³/s, 0.27 during the ventilation rate of 0.156 m³/s, and 0 for all other times. TRNFlow also required inputs such as wind speed, wind direction, and outside temperature from the weather component, as well as internal air temperature from the type-56 component to calculate the hourly ventilation rates.

3.6 Results and Discussion

Once the modeling of individual components was done, the TRNSYS simulation was executed, to estimate the output values. This section shows the different analyses that were considered to study the variation in the measured and the simulated values. Firstly, it includes the study of solar-to-air factor (f_{solair}) to identify an appropriate range for greenhouses consisting of plants and thermal storage. Secondly, it involves the comparison of the simulated internal air temperature of the greenhouse with the measured temperature and the simulated and measured supplemental heat provided to the greenhouse. This is

followed by the comparison of the ground temperature and the north wall temperature to observe the deviation offered by the energy modeling process.

3.6.1 Estimation of solar-to-air factor (f_{solair})

The internal air temperature profile for measured and simulated data with different values of solar-to-air factor (f_{solair}) is shown in Figure 3-7. This factor was varied from 0 to 1 in the interval of 0.2 for the analysis. Since no study focused on the estimation of this factor for greenhouses, it was crucial to understand the importance of this factor in the energy simulation using TRNSYS software. As the value of f_{solair} increases from 0 to 1, the spike in temperature also increases during the daytime, whereas the temperature almost remains the same during the nighttime for all the cases as seen in Figure 3-7. With $f_{\text{solair}} = 0$, the internal air temperature values were underestimated providing a lower temperature graph as compared to the measured internal air temperature, which tends to increase the heating load of the greenhouse. However, the value of f_{solair} greater than 0.4, indicates that the temperature values were overestimated during the daytime providing a much higher temperature graph as compared to the measured internal air temperature which tends to increase the cooling load. The values of f_{solair} between 0.2 to 0.4 indicate a much closer compliance with the measured internal air temperature. Hence, it was concluded that the f_{solair} value for greenhouses consisting of plants and thermal storage can vary from 0.2 to 0.4. To estimate the temperature profiles of the greenhouse for later analysis, three cases were considered with $f_{\text{solair}} = 0.2$, $f_{\text{solair}} = 0.3$, and $f_{\text{solair}} = 0.4$ because $f_{\text{solair}} = 0.2$ had values slightly below the measured values and $f_{\text{solair}} = 0.4$ has values above the measured values. The energy modeling results for the indoor air temperature with $f_{\text{solair}} = 0.3$ showed much closer compliance to measured values. Therefore, $f_{\text{solair}} = 0.3$ was used for the estimation of other output parameters.

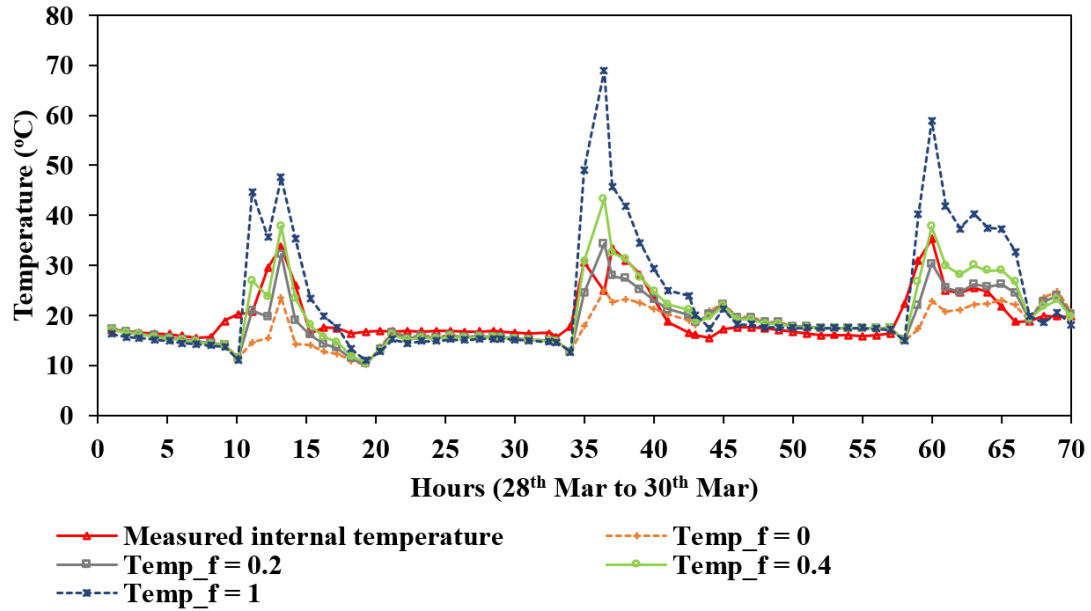


Figure 3-7 Comparison of measured internal air temperature with the simulated internal air temperature profiles for different values of solar-to-air factor (f_{solair}).

Note: The temperature profile for $f_{solair} = 0.6$ and $f_{solair} = 0.8$ was also studied and lies between the temperature profile $f_{solair} = 0.4$ and $f_{solair} = 1$, however, it was not included to maintain clarity in the figure.

3.6.2 Comparison of internal air temperature

The comparison between the measured internal air temperature with the simulated internal air temperature is illustrated in Figure 3-8. The graph shows that the simulated internal air temperature was in close compliance with the measured internal air temperature with $f_{solair} = 0.3$. During the early hours of 28th March, the temperature drops below 15 °C because ambient air temperature falls below 0 °C, leading to more conduction heat loss in the environment. However, during the nighttime, less fluctuation in indoor air temperature can be observed because of the thermal storage wall and thermal curtain. A spike in the indoor air temperature was observed during the daytime over all three days, caused by solar radiation entering the CSG through the south glazing and increasing the internal air temperature. Also, it can be observed that between 15 hours to 20 hours on 28th March, the simulated internal air temperature drops to 10 °C. This could be probably because of the natural ventilation. As already indicated in the literature, growers manually open the vents to allow fresh air to enter the greenhouse, whenever it was required. However, during the simulation, a daily schedule was added to open the vents. Even when the temperature was

not that high during that hour on 28th March, the vent was open because of the schedule and cooler air entered the greenhouse due to which the internal air temperature dropped.

The average value of the measured indoor temperature was 19.7 °C closely matching the simulated average indoor temperature of 19.4 °C. The mean absolute error (MAE) and root mean square error (RMSE) for the indoor air temperature were 2.4 °C and 3.1 °C, respectively, despite the assumption developed for natural ventilation and average weather inputs. Dong (2018) also validated the SOGREEN model with this experimental greenhouse, where the study recorded an average temperature difference of approximately 9.6%. However, the result from this simulation illustrates that the average prediction error in the internal air temperature was just 1.6 %. This leads to an important conclusion that this greenhouse energy model accurately predicted the temperature variation in an experimental greenhouse. However, the results were validated for only three days in March due to the limited availability of measured data during that year. Therefore, validation across different seasons was not conducted. Moreover, similar patterns were observed during both summer and winter, with trends remaining consistent throughout the day and night when the simulations were performed for a complete year.

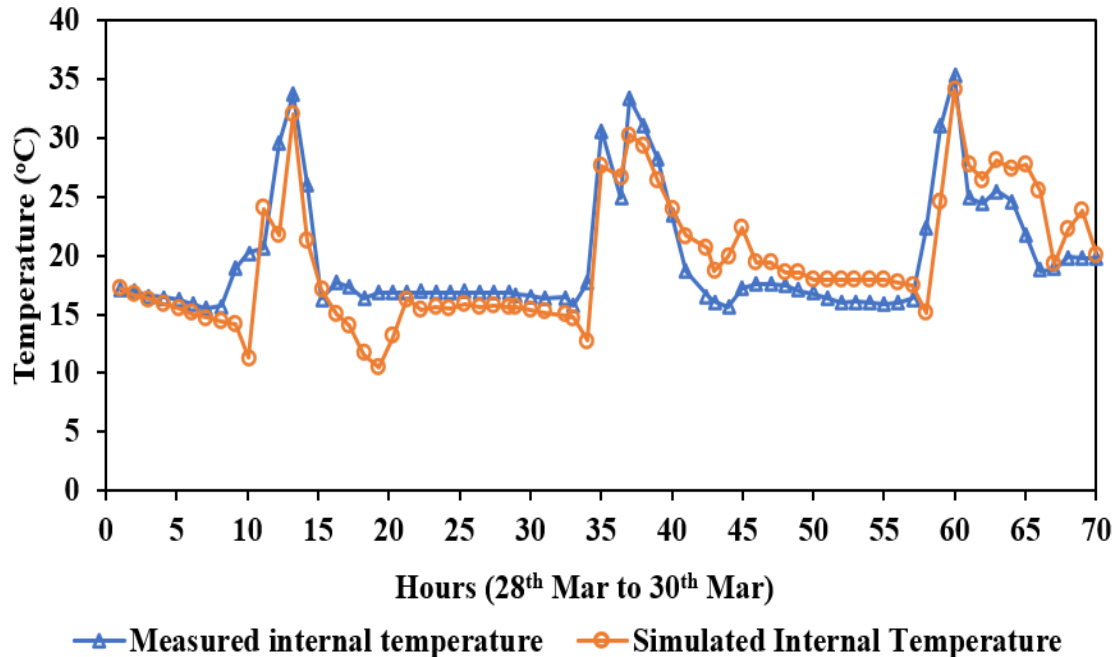


Figure 3-8 Comparison of measured internal air temperature with the simulated internal air temperature from 28th Mar 2017 to 30th Mar 2017.

3.6.3 Comparison of supplemental heating

The graph between the measured and simulated supplemental heat provided by an external electric heater is illustrated in Figure 3-9. A 3.6 kW electric heater was used every night to maintain optimal temperature inside CSG for tomato crop growth. The operation of this electric heater was controlled by a thermostat and would turn off when the temperature reached 18 °C (Dong *et. al.*, 2021). The supplemental heating requirements were accurately predicted by the greenhouse energy model from 28th March to 29th March with some deviations observed from 45 hours to 55 hours. This discrepancy in the heating load occurred because of the thermostat setting. As seen in Figure 3-8, the simulated internal air temperature of the greenhouse was more than 18 °C and gradually reduced to 16 °C for this period because of which the electric heater was turned off until the internal air temperature was 18 °C and then was gradually turned on when the temperature dropped below 18 °C. The total heat supplied by the electric heater from 28th March to 30th March was approximately 156 kWh for the measured supplemental heating and 110 kWh for simulated supplemental heating. The RMSE was approximately 1.4 kWh, and the MAE was 0.7 kWh. Ahamed *et. al.*, (2018) also studied this experimental greenhouse and compared it with the CSGHEAT model where discrepancies could be observed during the nighttime of 30th March. The percentage error recorded varies from 0.2% to 24.9%, and the average error was around 8.7% when the data for the night of 30th March was excluded from the analysis. However, the average prediction error of the current study was somewhat about 29 % for the complete period. Though this error was significant, it was most observed during some hours on 30th March due to thermostat settings and if the discrepancy due to thermostat setting was not accounted for, the error would reduce to 4.1%.

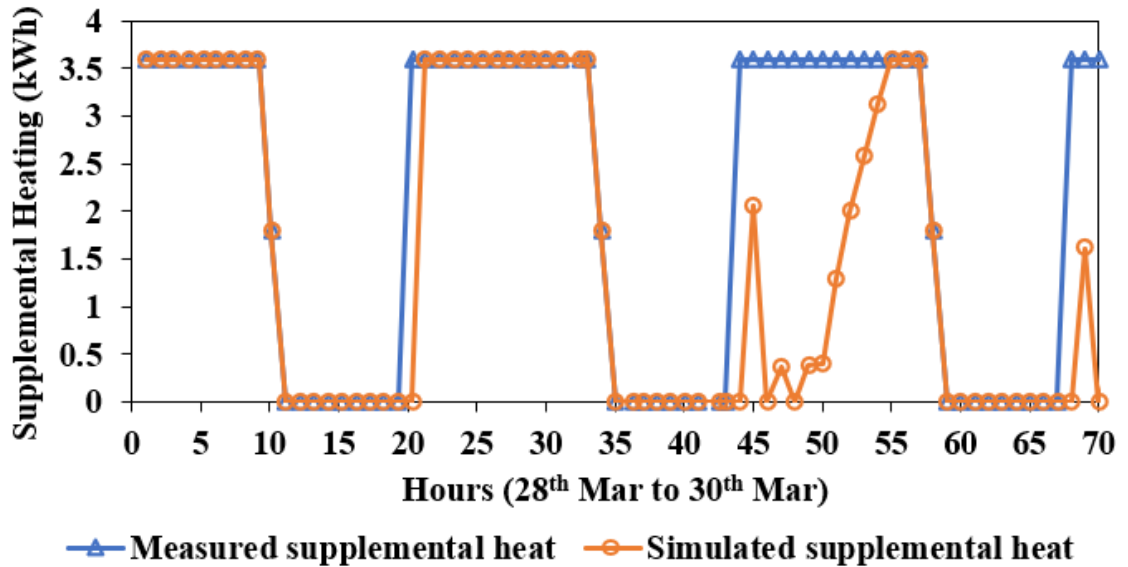


Figure 3-9 Comparison of measured supplemental heat with the simulated supplemental heat from 28th Mar 2017 to 30th Mar 2017.

3.6.4 Comparison of ground temperature:

The comparison of the measured ground temperature with the simulated ground temperature from 28th March 2017 to 30th March 2017 is indicated in Figure 3-10. It was observed that the simulated ground temperature shows the same trend as the measured ground temperature. However, there was a huge difference in estimating simulated temperature during the nighttime. This deviation in ground temperature may arise because of the differences in the thermal properties of the soil used in the simulation. Additionally, TRNSYS did not simulate the wet behavior of the soil as it was mentioned that the soil was wet with no cover (Dong, 2018). Secondly, the sensor was located 5 cm under the ground while measuring the temperature (Dong, 2018). However, in the greenhouse energy model using TRNSYS simulation, the temperature was calculated on the ground surface. It can be observed that the temperature rises as soon as solar radiation reaches the ground surface and drops because of conduction heat loss between the ground surface and the soil at night. TRNSYS software has a limitation, as it is designed for lumped body analysis i.e., it does not account for the temperature variation in the X and Y-axis. Ahamed *et. al.*, (2018) studied the variation in the ground temperature with a RMSE of 1.8 °C. The simulation for this study was performed without considering the greenhouse air exchange through the natural ventilation system. In this study with natural ventilation, the average measured value of the ground temperature was 19.8 °C and the simulated average value for this study

was 18.3 °C. The RMSE and the MAE were 6.4 °C and 5.6 °C respectively. The predicted error between the measured and simulated ground temperature was approximately 7.3%.

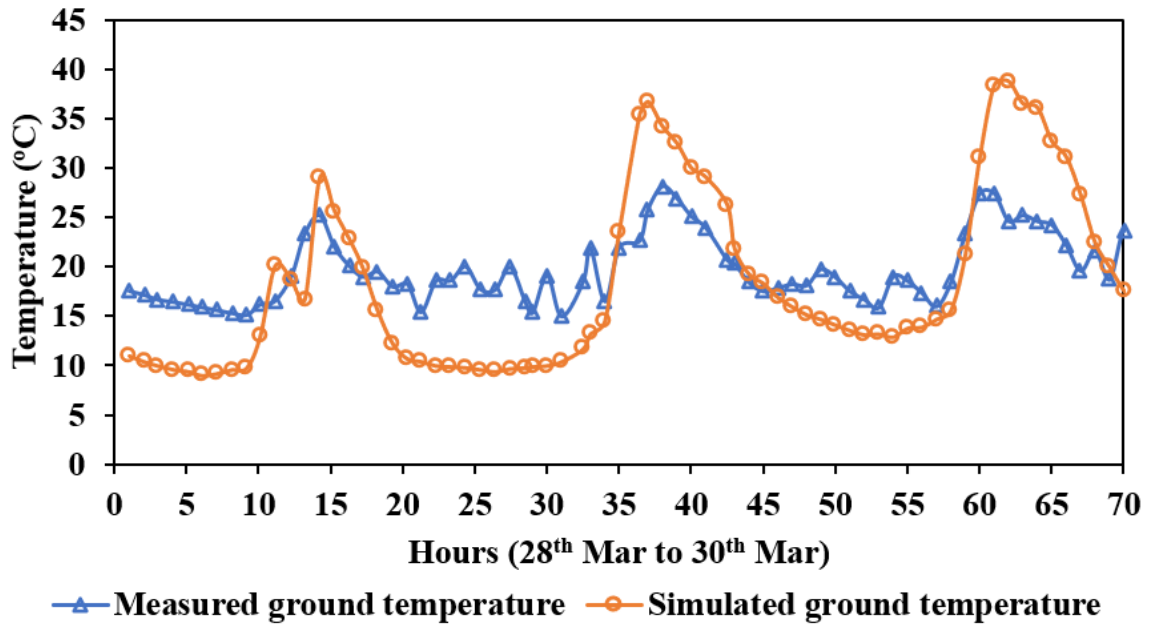


Figure 3-10 Comparison of measured ground temperature with the simulated ground temperature from 28th Mar 2017 to 30th Mar 2017.

3.6.5 Comparison of north wall temperature:

The difference between the measured and simulated north wall temperature is represented in Figure 3-11. It was clear from the graph that the simulated north wall temperature accurately predicts the measured values during some hours from 28th March to 30th March. Additionally, the greenhouse energy model results well predicted the peaks and valleys during the simulation period. The north wall temperature rises to above 30 °C during the daytime because it stores more heat during the day. However, the deviation was observed during the evening and nighttime for the 29th and 30th March. In the TRNSYS simulation, the energy gain by the internal greenhouse air from the north wall was gradual. However, the measured data shows a sharp reduction in the temperature. This may be due to the high wind speed and different wind directions in the actual weather conditions for the year 2017. This led to the increased heat loss from the north wall thereby maintaining slightly lower temperatures as compared to the simulated temperatures. The average measured value of the north wall temperature was 18.6 °C whereas the simulated average value was 21 °C. The RMSE and the mean absolute error were 4.3 °C and 3.5 °C respectively with a predicted error of about 13%. Dong (2018) predicted the north wall temperature with an

average discrepancy in the wall surface temperature of about 19.4%. In the study by Ahamed *et al.*, (2018), the RMSE in calculating the north wall temperature was estimated as 2.2 °C. This was because of the different modeling techniques and assumptions considered by each researcher.

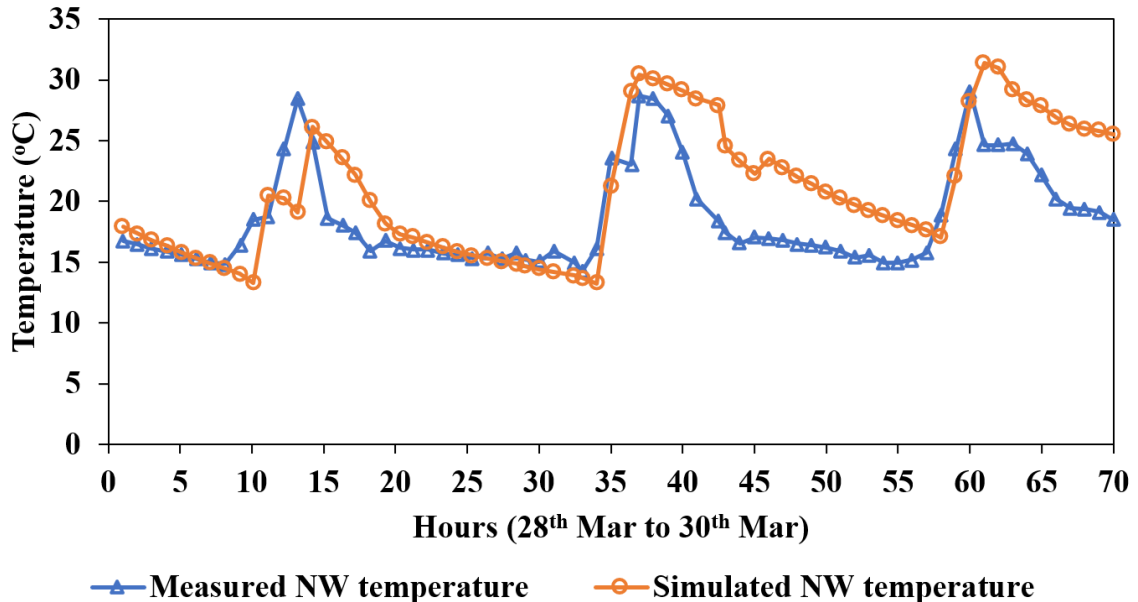


Figure 3-11 Comparison of measured north wall temperature with the simulated north wall temperature from 28th Mar 2017 to 30th Mar 2017.

3.7 Conclusion

The study demonstrated the importance of energy modeling for the greenhouse industry. Since no comprehensive guidelines or standards were available for greenhouse energy modeling, this study provided an in-depth energy modeling process for greenhouses. This study further used the mentioned energy modeling process to validate the thermal performance and the heating requirements of a greenhouse in Elie, Manitoba. The energy modeling had limitations in modeling the real experimental conditions of the greenhouse because of the absence of crucial data such as precise information on natural ventilation, and accurate weather data for the year 2017. Energy simulations were performed which led to the below conclusions:

1. Many studies used TRNSYS software for energy simulation, however, no researcher studied the solar-to-air factor. This study indicates the range of solar-to-air factor from 0.2 to 0.4 for greenhouses consisting of plants and thermal storage. However, this value may vary depending on the different configurations of a greenhouse.

2. Accurate weather inputs are essential for energy modeling, as the greenhouses directly interact with the external environment. However, if accurate weather inputs are unavailable, average weather data can be used.
3. The case study indicated that the natural ventilation was done by opening a vent near the ridge and no precise information about the vent size and opening factor was available. Therefore, assumptions were considered to perform the energy simulations which turned out to be quite accurate in calculating the internal air temperature and the heating requirement inside the greenhouse.
4. Evapotranspiration using the Stanghellini model can be used for a closed greenhouse. An average LAI and crop coefficient can be used to model the evapotranspiration effects without creating much error in the results.

The results obtained after the simulations show close compliance with the measured values. In a greenhouse validation process, the indoor air temperature is the most crucial parameter for verifying the accuracy of the simulation results as it majorly affects heating consumption (Dong, 2018). The validation results reveal that the mean predicted error between the measured and the simulated internal air temperature was only 1.6%. This demonstrates that the greenhouse energy model can be relied upon for further simulation processes. The validation study was not conducted for a complete year due to the limited availability of measured data during that year. However, discrepancies in the ground and north wall temperatures suggest a more refined modeling tool to be used to estimate other parameters. This study can be extended to check the uniformity and distribution of temperature in the greenhouse space, which was a limitation of TRNSYS software. However, this energy modeling can be expanded to model the various greenhouse designs under different climatic conditions and estimate the total energy needed to operate a greenhouse. The knowledge from the modeling process can be used to optimize the greenhouse design by maintaining a balance between heat gain and heat loss. This study contributes to the development of reliable modeling guidelines for further simulations to replicate dynamic greenhouse conditions.

Acknowledgments

The authors are very thankful to Dr. H. Guo for sharing the measured data for the experimental greenhouse as well as to MITACS for providing the research funding.

3.8 References

Acosta-Silva, Y. D. J., Torres-Pacheco, I., Matsumoto, Y., Toledano-Ayala, M., Soto-Zarazúa, G. M., Zelaya-Ángel, O., Mendez-Lopez, A., (2019) “Application of solar and wind renewable energy in agriculture: A review,” *Science Progress*, Vol. 102(2), pp. 127-140.

Ahamed, M. S., Guo, H., Tanino, K., (2017) “A quasi-steady state model for predicting the heating requirements of conventional greenhouses in cold regions,” *Information Processing in Agriculture*, Vol 5, pp. 33-46.

Ahamed, M. S., Guo, H., Tanino, K., (2018) “Development of a thermal model for simulation of supplemental heating requirements in Chinese-style solar greenhouses,” *Computers and Electronics in Agriculture*, Vol 150, pp. 235-244.

Ahamed, M. S., Guo, H., Tanino, K., (2019) “Modeling heating demands in a Chinese-style solar greenhouse using the transient building energy simulation model TRNSYS,” *Journal of Building Engineering*, Vol 29, 101114.

ASHRAE Handbook, (2013) “Fundamentals – ASHRAE Handbook” Copyright American Society of Heating, Refrigerating, and Air-conditioning Engineers, Inc. (Source: [2013 ASHRAE Handbook: Fundamentals - American Society of Heating, Refrigerating and Air-Conditioning Engineers, ASHRAE - Google Books](#))

Bartok, J. W., (2015) “Natural ventilation guidelines,” *Greenhouse Management* (Source: [Natural ventilation guidelines - Greenhouse Management \(greenhousemag.com\)](#))

Beaulac, A., Lalonde, T., Haillet, D., Monfet, D., (2024) “Energy modeling, calibration, and validation of a small-scale greenhouse using TRNSYS,” *Applied Thermal Engineering*, Vol 248, 123195.

Beshada, E., Zhang, Q., Boris, R., (2006) “Winter performance of a solar energy greenhouse in southern Manitoba,” Canadian Biosystems Engineering, Vol 48, pp. 5.1-5.8.

Chen, J., Yang, J., Zhao, J., Xu, F., Shen, Z., Zhang, L., (2016) “Energy demand forecasting of the greenhouses using nonlinear models based on model optimized prediction method,” Neurocomputing, Vol. 174, Part B, pp. 1087-1100.

Choab, N., Allouhi, A., Maakoul, A. E., Kousksou, T., Saadeddine, S., Jamil, A., (2021) “Effect of Greenhouse Design Parameters on the Heating and Cooling Requirement of Greenhouses in Moroccan Climatic Conditions,” IEEE Access, Vol 9, 3047851.

Climate.OneBuilding.Org (Source: [climatewebsite\WMO Region 4 North and Central America\CAN Canada \(onebuilding.org\)](https://climatewebsite/WMO_Region_4_North_and_Central_America/CAN_Canada(onebuilding.org)))

Donatelli, M., Bellocchi, G., Carlini, L., (2005) “Sharing knowledge via software components: Models on reference evapotranspiration,” European Journal of Agronomy, Vol. 24, pp. 186-192.

Dong, S., (2018) “Thermal environment modeling of the mono-slope solar greenhouse for cold regions,” [Thesis for Master of Science, University of Saskatchewan].

Dong, S., Ahamed, M. S., Ma, C., Guo, H., (2021) “A time-dependent model for predicting thermal environment of mono-slope solar greenhouses in cold regions,” Energies, Vol. 14, 5956.

Environment Canada, “Index of /cmc/climate/Engineer_Climate/CWEC_FMCCE,” (Source: [Index of /cmc/climate/Engineer Climate/CWEC FMCCE](https://www.ec.gc.ca/index-of-cmc-climate-engineer-climate-cwec-fmcce))

Golzar, F., Heeren, N., Hellweg, S., Roshandel, R., (2018) “A novel integrated framework to evaluate greenhouse energy demand and crop yield production,” Renewable and Sustainable Energy Reviews, Vol. 96, pp. 487-501.

Gong, X., Qiu, R., Sun, J., Ge, J., Li, Y., Wang, S., (2020) “Evapotranspiration and crop coefficient of tomato grown in a solar greenhouse under full and deficit irrigation,” Agricultural Water Management, Vol. 235, 106154.

Gorjian, S., Calise, F., Kant, K., Ahamed, M. S., Copertaro, B., Najafi, G., Zhang, X., Aghaei, M., Shamshiri, R., (2021) “A review on opportunities for implementation of solar energy technologies in agricultural greenhouses,” *Journal of Cleaner Production*, Vol. 285, 124807.

Government of Canada, “Past weather and climate historical data,” (Source: [Historical Data - Climate - Environment and Climate Change Canada \(weather.gc.ca\)](https://weather.gc.ca))

Greer, F., Raftery, P., Horvath, A., (2024) “Considerations for estimating operational greenhouse gas emissions in the whole building life-cycle assessments,” *Building and Environment*, Vol. 254, 111383.

Guo, H., Li, Z., Zhang, Z., Cui, Y., (1994) “Simulation of the temperature environment for solar greenhouse: Mathematic model and program verification,” *Journal of Shenyang Agricultural University*, Vol 25(4), pp. 438-443.

Hiller, M. D.E., Beckman, W. A., Mitchell, J.W., (2000) “TRNSHD – a program for shading and insolation calculations,” *Building and Environment*, Vol. 35, pp. 633-644.

Hiller, M., Kendel, C., (2023) “TRNSYS User Manual TRNSYS3d Sketch-Up Plugin,” Transsolar Energietechnik GmbH.

Imafidon, O. J., Ting, D. S-K., Carriveau, R., (2023) “Thermal modeling of a passive style net-zero greenhouse in Alberta: The effect of ground parameters and the solar to air fraction,” *Journal of Cleaner Production*, Vol. 416, 137840.

Jolliet, O., Danloy, L., Gay, J-B., Munday, G. L., Reist, A., (1991) “Horticern: an improved static model for predicting the energy consumption of a greenhouse,” *Agricultural and Forest Meteorology*, Vol 55, Issues 3-4, pp. 265-294.

Liu, X., Wu, X., Xia, T., Fan, Z., Shi, W., Li, Y., Li, T., (2022) “New Insights of designing thermal insulation and heat storage of Chinese solar greenhouse in high latitudes and cold regions,” *Energy*, Vol 242, 122953.

Liu, B., Jordan, R. C., (1961) “Daily insolation on surfaces tilted towards the equator,” *Journal of ASHRAE*, Vol. 10, pp. 53-53.

Liu, Y. H. B., Jordan, R. C., (1963) “The long-term average performance of flat plate solar collectors: With design data for the U.S., its outlying possessions and Canada,” *Solar Energy*, Vol. 7, Issue 2, pp. 53-74.

Ma, C., Han, J., Li, R., (2010) “Research and development of software for thermal environment simulation and prediction in the solar greenhouse,” *Northern Horticulture*, Vol. 15, pp. 69-75.

Ma, C., (2015) “Original Experiment Data,”.

Meng, L., Yang, Q., Bot, G. P. A., Wang, N., (2009) “Visual simulation model for the thermal environment in Chinese solar greenhouse,” *Transactions of the CSAE*. Vol. 25(1), pp. 164-170.

Mobtaker, H. G., Ajabshirchi, Y., Ranjbar, S. F., Matloobi, M., (2016) “Solar energy conservation in a greenhouse: Thermal analysis and experimental validation,” *Renewable Energy*, Vol 96, pp. 509-519.

Nauta, A., Lubitz, W. D., Tasnim, S., Han, J., (2022) “Using a greenhouse energy model to examine the potential for maintaining year-round growing conditions in off-grid greenhouses across Canada,” *The Canadian Society for Bioengineering*, Paper No. CSBE22-129.

Pamungkas, A. P., Hatou, K., Morimoto, T., (2014) “Evapotranspiration model analysis of crop water use in the plant factory system,” *Environmental Control in Biology*, Vol. 52(3), pp. 183-188.

Red River College and Proskiw Engineering Ltd, (2015) “Final Report: An investigation of airtightness in Manitoba,” (Sources: <https://www.rrc.ca/wpcontent/uploadssites/28/2016/03/MB-Hydro -Air-Leakage.pdf>)

Rorabaugh, P. A., Jensen, M. H., Giacomelli, G., (2002) “Introduction to controlled environment agriculture and hydroponics,” *Controlled Environment Agriculture Center*, Campus Agriculture Center, University of Arizona.

Santolini, E., Pulvirenti, B., Guidorzi, P., Bovo, M., Torreggiani, D., Tassinari, P., (2022) “Analysis of the effects of shading screens on the microclimate of greenhouse and glass façade buildings,” *Building and Environment*, Vol. 211, 108691.

Semple, L., Carriveau, R., Ting, D. S-K., (2017) “Assessing heating and cooling demands of closed greenhouse systems in a cold climate,” *International Journal of Energy Research*, Vol 41, Issue 13, pp. 1903-1913.

Sethi, V. P., (2009) “On the selection of shape and orientation of a greenhouse: Thermal modeling and experimental validation,” *Solar Energy*, Vol 83, pp. 21-38.

Sethi, V. P., Sharma, S. K., (2007) “Thermal modeling of a greenhouse integrated to an aquifer coupled cavity flow heat exchanger system,” *Solar Energy*, Vol. 81, pp. 723-741.

Sethi, V. P., Sumathy, K., Lee, C., Pal, D. S., (2013) “Thermal modeling aspects of solar greenhouse microclimate control: A review on heating technologies,” *Solar Energy*, Vol. 96, pp. 56-82.

The Mesh Company (Source: [0.42mm Hole Stainless Steel Woven Insect Mesh Midge Net - 0.22mm Wire - 40 LPI - The Mesh Company](#))

Tiwari, G. N., (2003) “Greenhouse technology for the controlled environment” Alpha Science International Ltd, pp. 160-330.

Tong, G., Christopher, D. M., Li, T., Wang, T., (2013) “Passive solar energy utilization: A review of cross-section building parameter selection for Chinese solar greenhouses,” *Renewable and Sustainable Energy Reviews* 26 (2013), pp. 540-548.

Tong, G., Li, B., Christopher, D. M., Yamaguchi, T., (2007) “Preliminary study on temperature pattern in Chinese solar greenhouse using computational fluid dynamics,” *Transactions of the CSAE*, Vol 23(7), pp. 178-185.

TRNFlow Manual, (2009) “A module of an airflow network for coupled simulation with Type-56 (multi-zone building of TRNSYS),” Version 1.4.

TRNSYS-18, (2017) “TRaNsient System Simulation program – Weather Data,” Volume 8, Solar Energy Laboratory, University of Wisconsin-Madison.

TRNSYS-18, (2021) “TRaNsient System Simulation program – Multizone Building Modeling with Type56 and TRNBuild” Volume 5, Solar Energy Laboratory, University of Wisconsin-Madison.

Typical Meteorological Year, (2024) “Wikipedia The free encyclopedia for a typical meteorological year,” (Source: [Typical meteorological year - Wikipedia](#))

Vadiee, A., (2011) “Energy Analysis of the closed greenhouse concept: Towards a sustainable energy pathway,” [PhD Thesis – KTH Royal Institute of Technology].

Vadiee, A., Martin, V., (2013) “Energy Analysis and thermo-economic assessment of the closed greenhouse – The largest commercial solar building,” Applied Energy, Vol 102 (2013), pp. 1256-1266.

Wang, T., Wu, G., Chen, J., Cui, P., Chen, Z., Yan, Y., Zhang, Y., Li, M., Niu, D., Li, B., Chen, H., (2017) “Integration of solar technology to a modern greenhouse in China: Current Status, challenges and prospect,” Renewable and Sustainable Energy Reviews, Vol 70, pp. 1178-1188.

Xu, H., Zhang, Y., Li, T., Wang, R., (2017) “Simplified Numerical Modeling of Energy Distribution in a Chinese Solar Greenhouse,” Applied Engineering in Agriculture, Vol. 33(3), pp. 291-304.

Yu, H., Chen, Y., Hassan, S. G., Li, D., (2016) “Prediction of the temperature in a Chinese solar greenhouse based on LSSVM optimized by improved PSO,” Computers and Electronics in Agriculture, Vol 122, pp. 94-102.

Zhao, X. T., Xu, H., Li, T. L., Wang, R., (2019) “Establishment of winter energy distribution model for solar greenhouses in Northeast China,” Journal of Shenyang Agricultural University, Vol. 50 (1), pp. 43-50.

CHAPTER 4
ECONOMIC AND ENERGY PERFORMANCE OPTIMIZATION FOR
CONTROLLED ENVIRONMENT AGRICULTURE: A REGIONAL VIGNETTE FOR
CANADA

4.1 Introduction

The agricultural industry is vital for developing countries, providing both food and income for the human population. An obvious transition in the agriculture industry involves utilizing advanced technologies and techniques to optimize crop growth conditions. This shift is driven by the ever-growing world population, leading to a rising demand for food crops to meet the needs of more people (FAO, 2009). Climate change and extreme weather patterns pose a significant challenge to agriculture, thereby diminishing overall productivity. Temperature plays a crucial role in determining which crops can be grown in a particular location and impacts the heating and cooling demands of buildings (Bush & Lemmen, 2019).

Canada, known for its cold climate, experiences significant temperature variation throughout the year and across different regions. For instance, the average temperature in the northern region, such as Nunavut, is around -11.6°C , while in the southern part, like Ontario, it averages around 3°C . The eastern region experiences temperatures of about 1.1°C , whereas the western region averages -3.7°C (Climate Atlas of Canada, 2023). Even within a single province, temperature variations can occur, making agriculture challenging in areas with extremely low temperatures, which in turn elevates heating costs. As a result, crops are not grown uniformly across Canada; instead, they are often transported from regions where they can be cultivated more efficiently. For example, the cost of producing one kilogram of lettuce varies significantly, with British Columbia having the lowest cost at \$4.12, followed by Alberta at \$4.87, while in Saskatchewan, it can go up to \$16, and in New Brunswick, it can reach \$21 (Statistics Canada, 2024). Additionally, growing crops such as lettuce contributes to varying levels of greenhouse gas (GHG) emissions across regions, with approximately 2500 kg CO₂ e/ha in the Atlantic Provinces, 3200 kg CO₂ e/ha in Quebec, 3100 kg CO₂ e/ha in Ontario, and 3500 kg CO₂ e/ha in other regions (Fouli *et al.*, 2021).

These temperature fluctuations, both daily and across different locations, are a major reason why agriculture is not prevalent in many parts of the world. To address this challenge, there is a need for a transition towards growing food which would reduce GHG emissions while potentially lowering crop production costs. Sustainable agriculture, particularly urban agriculture, is gaining traction, with Controlled Environment Agriculture (CEA) being a key component. Indoor farming is expected to see significant growth in the coming decades. In 2018, the global indoor agriculture market was valued at \$26.8 billion, with a projected growth rate of 9.19% between 2020 and 2025 (Grandview Research, 2019).

CEA is defined as cultivating crops within a carefully regulated environment, particularly in a structure, enabling precise management of variables such as temperature, humidity, carbon dioxide levels, and supplemental lighting. These variables play an important role in maximizing optimal plant development (Engler & Krarti, 2021). CEA offers a sophisticated approach to conventional agriculture, aiming to increase plant growth efficiency while providing clean and green crops, biosecurity, disease, and pest-free crops, and reduced use of transportation and fossil fuels (Benke & Tomkins, 2017). However, it is important to note that the installation and operational expenses for a CEA facility are quite substantial. Heating, ventilation, air-conditioning (HVAC), lighting, and dehumidification are the primary areas of energy consumption in such facilities. A study reveals that 60% of the total costs for CEA contribute towards energy, with lighting accounting for roughly one-half of energy use (Melancon, 2018). Moreover, intensive vertical farms may consume between 8,700 and 70,000 MWh each year depending on the crop and size of the facility (Electric Power Research Institute, 2018).

Research conducted for greenhouses in Southern California found that artificial lighting accounts for 38% of the electricity use, with HVAC accounting for 56% of the electricity use i.e., ventilation (30%), air-conditioning (21%), and heating (5%) (Schimelpfenig and Smith, 2021). This outlines the necessity to enhance the performance of CEA using energy-efficient measures (EEM) to make them profitable for growing crops. Engler and Krarti (2021) reviewed several CEA case studies and found that changes to the facility's envelope, HVAC, and lighting can reduce electricity consumption by up to 75%.

Researchers have investigated EEMs to utilize renewable energy as an alternative to reduce energy demand. Despite that, energy-efficient facilities are still not widely available due to the substantial supplemental energy requirements, which are typically met by natural gas or electricity.

This paper focuses on implementing EEMs that primarily reduce the heating and cooling demand of the facility. The remaining heating and cooling needs are then met using renewable energy, to create a facility that is nearly net-zero in energy consumption. Some of the existing literature only provides reviews on EEMs (Tong *et al.*, 2013; Ahamed *et al.*, 2019), while others largely focused on implementing single or paired EEMs rather than integrating multiple measures to enhance greenhouse efficiency (Tantau *et al.*, 2011; Rasheed *et al.*, 2019; Beaulac *et al.*, 2024). While these individual EEMs can reduce energy demand, their overall impact is often insufficient to significantly lower total energy consumption. Additionally, many studies have overlooked improvements in greenhouse design, which are crucial for reducing energy demand. There is also a gap in the literature concerning the optimization of CEA facilities to suit different regions, given that external weather conditions vary widely and significantly influence the internal conditions of greenhouses.

In response to these challenges, this study aims to develop an Advanced Growing Building (AGB), an energy-efficient greenhouse design featuring a double envelope that creates a buffer zone between the external environment and the growing space (GS). This design incorporates key EEMs, such as advanced construction materials, natural ventilation, thermal curtains, and shade curtains, to reduce energy demand without substantially increasing installation costs. Furthermore, an optimization study was conducted to enhance AGB efficiency by adjusting design parameters influencing heating and cooling demand and life-cycle costs (LCC). A comparative analysis was performed to estimate the heating and cooling demand per kilogram of crop and the LCC per kilogram for the AGB, the optimal design of AGB, and a conventional greenhouse (CG). This research offers insights into a new greenhouse design that offers superior energy efficiency compared to CGs, potentially increasing crop output, reducing heating and cooling demands, and lowering GHG emissions. Additionally, this study contributes to a deeper

understanding of EEMs and design parameters that significantly impact the thermal performance of greenhouses.

4.2 Literature Review

Energy consumption represents the greatest challenge in greenhouse operations. Researchers have reviewed various methods to reduce greenhouse heat losses and enhance energy efficiency. Gupta and Chandra (2001) studied various energy conservation measures, indicating that an east-west oriented gothic arch greenhouse requires 2% less heating compared to a north-south orientation. Adding north wall insulation in an east-west greenhouse saves 30% in heating costs, while night curtains reduce heating requirements by approximately 71%. Replacing a single cover on the south side with air-inflated double-wall glazing reduced the heating requirement by 23%. This study also combines these design features to reduce greenhouse heating requirements by 80%. Sethi (2008) analyzed the greenhouse shapes and orientations to compute transmitted solar radiation, revealing that greenhouse design varies the amount of solar radiation received and the inside air temperature rise. Tantau *et. al.*, (2011) predicted that closed greenhouses could elevate production yield by 20% and reduce energy demand by 30-40% based on the technology utilized. Vadiee and Martin (2013) studied energy conservation for various closed greenhouse configurations and a conventional design, illustrating that the payback period for the ideal closed greenhouse might be reduced by 50%. Pamungkas *et. al.*, (2014) developed a mathematical model to predict hourly evapotranspiration (EVT) rates, showing that solar radiation and vapor pressure deficit (VPD) are important factors driving EVT rates.

Mobtaker *et. al.*, (2016) investigated greenhouse shapes and orientation from an energy consumption aspect, showing that an east-west oriented single-span greenhouse had the lowest additional energy requirement. North wall insulation was found to further reduce heating requirements by 31.7%. Ahamed *et. al.* (2018) considered design parameters such as shape, orientation, and roof angle for greenhouses in the Canadian Prairies, showing that an east-west uneven-span greenhouse was more energy-efficient for heating and cooling in higher northern latitudes. Rasheed *et. al.*, (2019) studied the effect of different thermal screen materials and control strategies on greenhouse heating

requirements, achieving a maximum reduction of 30% when thermal screens were employed. Choab *et. al.*, (2021) investigated key design parameters such as cladding material characteristics, shape, orientation, and air change rate to analyze the greenhouse thermal behavior and heating and cooling energy needs. Dong *et. al.* (2021) developed a time-dependent model for predicting the thermal environment of a Chinese solar greenhouse (CSG) in Saskatoon, Canada, indicating that vegetable production could save about 55% on annual heating compared to traditional greenhouses. Beaulac *et. al.*, (2024) used greenhouse energy modeling to optimize energy consumption in a small-scale greenhouse consisting of plants and a ventilation system. Table 4-1 summarizes the EEMs employed in different studies.

Table 4-1 Summary of EEMs employed in different studies.

Author	Orientation	Design	Construction Material	Curtains	EVT	Ventilation	Combined EEMs
Gupta and Chandra (2001)	✓	✓	✓	✓			✓
Sethi (2008)	✓	✓					
Tantau <i>et. al.</i> , (2011)						✓	
Vadiee and Martin (2013)						✓	
Pamungkas <i>et. al.</i> , (2014)					✓		
Mobtaker <i>et. al.</i> , (2016)	✓	✓	✓				
Ahamed <i>et. al.</i> , (2018)	✓	✓					
Rasheed <i>et. al.</i> , (2019)				✓			
Choab <i>et. al.</i> , (2021)	✓	✓	✓		✓	✓	
Dong <i>et. al.</i> , (2021)			✓	✓	✓	✓	
Beaulac <i>et. al.</i> , (2024)					✓	✓	

Table 4-1 clearly shows that only Gupta and Chandra (2001) have focused on combining multiple EEMs to reduce energy consumption. Energy consumption and life-cycle costs are influenced by various factors, and the first step in reducing them is to identify the variables that impact these factors. Researchers have employed different optimization algorithms to maximize profits or minimize energy use, thereby improving energy efficiency. However, the objective function varies from study to study, with each study using different variables that affect the objective function. Table 4-2 highlights some of the various studies conducted in this field.

Table 4-2 Summary of optimization study conducted in this field

Author	Optimization Algorithm	Objective function	Controlled Variable
Pohlheim and Heibner, (1999)	Evolutionary algorithm	<ul style="list-style-type: none"> • Maximize profit • CO₂ enrichment 	<ul style="list-style-type: none"> • Heating • CO₂ injection • Ventilation
Blasco <i>et. al.</i> , (2001)	Genetic Algorithm	<ul style="list-style-type: none"> • Minimize energy use • Water use 	<ul style="list-style-type: none"> • Window opening percent • Heating power • Fog system flowrate
Ramirez-Arias <i>et. al.</i> , (2012)	Sequential quadratic programming	<ul style="list-style-type: none"> • Maximize profit • Product Quality • Water use efficiency 	<ul style="list-style-type: none"> • Actuation signals for heating • Window opening • Shade screen • Water • Electrical conductivity
Xu <i>et. al.</i> , (2013)	Rolling horizon optimization	<ul style="list-style-type: none"> • Minimize reference deviation • Variation of command 	<ul style="list-style-type: none"> • Temperature
Oliveira <i>et. al.</i> , (2015)	Quadratic programming	<ul style="list-style-type: none"> • Minimize reference deviation. • Variation of command 	<ul style="list-style-type: none"> • Ventilator actuation signals • Heater system • Irrigation system
Liang <i>et. al.</i> , (2018)	Exhaustive search	<ul style="list-style-type: none"> • Minimize reference deviation • Energy consumption 	<ul style="list-style-type: none"> • Switch signals for heating • Window opening

4.3 Methodology

The execution of this research was conducted in phases as indicated in Figure 4-1. Phase 1 of the research involves the development of the AGB and CG models using SketchUp software, followed by energy simulations using TRNSYS software and life-cycle cost analysis (LCCA). In phase 2, an optimization study was executed to determine the factors that influence heating and cooling demand and the LCC along with identifying an optimal design using a modified binary optimization approach. Different cases were defined using the design of experiments (DOE) approach, for each of them the energy simulation and LCCA were implemented. In the last phase, the performance of optimal design was studied for various locations across Canada.

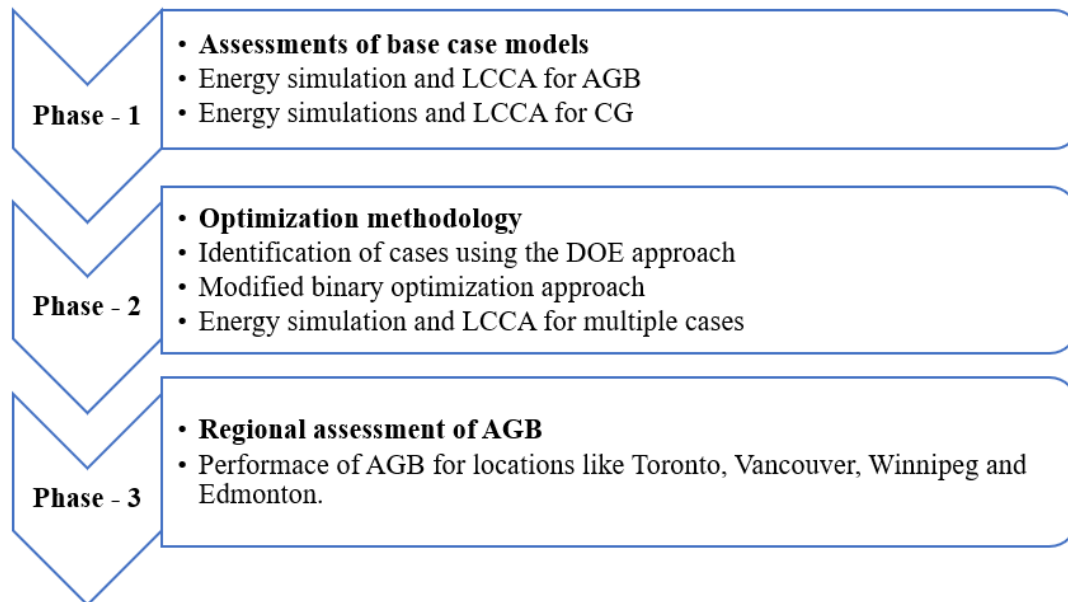


Figure 4-1 Represents the phases required to execute the research

4.3.1 Assessment of Base Case Models

This section explores the development of the AGB and CG models using the SketchUp software. The SketchUp file consists of each surface's dimension, orientation, volume, inclination, and orientation. Both these models were sized to accommodate 182,172 kilograms of lettuce crops. However, the difference between these two models is the method in which the crops were grown. The AGB was designed to have the benefits of vertical farms, thus lettuce crops were grown in three layers while CG grows lettuce crops only on the ground. The location selected for the initial study was Toronto, Ontario (43.8° N and -79.5° E). The weather file selected for the simulations was TMY-2, available in the

TRNSYS weather library (TRNSYS-18 Weather data, 2017). TMY files contain generated values from a data bank for a specific location of a minimum of 12 years (Typical Meteorological Year, 2024). The optimal temperature range for growing lettuce crops should be between 20°C to 25°C (Ahmed *et. al.*, 2020; Engler and Krarti, 2022). The initial temperature and relative humidity for the simulations were assumed to be 7.8 °C and 74.8% respectively, representing average values of outside ambient temperature and relative humidity.

The AGB design is a leading-edge greenhouse design featuring a double envelope. The inner envelope encloses the inside volume of air known as growing space (GS), where lettuce crops are grown. A buffer zone also known as outer space (OS) which surrounds the GS, provides additional safeguarding to reduce heat losses at night by minimizing the temperature gradient between the GS and the external environment. This helps to maintain a higher temperature in the GS during nighttime, thereby reducing overall heating demand. Additionally, the OS limits direct solar radiation entering the GS, decreasing cooling demand. The AGB design was constructed based on a preliminary study by Khanuja *et. al.*, (2024), which investigated the effects of orientation, design, and roof inclination on solar radiation availability. The AGB was oriented in an east-west direction, as the south side receives maximum solar radiation throughout the year, especially in winter when heating is maximum (Khanuja *et. al.*, 2024). Solar radiation enters the AGB through glazing on the south side.

The AGB design was inspired by a CSG design, an advanced version of the single-span greenhouse. Single-span greenhouses typically feature a vertical north wall and an inclined south wall to maximize solar radiation intake throughout the year (Khanuja *et. al.*, 2024). The AGB was modeled using two Trnsys3d zones, one for GS and the other for OS, to estimate the heating and cooling requirements solely for the GS. Additionally, the AGB design includes overlapping surfaces between the GS and OS envelopes, created in the SketchUp module as illustrated in Figure 4-2.

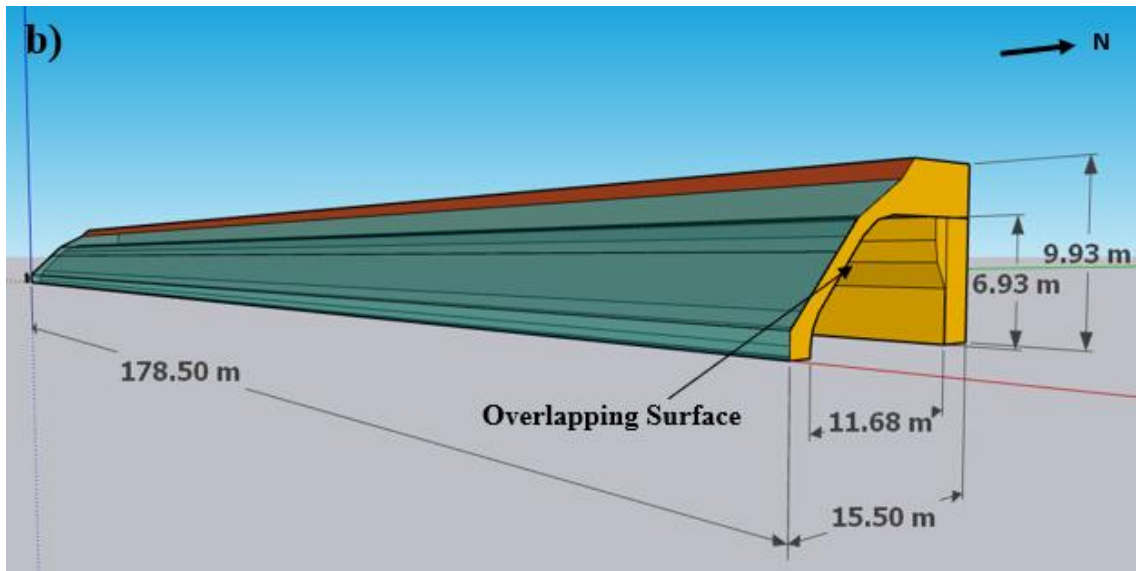
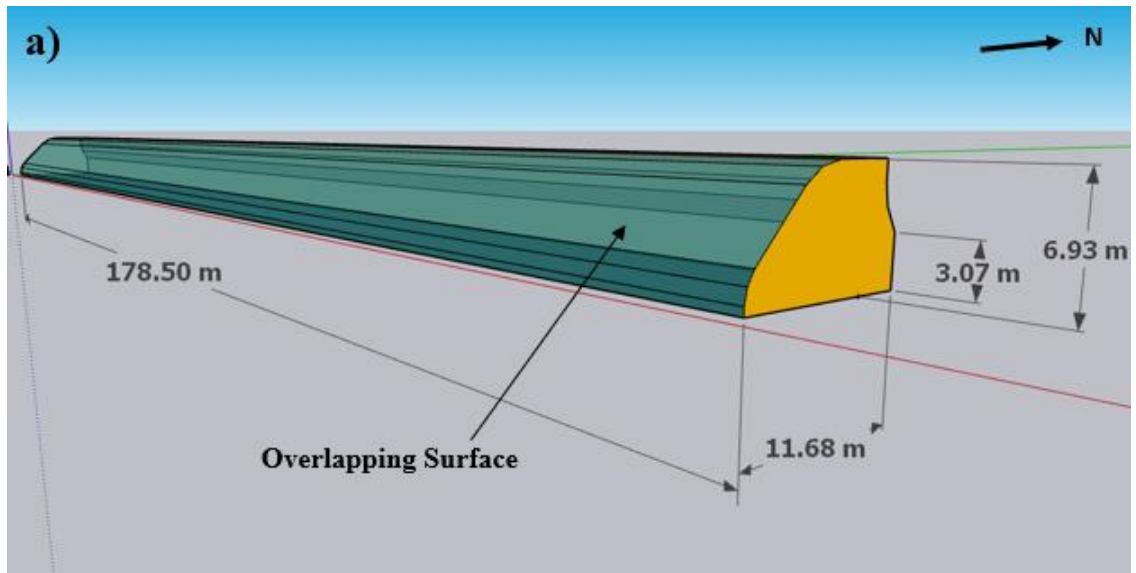


Figure 4-2 AGB model developed using the SketchUp software. (a) Trnsys3d zone -1 consisting of GS with a volume of 11336 m^3 (b) Trnsys3d zone-2 consisting of outer space (OS) with a volume of 9127 m^3

The north side of the AGB encompasses insulation to prevent heat losses, as it receives minimal solar radiation (Khanuja *et. al.*, 2024). Polycarbonate was used in the outer glazing because it has higher transmissivity to short-wave solar radiation along with the photovoltaic glass, a reinforced glass that maintains the same thermal insulation as traditional glass for the same amount of ambient light transmission as standard glass (Lowth, 2023). Polyethylene was used in the inner glazing as it transmits light in a scattered manner but has greater heat loss for the exchange of long-wave radiation (Ahamed *et. al.*,

2019). A single Trnsys3d zone was used to develop the CG model as presented in Figure 4-3. The CG comprised horticultural glass, accounting for approximately 99% of the total wall and roof area. The SketchUp files in the .idf format were transferred to the TRNSYS simulation studio for conducting the energy simulations. For more details related to AGB and CG, refer to Appendix A.

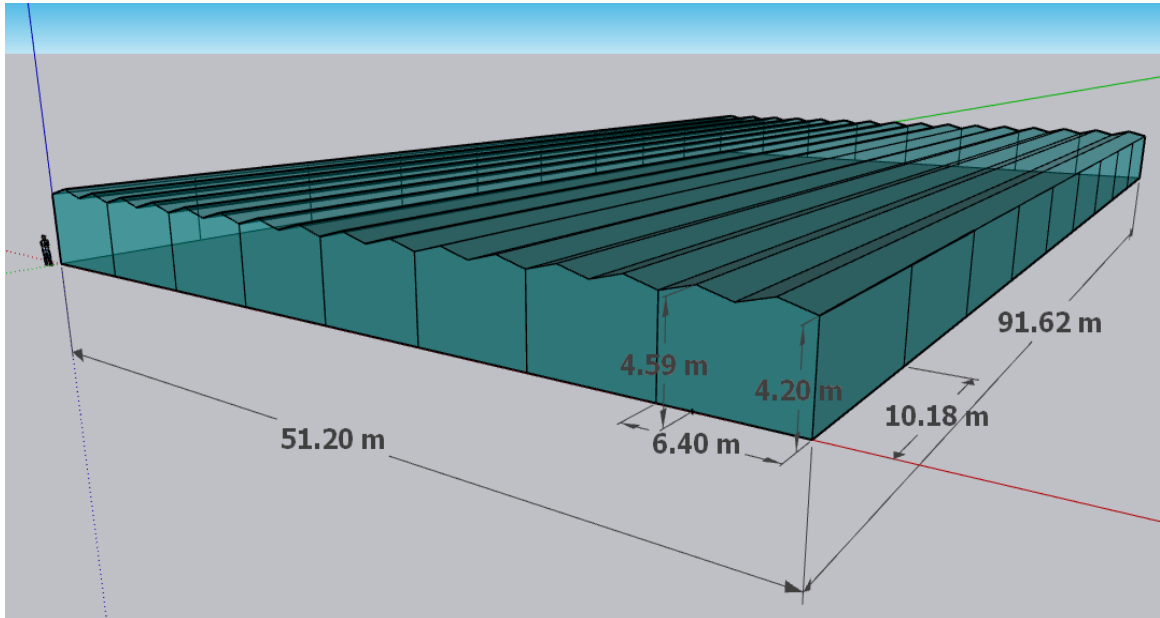


Figure 4-3 CG model developed using the SketchUp software with a volume of 20647 m^3 .

4.3.1.1 Energy Simulation for AGB and CG

The main components required to model energy requirements include the weather component (type-15), building component (type-56), evapotranspiration (sub-model), thermal curtain (type-56), shade curtain (type-56), ventilation schedule, integrators (type-55), plotters (type-65), and printers (type-25c). Figure 4-4 represents the interface of the TRNSYS simulation studio having connections between TRNSYS components.

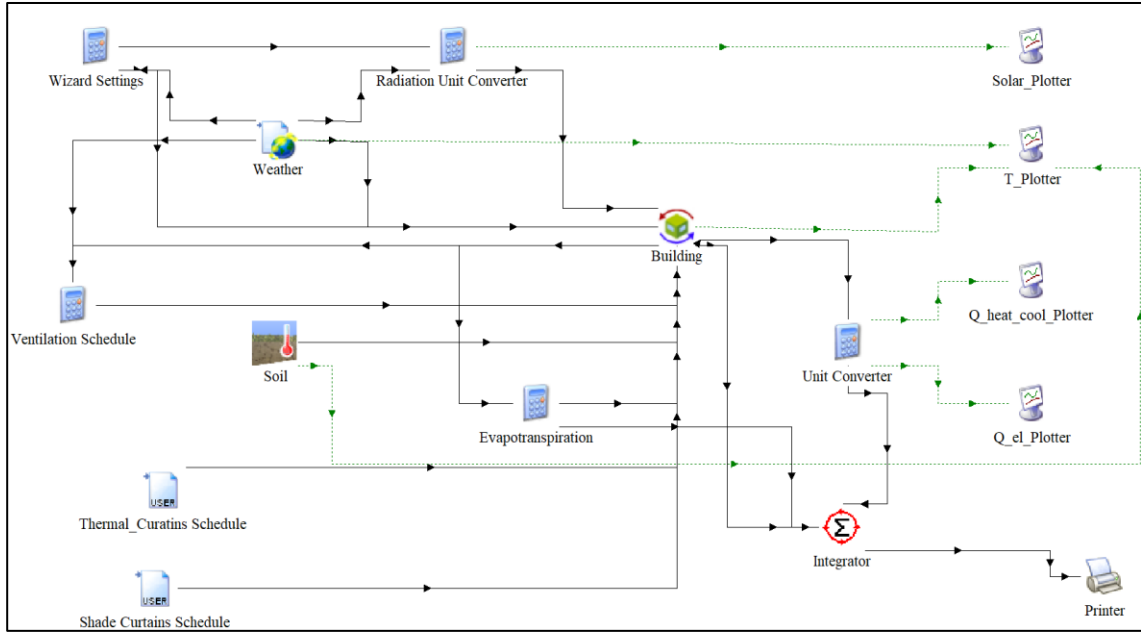


Figure 4-4 Represents the interface of the TRNSYS simulation studio indicating the inputs and outputs connection between individual components

The materials for opaque walls for the AGB were created using thermal properties such as conductivity, density, and specific heat in TRNBuild, which were then combined with thickness to form opaque walls, roofs, or floors. The optical and thermal properties of glazing materials used in AGB and CG were defined using the Lawrence Berkeley National Lab Window program. A DOE-2 file was then created and added to the TRNBuild. Table 4-3 represents the details of construction materials used in the TRNSYS software for thermal simulation.

Table 4-3 U-value of the construction material used in AGB and CG.

Surface	Materials	U-value	Thickness	Reference
Outer NW	IMP	0.14 W/m ² K	150 mm	Insulation UK, (2024)
Middle NW				
Inner NW	IMP	0.14 W/m ² K	150 mm	
	GSS	45300 W/m ² K	1 mm	
EW and WW	IMP	0.14 W/m ² K	150 mm	Insulation UK, (2024)
Inner NR		0.09 W/m ² K	204 mm	
Outer NR	FBG	0.15 W/m ² K	254 mm	
	IMP	0.18 W/m ² K	102 mm	
Floor - OS	Polystyrene	3 W/m ² K	40 mm	Periodic Table (2024)
Floor - GS	Concrete	1.56 W/m ² K	102 mm	

Glazing – OS (bottom part)	Triple-walled PC	2.9 W/m ² K	28 mm	Duralight Plastics (2023)
Glazing – GS	PE	6.29 W/m ² K	0.1 mm	Choab <i>et. al.</i> , (2021)
Glazing – OS (upper part)	PV glass	4.92 W/m ² K	19 mm	Onyx solar group
CG	HG	5.69 W/m ² K	6 mm	Adesanya <i>et. al.</i> , (2022)

*NW = North Wall, EW = East Wall, WW = West Wall, NR = North Roof, IMP = Insulated Metal Panel, GSS = Galvanized Sheet Steel, FBG = Fiberglass Insulation

While modeling the AGB and CG, infiltration was considered as it allows undesired cooler air to enter the greenhouse through leakages and openings, providing an imbalance in the thermal environment. Additionally, the effect of plants and the process of evapotranspiration was modeled in both models assuming the LAI and crop coefficient for the mid-season. The modeling of evapotranspiration was explained in detail in Appendix A. Moreover, energy-conserving parameters such as natural ventilation, thermal curtains, and shade curtains were implemented in the AGB whereas only natural ventilation was considered in CG. These parameters majorly influence the energy demand of the facility without significantly altering the capital expense. Table 4-4 presents the important parameters considered while modeling the AGB and CG. The operational schedule was solely selected based on the need for these curtains during the year and the solar radiation availability pattern.

Table 4-4 Important parameters considered during the modeling of AGB and CG.

AGB			CG		
Parameters	Values	Reference	Parameters	Values	Reference
Infiltration	0.3 ACH	Vadiee and Martin (2013)	Infiltration	1.5 ACH	Younes <i>et. al.</i> , (2012)
TC resistance	3.45 m ² K/W	Focus Technology (2024)	TC resistance	-	-
SC resistance	0.004 m ² K/W	Svensson, 2018	SC resistance	-	-
TC schedule	TC schedule 1	Refer Appendix A	TC schedule	-	-
SC schedule	SC schedule 1	Refer Appendix A	SC schedule	-	-

Natural ventilation was modeled using TRNFlow, which employs COMIS to model the airflow between the greenhouse and the environment (TRNFlow Manual, 2009). Natural ventilation allowed outside fresh air to enter the GS when it was in the desirable temperature range. For all other times, the ventilation vents were kept closed. The outside air was exchanged with GS as indicated in Figure 4-5. The ambient air enters the

greenhouse through point 1 of size 0.31 m^2 , which consists of the duct system. This air is then transferred to the section between the inner north wall and the middle north wall. The cooler air starts to diffuse in through small openings of 0.036 m^2 represented by points 2 and 3. This air mixes with GS air which lowers the GS temperature, as well as providing uniformity to heat distribution. Further, the hot air tends to move upwards, which moves from GS to OS from points 4 (0.057 m^2) and 5 (0.21 m^2). Lastly, point 6 of size (0.99 m^2) was used to allow air from the OS to move out to the external environment. This ventilation network was considered at 17 locations at a distance of 10.5 m along the length of the building.

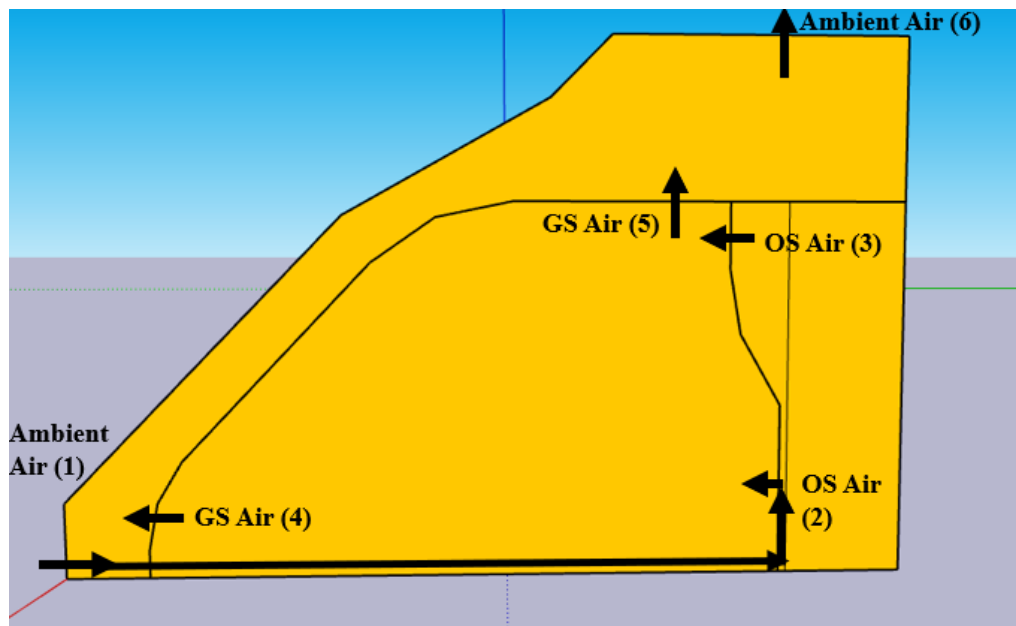


Figure 4-5 Airflow network for natural ventilation in AGB.

Natural ventilation was also considered in CG. The sizing of the vents for CG was assumed based on the recommendation provided by the American Society of Agricultural and Biological Engineers standards that the combined roof vent area should equal the combined sidewall vent area and each should be at least 15 to 20% of the floor area. For northern climates, 15% may suffice, but warmer climates require greater amounts (Bartok, 2015). Therefore, based on the sizing criteria, 2 vents of size 4.7 m by 2.3 m were considered on each roof, along with a total of 34 vents on the side walls of size 6.6 m by 3.3 m. The vents were operated using an algorithm that when the need for ventilation vents was maximum i.e. temperature of the greenhouse air reaches beyond 45°C , 80% of each vent gets open, when the temperature was between 30 and 45°C , 30% of vents opened,

and when the temperature was between 25°C and 30°C, 10% of vents get open. Once the model was created, a simulation was performed to estimate the energy demand of the AGB and CG. However, the energy demand per kilogram of lettuce crop was calculated using equation (4-1).

$$\text{Energy demand(kWh/kg)} = \frac{\text{Heating load (kWh)} + \text{Cooling load (kWh)}}{\text{Crop Output}} \dots (4 - 1)$$

4.3.1.2 Life-cycle cost analysis (LCCA)

The LCCA includes the installation cost of the facility along with the cost to provide heating and cooling for 10 years of operation. The installation costs include the cost of materials including the PE layer, triple-walled PC, PV glass, IMP, GSS, FBG insulation, polystyrene, concrete, steel frame, thermal curtain, shade curtain, ventilation vents, and duct system for the AGB. Similarly, the installation costs for CG involve the cost of HG, steel frame, concrete, and ventilation vents. The quantity of materials required to build the model was determined using the SketchUp file. A 10% allowance was also considered while estimating the installation cost to account for variations in the vendor’s price and inflation. The energy demand of AGB and CG included the additional heating and cooling required to maintain optimal temperature. It was assumed that the heating is provided by natural gas and cooling is provided using electricity. The cost of natural gas providing per kWh of heat was approximately 5.58 cents (Canadian Gas Association, 2022) and the cost of electricity providing per kWh of cooling was approximately 13.03 cents (Ontario Energy Board, 2022). The total LCC in cents per kilogram can be calculated using equation (4-2)

$$\text{LCC} = \frac{\sum \text{MC} + ((\text{HL} * 0.055) + (\text{CL} * 0.1303)) * \text{NOY}}{\text{CO} * \text{NOY}} \dots (4 - 2)$$

Where,

MC is the sum of all materials cost in \$

HL is the heating demand in kWh

CL is the cooling demand in kWh

NOY is the number of years

CO is the lettuce crop output in kilograms per year

In this study, the number of operating years was considered as 10 years. The costs of providing natural gas and electricity were assumed constant for 10 years. The unit cost of each material was identified from the vendor’s website explained in Appendix A.

4.3.2 Optimization Methodology

An optimization study was only conducted on the AGB model with two objective functions. The multi-objective functions include the minimization of heating and cooling energy per kilogram along with the reduction in LCC per kilogram of crop output. A modified binary optimization approach was implemented to minimize the multi-objective function (X_i and Y_i) which are indicated in equations (4-3) and (4-4).

$$X_i = \text{Minimize } \sum_{i=1}^n \frac{(HL)_i + (CL)_i}{(CO)_i} \dots\dots\dots (4 - 3)$$

$$Y_i = \text{Minimize } \sum_{i=1}^n \frac{\sum(MC)_i + (((HL)_i * 0.055) + ((CL)_i * 0.1303)) * NOY}{(CO)_i * NOY} \dots\dots (4 - 4)$$

Where,

X_i is the objective function to minimize heat and cooling demand per kilogram of crop output

HL_i is the heating demand in kWh when variable ‘i’ was implemented

CL_i is the cooling demand in kWh when variable ‘i’ was implemented

CO_i is the crop output of the facility with variable ‘i’

Y_i is the objective function to minimize LCC per kilogram of crop output

MC_i is the total material cost of the facility when variable ‘i’ was implemented

NOY is the number of years = 10 years (for this study)

Step 1: After defining the objective function, the next step was to identify the variables that affect either the energy demand or the LCC, which is the sum of installation and operating costs. The identified variables are indicated in Table 4-5.

Table 4-5 Variables affecting either the heating and cooling demand or the LCC.

Variable	Multi-objective function		
	Heating and cooling demand	Installation Cost	Operating Cost
Orientation	✓	X	✓
Envelope geometry	✓	✓	✓
Envelope materials	✓	✓	✓
Envelope material thickness	✓	✓	✓
TC and SC resistance	✓	✓	✓
TC and SC schedule	✓	X	✓
TC and SC location	✓	X	✓
Size of ventilation vents	✓	✓	✓
Opening schedule of ventilation vents	✓	X	✓
Location of vents	✓	X	✓

Step 2: The identified variables were broken down to identify the possible scenarios under each variable as presented in Table 4-6. Here, the important aspect was to see the availability of the material in the market as well as the cost. In-depth research was conducted to identify the possible scenarios closest to the base case of AGB. Market research was done to identify better materials for thermal and shade curtains. However, the materials available correspond to the same or lesser R-value of thermal curtains, which would not be beneficial for the energy demand. Therefore, no possible scenarios were identified for thermal curtains and shade curtains resistance.

Table 4-6 Possible scenarios considered under each variable

Variable		Possible scenario	X-value
Variable 1	Orientation	East-west	A
		15° north of east	B
Variable 2	Envelope geometry	Profile 1 (refer to Appendix A)	1
		Profile 2 (refer to Appendix A)	2
		Profile 3 (refer to Appendix A)	3
Variable 3	Outer glazing material (thickness)	PC (28 mm)+PV glass (19 mm)	Base case
		PC (28 mm)	A
		PV glass (19 mm)	B
		PVC (1.8 mm)	C
		HG (6 mm)	D

		PC (4 mm)	E
		PC (10 mm)	F
		PC (16 mm)	G
		PV glass (6 mm)	H
		PV glass (26 mm)	I
		PVC (3.18 mm)	J
		HG (4 mm)	K
		HG (10 mm)	L
		PC (28 mm)+PV glass (26 mm)	M
		PC (16 mm)+PV glass (26 mm)	N
Variable 4	Internal glazing material (thickness)	PE (0.1 mm)	Base case
		PE (0.05 mm)	1
		PE (0.15 mm)	2
		Double PE layer (2.2 mm)	3
Variable 5	Opaque surface thickness	Thickness as per Table 4-3	Base case
		50% reduction in thickness	A
		50% increment in thickness	B
Variable 6	TC resistance	3.45 m ² K/W	Base case
Variable 7	TC schedule	Schedule 1(refer to Appendix A)	Base case
		Schedule 2 (refer to Appendix A)	1
Variable 8	SC resistance	0.004 m ² K/W	Base case
Variable 9	SC schedule	Schedule 1(refer to Appendix A)	Base case
		Schedule 2 (refer to Appendix A)	2
Variable 10	Ventilation vents size	Original vents size	Base case
		50% increment in vents size	3
		100% increment in vent size	4

Step 3: In this step, the possible scenarios were taken one by one to identify variables that significantly influence either the heating or cooling demand or the LCC. The results of the individual possible scenarios were recorded. Based on the performance of each possible scenario, the combination of possible scenarios was developed using the design of experiments (DOE) approach. DOE is a systematic, efficient technique to determine individual and interactive effects of various factors that can influence the objective function. It also helps to optimize and better understand how the most important factors can regulate the output. The benefit of using DOE is that it is a more organized approach providing a direction of flow to conduct simulation (Sartorius, 2020). The total number of

cases that were developed using the DOE approach counts up to 12,960 cases. The method of reading a case number is explained below:

Case XXXX-X

The first ‘X’ indicates the envelope geometry. Refer to Table 4-6 to determine the value of X for each possible scenario. The second ‘X’ indicates the orientation. A combination was developed to ease the case's readability, where 1A = 4, 1B = 5, 2A = 6, 2B = 7, 3A = 8, 3B = 9. The outer glazing material (thickness) was represented by the letter. The third ‘X’ indicates the material and thickness of the inner glazing. The fourth ‘X’ indicates the thickness of opaque surfaces. The fifth ‘X’ denotes the energy-conserving parameters being implemented.

Step 4: Using the DOE approach, the total number of all the possible cases was determined which accounted for 12,960 cases. However, it was impossible to simulate all 12,960 cases to estimate the heating and cooling load. Thus, to avoid this tedious task, modified binary optimization was employed. This optimization is usually employed for problems involving a few interrelated “Yes-or-No decisions”. In such cases, there are only two possible choices i.e. “Yes” or “No”. For this study, modified binary optimization was implemented in the below manner:

For a case,

$$C_i = \begin{cases} 1, & \text{when both } (ED)_i \leq (ED)_{BC} \text{ and } (LCC)_i \leq (LCC)_{BC} \\ 0, & \text{when either } (ED)_i \geq (ED)_{BC} \text{ or } (LCC)_i \geq (LCC)_{BC} \end{cases}$$

Where,

C_i is the case ‘i’

$(ED)_i$ is the energy demand per kilogram of crop output for case ‘i’

$(ED)_{BC}$ is the energy demand per kilogram of crop output for the base case

$(LCC)_i$ is the life-cycle cost per kilogram of crop output for case ‘i’

$(LCC)_{BC}$ is the life-cycle cost per kilogram of crop output for the base case

Based on this Boolean algorithm, it was decided whether the case is required to be simulated or not. The algorithm was initially applied to individual scenarios to identify

those that significantly reduced both energy demand and LCC per kilogram of crop output. The cases formed with the individual possible scenarios were analyzed in detail, as some had a small impact on increasing either energy demand or LCC while substantially reducing the other. Based on the results, each scenario was evaluated with a decision of Yes (1) or No (0) for further consideration in combination with other cases. This approach aids in developing the optimal case with the lowest energy demand and LCC per kilogram of the crop output. In cases where the decision received was No (0), the possible scenario was dropped from the optimization study whereas, in the cases where the decision was Yes (1), they were further combined with the other positive cases. All the cases that fall under decision Yes (1), were simulated one by one using the modeling approach mentioned in section 4.3.1.1, and the LCCA was implemented as mentioned in section 4.3.1.2. Energy demand and LCC per kilogram of crop output for all the available cases were finally compared relative to the base case of AGB to identify the best optimal cases. The complete optimization methodology is explained in Figure 4-6.

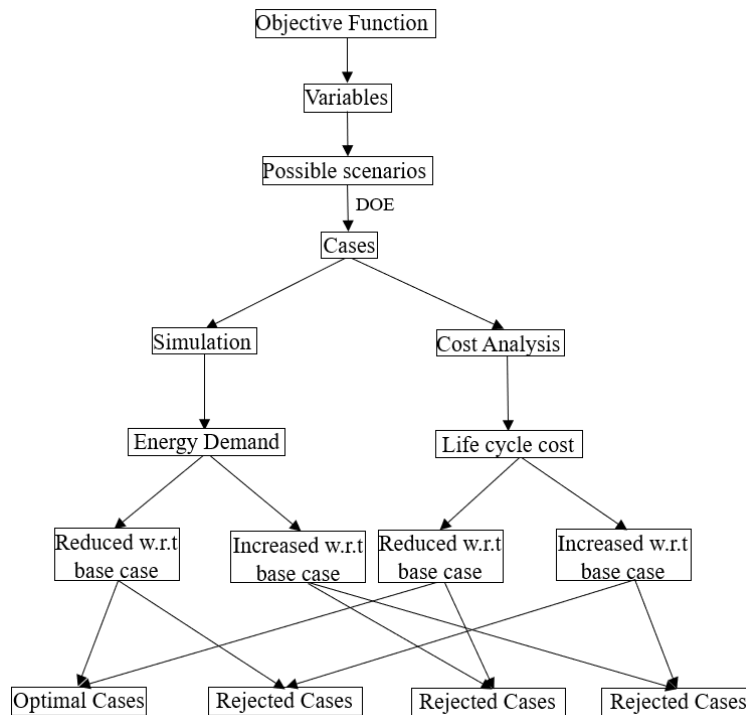
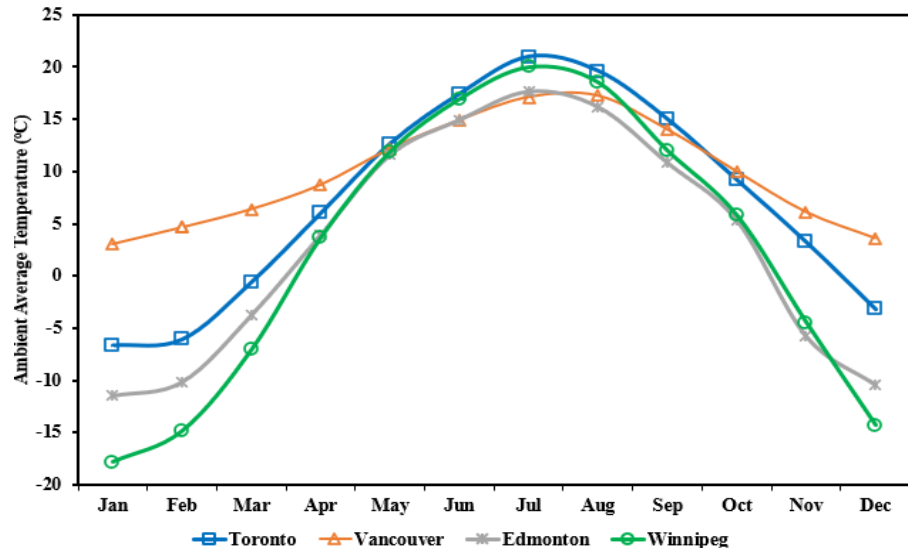


Figure 4-6 Represents the process of complete optimization methodology

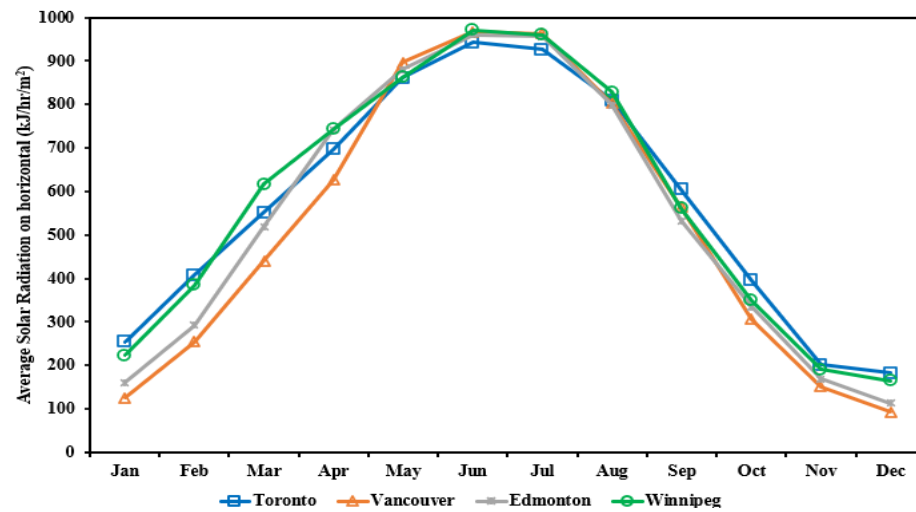
4.3.3 Regional Assessment of AGB

The study also examines the performance of AGB across different Canadian locations such as Toronto, Vancouver, Winnipeg, and Edmonton. It is important to understand that the

greenhouse performance is largely affected by factors like ambient temperature, intensity and duration of solar radiation, transmission of solar radiation inside the greenhouse, overall heat transfer coefficient, type of covering material, wind speed, and direction, and the specific crop being cultivated (Ali, 2008). With the location change, weather conditions are also altered like ambient temperature, solar radiation intensity and duration, and wind speed and direction. The change in weather parameters across different locations is depicted in Figure 4-7.



a)



b)

Figure 4-7 Variation of weather parameters for different locations under study (a) Average ambient temperature (°C) (b) Average solar radiation on horizontal (kJ/hr/m²)

Figure 4-7 illustrates the variation in average ambient temperature and average horizontal solar radiation across different locations. Vancouver (49.25°N, -123.25°E) stands out as having a higher average ambient temperature compared to other locations along with lesser solar radiation intensity during the winter months when heating demand is highest. The ambient temperature profiles of Edmonton (53.5°N, -114.1°E) and Winnipeg (49.9°N, -97.23°W) are quite similar, both characterized by extremely cold conditions with negative temperatures. Toronto (43.8°N, -79.5°E) appears to be a more moderate location, with temperatures ranging from about -7°C in winter to 22°C in summer, along with adequate solar radiation. All the weather files used for the simulations were TMY-2 data from the TRNSYS weather library (TRNSYS-18 Weather data, 2017).

The energy simulations on AGB with various Canadian locations were conducted. Toronto location was used as the baseline location with lettuce crops as the reference case, and variations were analyzed relative to this scenario. Additionally, it is important to note that the costs of natural gas and electricity differ across provinces in Canada, as indicated in Table 4-7.

Table 4-7 Unit cost of natural gas and electricity for different locations

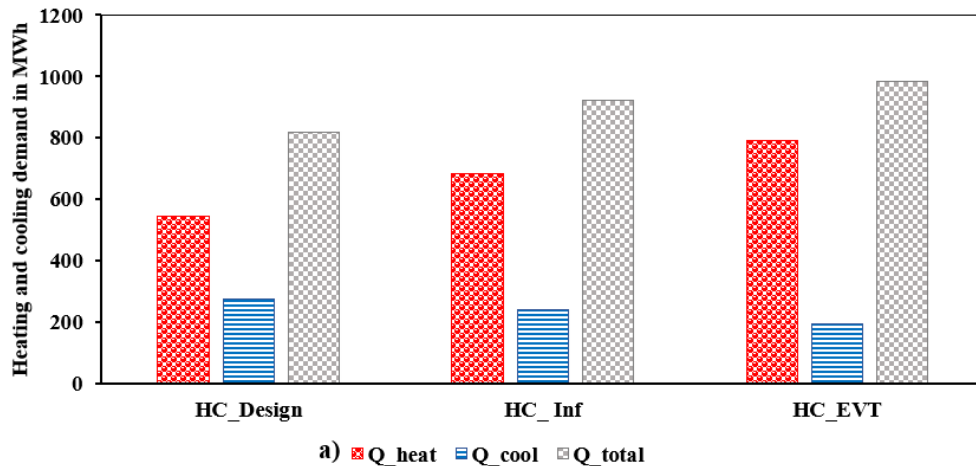
Locations	Natural Gas (Cents/kWh)	Electricity (Cents/kWh)
Toronto, ON	5.58	13.03
Vancouver, BC	4.82	11.4
Edmonton, AB	7.25	25.8
Winnipeg, MB	5.86	10.2
Reference	Canada Energy Regulator (2023)	Energy hub (2023)

4.4 Results and Discussion

All the simulations were performed for different cases received from optimization, including the AGB base case and CG. The simulation runtime was considered as 3 years. However, the results were taken for 1 year, which are the values of 2nd year. The objective was to simulate the effects of greenhouse air for 1 year so that actual working conditions could be developed. This section explores the performance of the energy-efficient design of AGB with CG. It further includes the results of the optimization study. The primary focus of this study was to estimate the energy demand of the facility. The actual heating and cooling input to the facility needs to account for the efficiency of the heating and cooling systems.

4.4.1 Performance Assessment for AGB

The performance of AGB and the effects of design, process, and energy-conserving parameters are illustrated in Figure 4-8(a). The results indicated that incorporating infiltration in greenhouse modeling increased heating energy demand by 25% while reducing the cooling demand by 13% because of air leakage to the GS from the external environment. An increment of 12% in the total heating and cooling requirement was observed. Furthermore, the effect of evapotranspiration was also seen in Figure 4-7a, which showed that evapotranspiration created a cooling effect in the growing environment which further reduced the cooling demand by 29% and increased the heating demand by 45%, with a total change in the heating and cooling consumption by 20%. These results revealed the importance of infiltration and evapotranspiration to accurately estimate the greenhouse energy demand. Figure 4-8(b) indicates the use of energy-conserving parameters such as natural ventilation, thermal curtains, and shade curtains in optimizing the heating and cooling demand of the AGB. The total heating and cooling demand was reduced by 30% when only natural ventilation was considered, 52% when only a thermal curtain was installed as per thermal curtain schedule 1, and 34% when only a shade curtain was installed as per shade curtain schedule 1. The results when natural ventilation, thermal curtains, and shade curtains were installed together reduced the heating load by 54%, the cooling load by 71%, and the total energy demand by 58%. The results showed that installing energy-efficient parameters can lead to reducing the energy requirement of the facility.



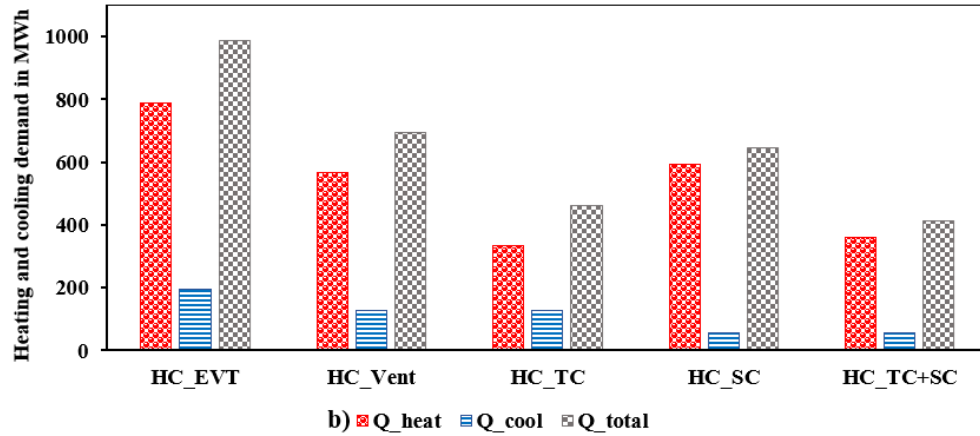


Figure 4-8 Graphs representing the effects of design parameters, process parameters, and energy-conserving parameters on the heating and cooling demand of AGB. (a) Effects of design, infiltration (inf), and evapotranspiration (evt) (b) Effects of natural ventilation (vent), thermal curtain (TC), shade curtain (SC), and combined parameters (TC+SC)

4.4.2 Performance Assessment for CG

The performance graph for the CG is presented in Figure 4-9. The results showed that the heating and cooling requirement for CG is significantly high i.e. approximately 2400 MWh of heating and 1400 MWh of cooling for the design aspect. It is evident that the design of CG is not energy-efficient, and it consumes more heating and cooling to grow the same crop output. This is also because the volume of CG is three times more than the volume of GS of the AGB. Therefore, new greenhouse designs are being developed to grow crops in layers that would increase the crop output. The effect of infiltration and evapotranspiration can be seen in the results of CG. The heating and cooling requirements were elevated by 27% when infiltration and evapotranspiration were considered while natural ventilation helped to minimize the energy demand by 3%.

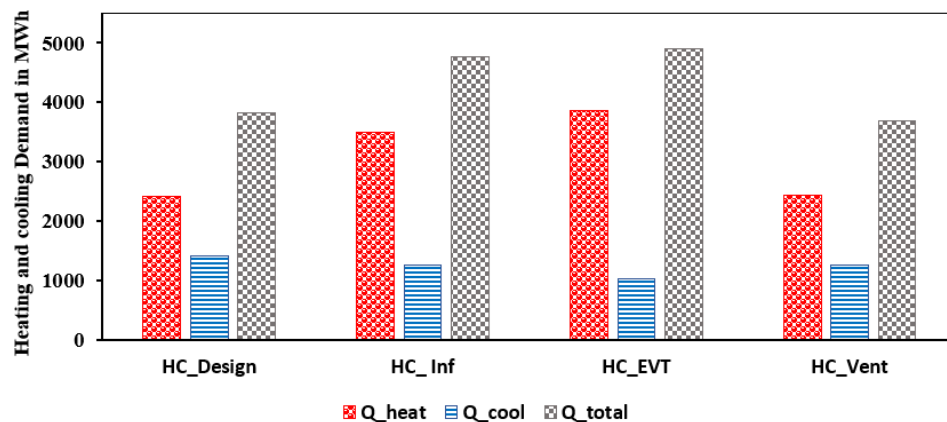


Figure 4-9 Graphs representing the effects of design parameters, process parameters, and energy-conserving parameters on the heating and cooling demand of CG.

4.4.3 Comparison of performance and LCC for AGB and CG

The comparison of heating and cooling demand and LCC between AGB and CG is illustrated in Figure 4-10. The heating and cooling requirements per kilogram for CG was approximately 20.2 kWh/kg while that of the AGB was around 2.27 kWh/kg, which was approximately 10 times less. This difference in the heating and cooling demand per kilogram of the crop was because of the advanced construction material, design, and energy-conserving parameters including natural ventilation, thermal curtains, and shade curtains implemented in the AGB. Despite having the same crop output, the volume for CG was more than the AGB, which also increased the heating and cooling demand of CG. The results further indicated that AGB was approximately 88% more energy-efficient than CG. Additionally, AGB had the advantage of OS which limits the heat interaction between the GS and the external environment. Since AGB was constructed using advanced construction materials such as insulated metal panels, photovoltaic glass, and triple-walled polycarbonate, the installation cost for AGB was 51% more than that of CG. Despite higher installation costs, the life-cycle cost of the AGB was 56% less than the CG. This indicates that the AGB can be cost-effective in the long term with lower heating and cooling demand. This will also lead to less use of natural gas and electricity, eventually minimizing the GHG emission. However, these results have a limitation in that they purely include thermal analysis to calculate the energy demand. However, the total energy demand also accounts for the cost of electricity to run the artificial lights which are predominantly required in AGB as crops are grown in layers and sufficient light is not available for all the crops. Hence, the analysis will be complete when the cost of electricity for artificial light is accounted.

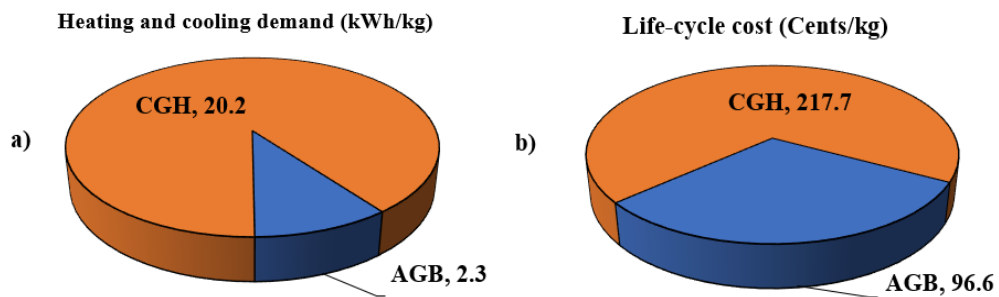


Figure 4-10 Comparison of performance and LCC for AGB and CG (a) Heating and cooling demand in kWh/kg (b) Life-cycle costs in Cents/kg

4.4.4 Comparison of performance and LCC of individual possible scenarios

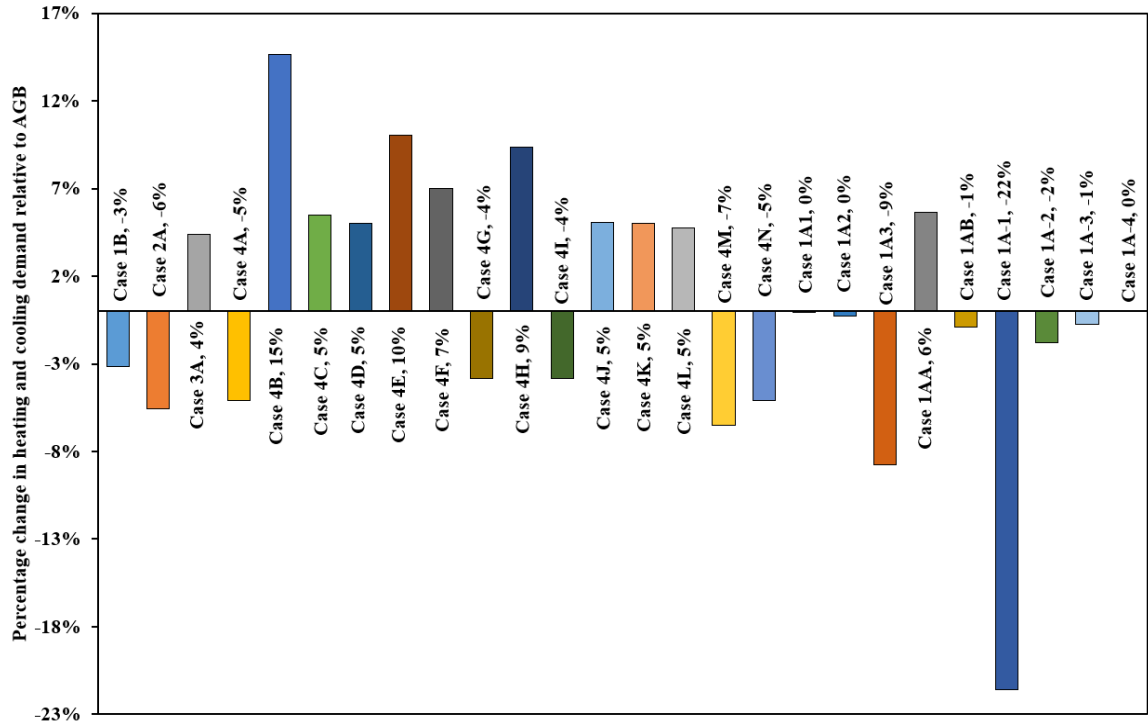
This section compares the effects of individual possible scenarios considered under the optimization study. The best possible scenario (Case 1A-1) to minimize the energy requirement was to change the thermal curtain from schedule 1 to schedule 2, reducing the heating and cooling requirements by 22%. The additional advantage of changing the schedule was that there was no increase in the installation cost of the facility. The best possible scenario (Case 4L) to minimize the LCC was to use a horticultural glass of 10 mm thickness in the outer glazing. This would lead to a decrease in LCC by 14% relative to the base case. However, using horticultural glass increases energy demand by 5%. Table 4-8 details the comparison of all the possible scenarios under the optimization study.

Table 4-8 Comparison of performance and LCC for possible scenarios relative to AGB

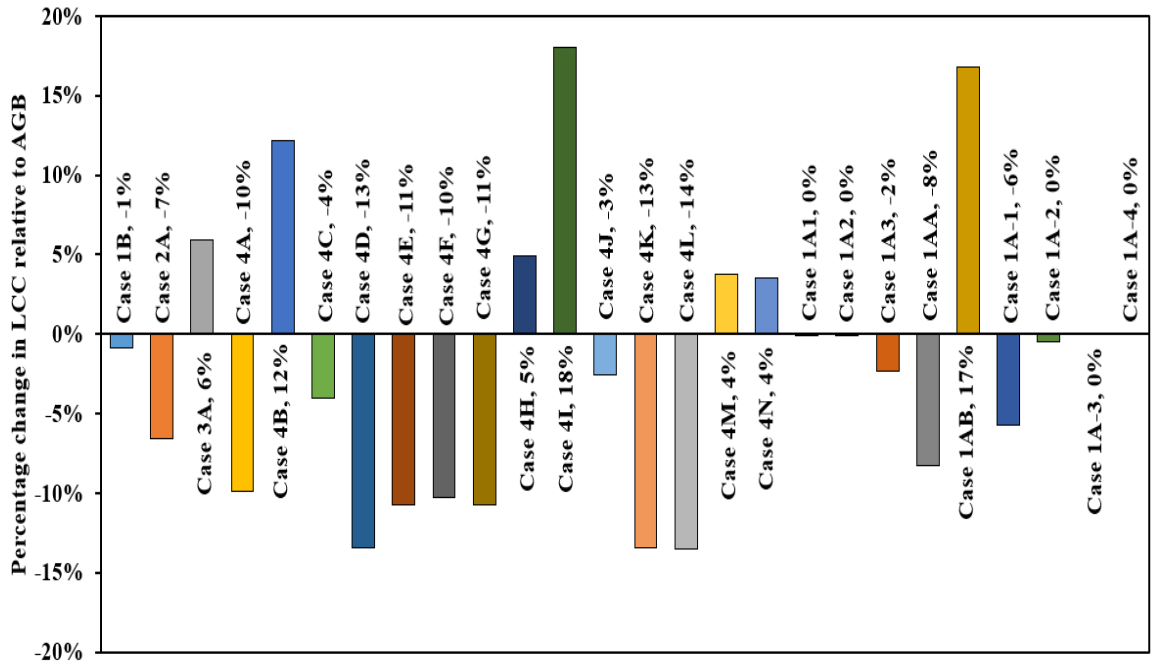
Possible scenarios	Cases	Variation in energy demand	Variation in LCC	Reasons
E-W	Case 1A	-	-	Base case
15° NOE	Case 1B	-3%	-1%	The advantage of capturing more solar radiation
Profile 1	Case 1A	-	-	Base case
Profile 2	Case 2A	-6%	-7%	More crop output – reduced energy demand and LCC per kilogram
Profile 3	Case 3A	4%	6%	Less crop output – increased energy demand and LCC per kilogram
PC(28 mm)+PV glass (19 mm)	Case 1A	-	-	Base case
PC (28 mm)	Case 4A	-5%	-10%	Better thermal properties at a lower cost
PV glass (19 mm)	Case 4B	15%	12%	Worst thermal properties + expensive material
PVC (1.8 mm)	Case 4C	5%	-4%	Slight increase in energy demand but have the advantage of lower capital cost
HG (6 mm)	Case 4D	5%	-13%	
PC (4 mm)	Case 4E	10%	-11%	
PC (10 mm)	Case 4F	7%	-10%	
PC (16 mm)	Case 4G	-4%	-11%	Better thermal properties at a lower cost
PV glass (6 mm)	Case 4H	9%	5%	Worst thermal properties + expensive material
PV glass (26 mm)	Case 4I	-4%	18%	Better thermal properties but has an expensive material
PVC (3.18 mm)	Case 4J	5%	-3%	
HG (4 mm)	Case 4K	5%	-13%	

HG (10 mm)	Case 4L	5%	-14%	Slight increase in energy demand but have the advantage of lower capital cost
PC(28 mm)+PV glass (26 mm)	Case 4M	-7%	4%	Better thermal properties but has an expensive material
PC(16 mm)+PV glass (26 mm)	Case 4N	-5%	4%	
PE (0.1 mm)	Case 1A	-	-	Base case
PE (0.05 mm)	Case 1A1	0%	0%	Neither a reduction in energy demand nor LCC
PE (0.15 mm)	Case 1A2	0%	0%	
Double PE layer (2 mm)	Case 1A3	-9%	-2%	More better heat retention in GS at almost the same capital cost.
Original thickness	Case 1A	-	-	Base case
50% thickness reduction	Case 1AA	6%	-8%	Increases energy demand because of more heat loss from the north side - reduced LCC by around \$ 200,000.
50% thickness increment	Case 1AB	-1%	17%	Reduces energy demand because of less heat loss from the north side - increased LCC by around \$ 345,000.
TC Schedule -1	Case 1A	-	-	Base case
TC Schedule -2	Case 1A-1	-22%	-6%	Reduces energy demand significantly without increasing capital cost.
SC Schedule -1	Case 1A	-	-	Base case
SC Schedule -2	Case 1A-2	-2%	0%	The effect of changing the SC schedule was not significant
Original vents size	Case 1A	-	-	Base case
Vents size increased by 50%	Case 1A-3	-1%	0%	Increasing the vent size reduced the energy demand, but the effect was not significant.
Vents size increased by 100%	Case 1A-4	0%	0%	

Some scenarios did not influence the energy requirements as well as the LCC such as the PE layer with 0.05 mm thickness, the PE layer with 0.15 mm thickness, shade curtain schedule 2, and increasing the ventilation vents sizes. Since they did not affect the objective function, they were removed from the optimization study. The cases and the influence factor in percentage for different possible scenarios are indicated in Figure 4-11.



a)



b)

Figure 4-11 Comparison of performance and LCC for different possible scenarios (a) Heating and cooling demand per kilogram w.r.t the base case (b) Life-cycle costs per kilogram w.r.t the base case

4.4.5 Optimal cases from the optimization

The identified cases in the optimization study were simulated to identify the energy demand per kilogram of crop out and LCC per kilogram of crop output. The distribution of these cases is indicated in Figure 4-12. The life-cycle cost in cents per kilogram is shown in the Y-axis and the heating and cooling demand in kWh/kg is indicated in the X-axis. The origin of this graph represents the heating and cooling demand and LCC of the base AGB design. All the cases falling to the left-lower corner in the green zone are optimal cases i.e. they reduce both energy demand and LCC per kilogram of crop output, while the cases falling to the upper right corner in the red zone are the rejected cases because they increase both the energy demand and the LCC. The cases that come under the upper-left corner and the lower-right corner are the ones that are either increasing the energy demand or increasing the LCC. These cases were rejected because they do not comply with the objective of the optimization study.

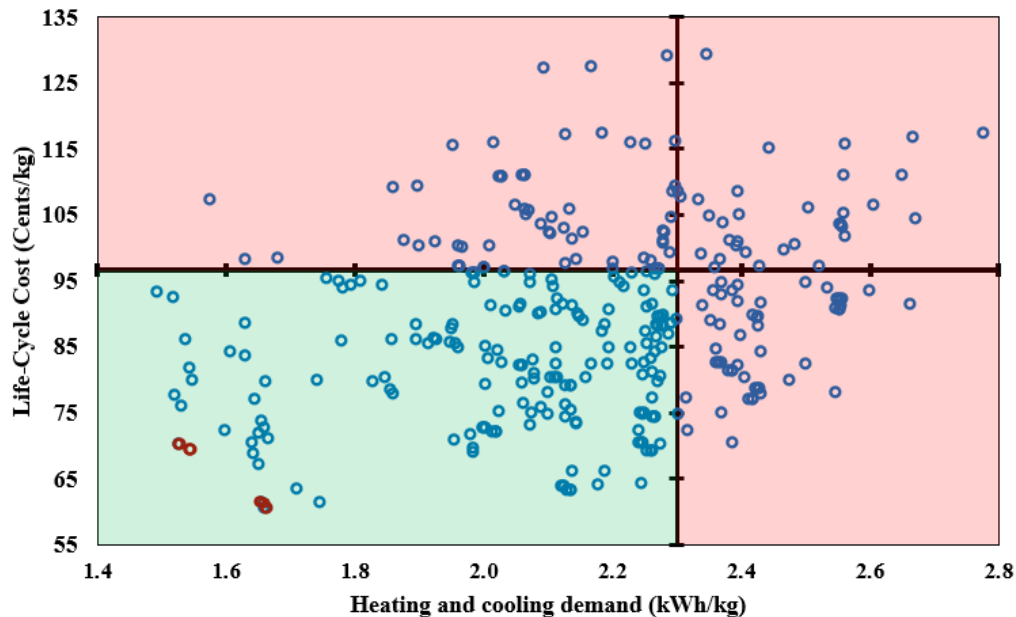


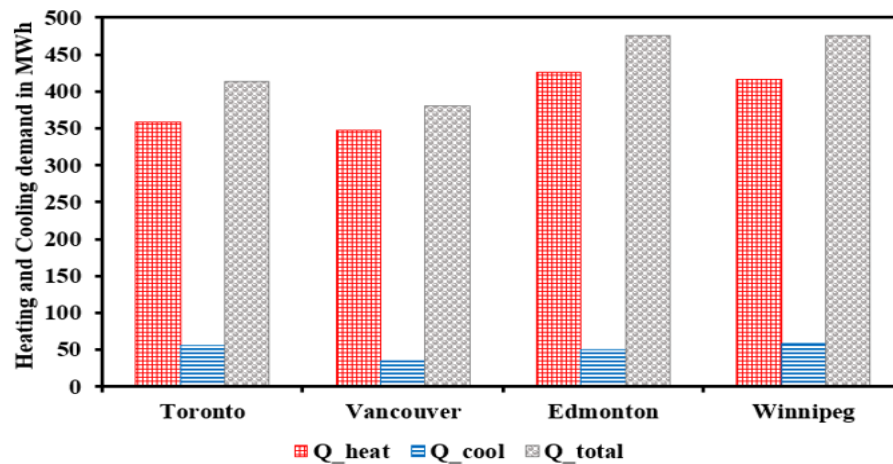
Figure 4-12 Distribution of all cases considered under optimization study

The cases that are to the extreme left and lower corner marked in red in Figure 4-12 represent the best optimal cases with the least energy demand and the LCC. The cases 6D3A-1, 6K3A-1, and 6L3A-1 were the combination of best possible scenarios that include profile 2, with east-west orientation. All three cases used horticultural glass in the outer glazing with thicknesses 4 mm, 6mm, and 10 mm, indicating that thickness does not substantially vary the heating and cooling demand and the LCC. Additionally, these cases

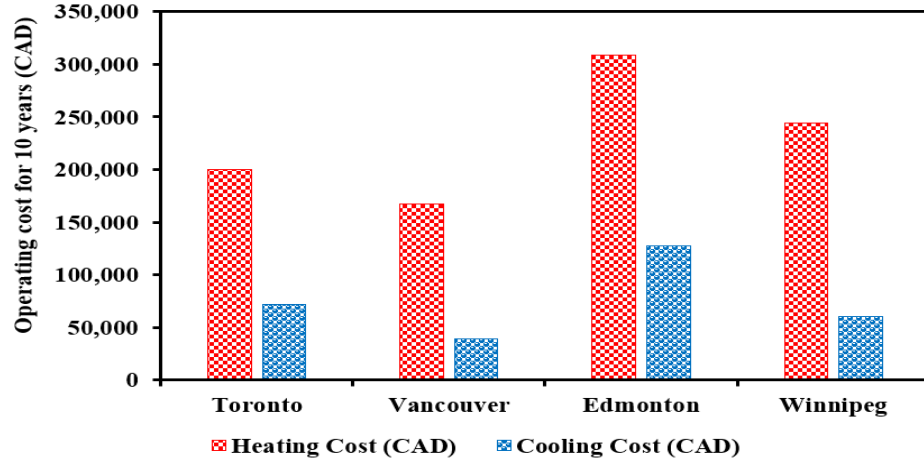
incorporated a double-layer polyethylene layer in the inner glazing with a 50% reduction in the thickness of opaque surfaces. The thermal curtain was operated using schedule 2 in all three cases. The results also showed that the energy demand of the optimal AGB designs will be 27% more energy-efficient than the base case AGB. Furthermore, the LCC was also reduced further by 37%, indicating the benefits of using cheaper horticultural glass.

4.4.6 Performance of AGB with variation in locations

The results indicated that Vancouver was the most favorable location for growing lettuce, as it had the lowest heating and cooling requirements. The total energy demand in Vancouver was approximately 381 MWh, which was 8% lower than in Toronto. This is due to Vancouver's favorable external weather conditions for crop growth. In contrast, both Edmonton and Winnipeg have a total energy demand of 476 MWh, about 15% higher than Toronto's energy demand. However, the heating and cooling demand differs between these two locations, with Edmonton requiring more heating and less cooling, likely due to its lower solar radiation availability. These results are further influenced by variations in the cost of natural gas and electricity across locations. Vancouver's lower energy prices make it even more advantageous for crop production by reducing operating costs by 24%, while Edmonton's high energy requirements and unit costs make it less favorable, resulting in a 60% increase in total costs over 10 years of operation as depicted in Figure 4-13. In addition to heating and cooling requirements, adequate light availability is crucial for any greenhouse facility. According to weather data, Vancouver receives comparatively less solar radiation than other locations, leading to higher costs for artificial lighting.



a)



b)

Figure 4-13 Variation in performance and operating costs for AGB in different locations. (a) Heating and cooling demand in MWh (b) Operating cost for 10 years in Canadian Dollars

4.5 Conclusion

This research focused on the development of a greenhouse facility designed to be more energy-efficient than CG. The design of AGB was inspired by a CSG but included an additional zone between the GS and the ambient environment. AGB was designed to incorporate design parameters like advanced construction materials, and energy-conserving parameters like natural ventilation, thermal, and shade curtains. The energy modeling was performed to analyze the energy demand of the AGB and CG. Moreover, an optimization study was executed using modified binary optimization, that identified the possible scenarios that substantially affected the heating and cooling demand or the LCC. The possible scenarios that most affected these two parameters were taken forward to combine with other best scenarios to identify the best optimal design. The outcomes of this study are as follows:

- 1) AGB proved to be 88% more energy efficient as compared to CG by using energy-efficient materials, natural ventilation, thermal curtains, and shade curtains.
- 2) AGB uses advanced and expensive materials in its construction, and as a result, the installation cost of CG was 51% less as compared to the AGB.
- 3) The LCC for the AGB was 56% less than the CG. Despite having a high installation cost, the operating cost for the AGB was less. This shows that AGB can be cost-effective in the long term, along with reducing GHG emissions.

- 4) Using high-quality materials for greenhouse envelopes not only reduces energy demand but also increases the installation costs drastically. This is reflected in the best optimal cases also.
- 5) The best optimal AGB design was 27% energy-efficient with a 37% reduction in LCC. The major contribution in reducing the heating and cooling requirements was because of double layer PE and schedule 2 while using HG and reducing the opaque surface thickness by 50% reduced the LCC.

The optimal design indicates that these energy-efficient measures significantly influence the energy requirement and the LCC. This study utilized average TMY (Typical Meteorological Year) files for various locations in the simulations, rather than relying on weather data from a single year. As a result, the analysis accounts for variations in weather conditions over several years. Additionally, the cost of additional energy was assumed to be constant, though it may fluctuate in the future. Therefore, an appropriate factor should be applied to adjust costs for future projections. This study mainly focused on maintaining an optimal temperature inside the GS. However, to maintain an optimal condition for plant growth other parameters like relative humidity, supplemental lighting, CO₂ concentration, and air velocity need to be balanced. Further, this study used TRNSYS software for simulations, which does not encompass uniformity analysis. Hence, a more detailed study is required to see the distribution of these parameters inside the GS. This study can further be extended to simulate the latent energy demand to balance relative humidity. The results of this study are subjected to change when artificial light analysis is considered. Since AGB grows crops in layers, a sufficient amount of light would be required for the plant to grow optimally. The cost of electricity to run the artificial lights in the AGB would be tremendously higher compared to that of CG and may also affect the heating and cooling load. This research will help the researchers and growers to understand the effects of infiltration and evapotranspiration in the GS, along with the parameters that significantly affect the energy requirement and LCC.

4.6 References

Adesanya, M. A., Na, W. H., Rabi, A., Ogunlowo, Q. O., Akpenpuun, T. D., Rasheed, A., Yoon, Y. C., Lee, H. W., (2022) "TRNSYS simulation and experimental validation of

internal temperature and heating demand in a glass greenhouse,” *Sustainability*, Vol, 14, 8283.

Ahamed, M. S., Guo, H., Tanino, K., (2018) “Energy-efficient design of greenhouse for Canadian Prairies using a heating simulation model,” *International Journal of Energy Research*, Vol. 42, pp. 2263-2272.

Ahamed, M. S., Guo, H., Tanino, K., (2019) “Energy saving techniques for reducing the heating cost of conventional greenhouses,” *Biosystems Engineering*, Vol 178, pp. 9-33.

Ahmed, H. A., Xin, T. Y., Chang, Y. Q., (2020) “Optimal control of environmental conditions affecting lettuce plant growth in a controlled environment with artificial lighting: A review,” *South African Journal of Botany*, Vol 130, pp. 75-89.

Ali, S. A., (2008) "Modeling of solar radiation available at different orientations of a greenhouse," Agriculture Engineering Department.

Bartok, J. W., (2015) “Natural ventilation guidelines,” *Greenhouse Management* (Source: [Natural ventilation guidelines - Greenhouse Management \(greenhousemag.com\)](http://greenhousemag.com))

Benke, K., Tomkins, B., (2017) “Future food-production systems: vertical farming and controlled environment agriculture” *Sustainability: Science, Practice, and Policy*, Vol 13:1, pp. 13-26.

Beaulac, A., Lalonde, T., Haillet, D., Monfet, D., (2024) “Energy modeling, calibration, and validation of a small-scale greenhouse using TRNSYS,” *Applied Thermal Engineering*, Vol 248, 123195.

Blasco, X, Martinez, M, Herrero, J. M., Ramos, C., Sanchis, J., (2007) “Model-based predictive control of greenhouse climate for reducing energy and water consumption,” *Computers and Electronics in Agriculture*, Vol, 55(1), pp. 49–70.

Bush, E., Lemmen, D. S., (2019) “Canada’s Changing Climate Report; Government of Canada”, Ottawa, ON. 444 p.

Canada Energy Regulator, (2022) “Data and analysis of Energy commodities,” (Source: [CER – Natural gas bills \(cer-rec.gc.ca\)](https://www.cer-rec.gc.ca/natural-gas-bills))

Canadian Gas Association, (2022) “Natural gas statistics,” (Source: [Natural Gas Statistics | Canadian Gas Association \(cga.ca\)](https://www.cga.ca/natural-gas-statistics))

Choab, N., Allouhi, A., Maakoul, A. E., Kousksou, T., Saadeddine, S., Jamil, A., (2021) “Effect of Greenhouse Design Parameters on the Heating and Cooling Requirement of Greenhouses in Moroccan Climatic Conditions,” IEEE Access, Vol 9, 3047851.

Climate Atlas of Canada, (2024) “Canada’s Cities and Climatic Change,” (Source: [Climate Change in Canada | Climate Atlas of Canada](https://climateatlas.ca/canada-cities-climatic-change))

Dong, S., Ahamed, M. S., Ma, C., Guo, H., (2021) “A time-dependent model for predicting thermal environment of mono-slope solar greenhouses in cold regions,” Energies 2021, 14, 5956.

Duralight Plastics (2024) “Multiwall Polycarbonate,” (Source: [Multiwall Polycarbonate - Duralight Plastics](https://www.duralight.com/multiwall-polycarbonate))

Electric Power Research Institute, (2018) “Indoor Agriculture: A utility, water, sustainability, technology, and market overview,” (Source: [www.epri.com/ - pages/product/000000003002014056/?lang=en.](https://www.epri.com/pages/product/000000003002014056/?lang=en))

Energy hub, (2023) “Electricity prices in Canada 2023,” (Source: [Electricity Prices in Canada 2023 \(energyhub.org\)](https://energyhub.org/electricity-prices-in-canada-2023))

Engler, N., Krarti, M., (2021) “Review of energy efficiency in controlled environment agriculture,” Renewable and Sustainable Energy Reviews, Vol 141, 110786.

Engler, N., Krarti, M., (2022) “Optimal designs for net zero energy-controlled environment agriculture facilities,” Energy and Buildings, Vol 272, 112364.

Food and Agriculture Organization (FAO), (2009) “How to feed the world in 2050,” UN Food and Agriculture Organization, Rome.

Focus Technology, (2024) “PE Waterproof Thermal Heat Insulation Warmer Quilt for Greenhouse,” Made-in-China (Source: [PE Waterproof Thermal Heat Insulation Warmer Quilt for Greenhouse - China PE Insulation Quilt and Customized Thermal Insulation \(made-in-china.com\)](#))

Fouli, Y., Hurlbert, M., Krobek, R., (2021) “Greenhouse gas emissions from Canadian Agriculture: Estimates and Measurements,” The School of Public Policy, Vol, 14:35.

Grand View Research, (2019) “Indoor farming market size, share and trends analysis report by facility type (greenhouses, vertical farms), by component (hardware, software), by crop category, by region, and segment forecasts,” (GVR- 3-68038-942-5). Retrieved from, <https://www.grandviewresearch.com/industry-analysis/indoor-farming-market>.

Gupta, M. J., Chandra, P., (2001) “Effect of greenhouse design parameters on conservation of energy for greenhouse environmental control,” Energy, Vol. 27, pp. 777-794

Insulation, UK (2024) “Celotex PIR Insulation Board (2400 mm x 1200 mm) All sizes,” (Source: [Celotex PIR Insulation Board | 2400mm x 1200mm | \(All Sizes\) | Insulation UK](#))

Khanuja, G., Ruparathna, R., Ting, D. S-K., “Enhancing solar insolation in agricultural greenhouses by adjusting its orientation and shape,” Clean energy for low-income communities: technology, deployment, and challenges, Chapter 8.

Liang, M. H., Chen, L. J., He, Y. F., Du, S. F., (2018) “Greenhouse temperature predictive control for energy saving using switch actuators,” IFAC-PapersOnLine, Vol 51, Issue 17, pp. 747-751

Lowth, M., (2023) “Solar glass, a building-integrated photovoltaic technology: Engineering innovation to generate solar-based electricity by replacing normal glass in buildings,” (Source: [Solar Glass, a building-integrated photovoltaic technology: Engineering innovation to generate solar-based electricity by replacing normal glass in buildings | by Marc Lowth | Medium](#))

Melancon, M., (2018) “US (GA): \$5 million to help reduce energy costs of Indoor Farming,” HortiDaily, September 11, 2018.

Mobtaker, H. G., Ajabshirchi, Y., Ranjbar, S. F., Matloobi, M., (2016) “Solar energy conservation in a greenhouse: Thermal analysis and experimental validation,” *Renewable Energy*, Vol 96, pp. 509-519.

Oliveira, J. B., Cunha, J. B., Oliveira, P. B. M., (2015) “A feasibility study of sliding mode predictive control for greenhouses,” *Optimal control applications and methods*, Vol 37, Issue 4, pp. 730-748.

Ontario Energy Board, (2022) “Ontario electricity rates,” (Source: [Electricity rates | Ontario Energy Board \(oeb.ca\)](https://www.ontarioenergyboard.ca/electricity-rates))

Onyx solar group, “Technical specifications for photovoltaic glass,” (Source: [TECHNICAL SPECIFICATIONS \(onyxsolar.com\)](https://www.onyx-solar.com/technical-specifications))

Pamungkas, A. P., Hatou, K., Morimoto, T., (2014) “Evapotranspiration model analysis of crop water use in plant factory system,” *Environmental Control in Biology*, 52(3), pp. 183-188.

Periodic table (2024) “Materials table,” (Source: [Material Properties | Website about Elements and Materials \(material-properties.org\)](https://www.material-properties.org/))

Pohlheim, H., Heibner, A., (1999) “Optimal Control of Greenhouse Climate using Real-World Weather Data and Evolutionary Algorithms,” *Proceedings of the Genetic and Evolutionary Computation Conference*, pp. 1672-1677.

Ramirez-Arias, A., Rodriguez, F, Guzman, J. L., Berenguel, M., (2012) “Multi-objective hierarchical control architecture for greenhouse crop growth,” *Automatica*, Vol 48(3), pp. 490–8.

Rasheed, A., Na, W. H., Lee, J. W., Kim, H. T., Lee, H. W., (2019) “Optimization of greenhouse thermal screens for maximized energy conservation,” *Energies*, Vol. 12, 3592.

Sartorius, (2020) “What is DOE? Design of Experiments Basics for Beginners,” *Science Snippets* (Source: [What is DOE? Design of Experiments Basics for Beginners \(sartorius.com\)](https://www.sartorius.com/what-is-doe))

Schimelpfenig, G., Smith, D., (2021) “Controlled Environment Agriculture Market Characterization Report, Supply Chains, Energy Sources and Uses, and Barriers to Efficiency,” Resource Innovation Institute and United States, Department of Agriculture.

Sethi, V. P., (2008) “On the selection of shape and orientation of a greenhouse: Thermal modeling and experimental validation,” *Solar Energy*, Vol. 83, pp. 21-38.

Statistics Canada, (2024) “Production and value of greenhouse fruits and vegetables,” (Source: [Production and value of greenhouse fruits and vegetables \(statcan.gc.ca\)](https://www150.statcan.gc.ca/n1/pub/26390270000000000001/00001-eng.htm))

Svensson, (2018) “Outdoor shading and weather protection SOLARO 5120,” (Source: [SOLARO 5120 O E AW | Find your screen | Svensson \(ludvigsvensson.com\)](https://www.ludvigsvensson.com/en/solaro-5120))

Tantau, H. J., Meyer, J., Schmidt, U., Bessler, B., (2011) “Low energy greenhouse – A system approach,” International Symposium on High Technology for Greenhouse Systems: GreenSys2009, *Acta Horticulturae*, 893, pp. 75-84

Tong, G., Christopher, D. M., Li, T., Wang, T., (2013) “Passive solar energy utilization: A review of cross-section building parameter selection for Chinese solar greenhouses,” *Renewable and Sustainable Energy Reviews* 26 (2013), pp. 540-548.

TRNFlow Manual, (2009) “A module of an airflow network for coupled simulation with Type-56 (multi-zone building of TRNSYS),” Version 1.4.

TRNSYS-18, (2017) “TRaNsient System Simulation program – Weather Data,” Volume 8, Solar Energy Laboratory, University of Wisconsin-Madison.

Vadiee, A., Martin, V., (2013) “Energy Analysis and thermo-economic assessment of the closed greenhouse – The largest commercial solar building,” *Applied Energy*, Vol 102 (2013), pp. 1256-1266.

Typical Meteorological Year, (2024) “Wikipedia The free encyclopedia for a typical meteorological year,” (Source: [Typical meteorological year - Wikipedia](https://en.wikipedia.org/wiki/Typical_meteorological_year))

Xu, Z. T., Yao, Z. Y., Chen, L. J., Du, S. F., (2013) "Greenhouse air temperature predictive control using the dynamic matrix control," Fourth International Conference on Intelligent Control and Information Processing, pp. 349-353.

Younes, C., Shdid, C. A., Bitsuamlak, G., (2011) "Air infiltration through building envelopes: A review," Journal of Building Physics, Vol 35, Issue 3.

CHAPTER 5

CONCLUSIONS, RECOMMENDATIONS, AND FUTURE WORKS

This research provides insight into CEA, which can be employed in the future as a sophisticated solution to conventional agriculture, as it has many benefits over conventional agriculture. It can offer biosecurity, clean and green crops year-round, and reduced transportation costs and distance, which would ultimately reduce fossil fuel consumption. However, the success of CEA will be subject to reduced energy consumption, minimum capital costs, and minimizing greenhouse gas emissions. This research was conducted in three phases to resolve these problems.

Firstly, energy-efficient parameters including greenhouse orientation, roof inclinations, and greenhouse shapes were identified which alters the solar insolation availability on the greenhouse surfaces. Some parameters have a major impact on solar insolation availability such as greenhouse shapes and roof inclinations. However, some parameters do not have much effect on the solar insolation falling on the greenhouse such as greenhouse orientation. For a greenhouse located in Toronto, Ontario, 30° North of East was the best orientation to increase solar radiation availability. The solar radiation percentage difference between the maximum (30° North of East) and minimum (east-west orientation) solar radiation availability for different greenhouse orientations was only 0.6%. The results indicated that the south side receives maximum solar radiation during the winter months which was 50% to 70% more as compared to the other greenhouse surfaces. Roof inclination played a major role in optimizing solar radiation availability. The increase in the inclination of the south roof leads to an increase in solar radiation availability, resulting in approximately 40% more solar radiation availability. The solar radiation percentage difference between the maximum (single span) and minimum (semi-circular) solar radiation availability for different greenhouse shapes was approximately 17%. This preliminary study would help to make greenhouses in cold climates more sustainable, by capturing more solar insolation falling on the roofs and walls of the greenhouse, which could be used for greenhouse heating.

Secondly, this research demonstrated the importance of energy modeling for the greenhouse industry. Due to the lack of comprehensive energy modeling guidelines, this study provided an in-depth energy modeling process for greenhouses. The study further indicated the importance of modeling parameters such as weather conditions, greenhouse models, solar distribution within the greenhouse, evapotranspiration, infiltration, and energy-efficient parameters. This research validated an experimental CSG using the proposed methodological framework to check the accuracy of the greenhouse energy model. The energy modeling had limitations in modeling the real experimental conditions of the greenhouse because of the absence of crucial data such as precise information on natural ventilation, and accurate weather data for the year 2017. The simulation results were in close compliance with measured values. The validation results reveal that the mean predicted error between the measured and the simulated internal air temperature was only 1.6%. Additionally, the RMSE was approximately 1.4 kWh, and the MAE was 0.7 kWh while calculating the supplemental heating. This demonstrated that the greenhouse energy model was accurate and can be relied upon for further simulation processes.

Lastly, the insights gained from the preliminary study were used to develop an energy-efficient design for an AGB, incorporating design parameters like advanced construction materials, process parameters like infiltration and evapotranspiration, and energy-conserving parameters like natural ventilation, thermal, and shade curtains. AGB proved to be 88% more energy efficient compared to CG. However, the installation cost of CG was 51% less as compared to the AGB, because AGB used advanced and expensive materials in its construction. The LCC for the AGB was 56% less than the CG. Despite having a high installation cost, the operating cost for the AGB was less. This shows that AGB could be cost-effective in the long term, along with reducing GHG emissions. Moreover, an optimization study was executed using modified binary optimization, that identified the possible scenarios that substantially affected the heating and cooling demand or the LCC. The best optimal AGB design was 27% energy-efficient with a 37% reduction in LCC. The major contribution in reducing the heating and cooling requirements was because of double layer PE and schedule 2 while using HG and reducing the opaque surface thickness by 50% reduced the LCC.

5.1 Contributions

The major contributions of this thesis are as follows:-

- 1) The development of reliable guidelines for greenhouse energy modeling to accurately simulate and replicate dynamic greenhouse conditions. These guidelines address the current lack of comprehensive energy modeling literature, enabling researchers to predict energy requirements and assess the economic viability and profitability of greenhouses in advance.
- 2) The development of an energy-efficient greenhouse design featuring a double envelope along with advanced envelope design, construction material, natural ventilation, thermal curtains, and shade curtains proved to be 88% more energy-efficient compared to a conventional greenhouse.
- 3) Highlighting the performance of energy-efficient greenhouse designs across various provinces in Canada, considering the significant impact of diverse external weather conditions on the internal environment of greenhouses.
- 4) Integrating a methodology to accurately model evapotranspiration within greenhouses for precise heating and cooling requirements, addressing the complexity that led many studies to either eliminate it or assume constant evapotranspiration rates.
- 5) Identifying energy-efficient parameters that significantly impact heating, cooling requirements, and life-cycle costs within greenhouses. This will provide researchers and growers with a deeper understanding of energy efficiency measures and help optimize greenhouse energy demand.

5.2 Limitations and Future-works

Some of the identified limitations and potential areas for future research in this study are as follows:

- 1) While the proposed methodology for greenhouse modeling accurately predicted internal air temperature, significant discrepancies were found in estimating ground and north wall temperatures. This indicates the need for a more refined modeling tool to estimate these and other parameters more precisely.

- 2) The simulation tool TRNSYS was used to simulate the thermal performance of greenhouses; however, it lacked uniformity analysis, meaning it does not account for temperature distribution within the greenhouse space. To address this, a CFD tool such as ANSYS or COMSOL could be employed to analyze the distribution of temperature and other variables inside the greenhouse.
- 3) The results of the AGB design may vary when the impact of artificial lighting is included in the energy modeling. Since AGB grows crops in layers, adequate lighting is necessary for optimal plant growth. The cost of electricity for artificial lighting in the AGB would be significantly higher than in conventional greenhouses, potentially reducing some of the AGB's energy efficiency.
- 4) This study primarily focused on maintaining optimal temperatures within the greenhouse structure. However, achieving optimal plant growth requires balancing other factors, such as relative humidity, supplemental lighting, CO₂ concentration, and air velocity. Future research could explore strategies for balancing these variables to create optimal growing conditions in the greenhouse while minimizing life-cycle costs.

APPENDICES

Appendix A COMPREHENSIVE INFORMATION TO MODEL ADVANCED GROWING BUILDING

The appendix of the paper includes additional information required to support the work in the main paper.

A.1 Details of AGB and CG

The physical details of the AGB and CG are explained in Table A-1. The AGB was designed to combine the advantages of both vertical farms and conventional greenhouses. The south side consists of glazing, which allows for increased interception of solar radiation, a characteristic common in conventional greenhouses. Meanwhile, the north side is insulated with crops grown in layers, as typically observed in vertical farms. Assuming that the AGB incorporates the benefits of a vertical farm, the canopy unit yield was assumed as 76 kilograms of lettuce per m² per year (Eden Green Technology, 2023), which determined the canopy area.

Table 5-1 Represents the physical details of the AGB and CG

Parameters	AGB	CG
Annual lettuce output	182,172 kg	182,172 kg
Canopy Area	2397 m ²	2760 m ²
Footprint	2767 m ²	4691 m ²
Length (L) x Breadth (B) x Height (H)	178.5 m x 15.5 m x 10 m	51.2 m x 91.6 m x 4.6 m
GS volume	11336 m ³	20648 m ³
OS volume	9127 m ³	-
Number of layers	3	1

A.2 Modeling of evapotranspiration

Evapotranspiration is the process of plant transpiration within a greenhouse. Many studies did not consider the effects of plants or assume a constant evapotranspiration rate due to the complexity of modeling the dynamic nature of plants, leading to huge inaccuracies in predicting the energy requirements (Ahamed *et. al.*, 2019). Plants have a thermal capacity to absorb solar radiation, transferring less heat to the internal air. Since it was difficult to simulate the changing LAI throughout the year, an average LAI is often used for energy

modeling. LAI is defined as the ratio of total leaf area (m²) to ground area (m²). The crops grow to their maximum extent during the mid-season; therefore, most studies assume the LAI and crop coefficient for the mid-season. The reference crop evapotranspiration (ET_o) is estimated using the Stanghellini model suitable for closed greenhouses where the wind speeds are typically less than 1 m/s (Pamungkas *et.al.*, 2014) and is given by equation (A-1). Table A-2 was used to calculate the individual terms of this equation. The crop coefficient (K_c) was multiplied by the reference evapotranspiration rate given by equation (A-2). The crop coefficient for mid-season conditions is around 1.10 ± 0.04 (Pamungkas *et.al.*, 2014).

$$ET_o = 2 \times LAI \times \frac{1}{\lambda} \times \frac{s \times (R_n - G) + K_t \frac{VPD \times \rho \times C_p}{r_a}}{s + \gamma \left(1 + \frac{r_c}{r_a}\right)} \dots\dots\dots (A - 1)$$

$$ET_{actual} = K_c \times ET_o \dots\dots\dots (A - 2)$$

Table 5-2 List of parameters, symbols, and formulas used for determining ET_o using the Stanghellini model.

Parameters	Symbol	Formula	Units	References
Saturation vapor pressure	e _s	$e_s = 0.61078 \times \exp\left(\frac{17.269 T}{237.3 + T}\right)$	kPa	Pamungkas <i>et. al.</i> , (2014)
Actual vapor pressure	e _a	$e_a = \frac{e_s \times RH}{100}$		
Vapor pressure deficit	VPD	$VPD = e_s - e_a$		
Slope of the saturation vapor pressure curve	s	$s = 0.04145 \times \exp^{(0.06088.T)}$	kPa/°C	
Atmospheric pressure	P	P = 101.325	kPa	-
Latent heat of vaporization	λ	λ = 2.26	MJ/kg	-
Specific heat of air	C _p	C _p = 0.001013	MJ/kg °C	Pamungkas <i>et. al.</i> , (2014)
Psychrometric constant	γ	$\gamma = \frac{C_p P}{\epsilon \lambda}$	kPa/°C	Donatelli <i>et. al.</i> , (2005)
Atmospheric density	ρ	ρ = 1.204	kg/m ³	-

Leaf Temperature	T_o	$T_o = 2.52 + (0.84 \times T) + (-0.54 \times VPD)$	°C	Pamungkas <i>et. al.</i> , (2014)
Canopy resistance	r_c	$r_c = \frac{100}{0.5 \times LAI}$	s/m	
Aerodynamics resistance	r_a	$r_a = \frac{665}{1 + 0.54 \times U}$		Donatelli <i>et. al.</i> , (2005)
Net radiation	R_n	$R_n = R_{ns} - R_{nl}$	MJ/m ² /hr	Pamungkas <i>et. al.</i> , (2014)
Net shortwave radiation	R_{ns}	$R_{ns} = (0.07 \times GLSR)/1000/CA$		
Net outgoing longwave radiation	R_{nl}	$R_{nl} = \frac{(0.16)(3600) \rho \times C_p \times (T - T_o)}{r_R}$		
Radiative resistance	r_R	$r_R = \frac{\rho \times C_p}{4 \times \sigma \times (T + 273.16)^3}$	s/m	
Emissivity	ϵ	$\epsilon = 0.622$	-	
Specific gas constant	R	R = 287	J/kg K	
Stefan-Boltzmann constant	σ	$\sigma = 5.669 \times 10^{-14}$	MJ/ K ⁴ m ² s	
Soil heat flux	G	G = 0	MJ/m ² h	Pamungkas <i>et. al.</i> , (2014)
Leaf area index	LAI	LAI = 4	m ² / m ²	Sandmann <i>et. al.</i> , (2013)
Air velocity	U	U = 0.34	m/s	Baglivo, <i>et. al.</i> , (2020)

A.3 Operational schedule for thermal curtain and shade curtain

The operational schedule was solely selected based on the need for these curtains during the year and the solar radiation availability pattern. However, this schedule was finalized after many iterations which as updated based on the previous results. Schedules 1 and 2 for the thermal curtains and shade curtains are mentioned in Table A-3.

Table 5-3 Schedules 1 and 2 for thermal curtains and shade curtains.

Thermal Curtains	
Schedule 1	Nov-Feb: 19:00 - 7:00
	Mar-Apr; Oct: 20:00 - 5:00
	May-Sep: 23:00 - 04:00
Schedule 2 (Dong <i>et. al.</i> , 2021)	Jan: 16:30 - 10:00

	Feb: 17:00 - 09:30
	Mar: 18:00 - 08:30
	Apr: 19:00 - 07:00
	May: 19:30 - 06:30
	Jun: 21:00 - 06:00
	Jul: 24:00 - 05:30
	Aug: 23:00 - 06:30
	Sep: 18:00 - 07:40
	Oct: 17:00 - 08:30
	Nov: 16:00 - 10:00
	Dec: 16:00 - 10:30
Shade Curtains	
Schedule 1	01 Jan-31 Jan: 12:00-12:59
	01 Feb-19 Mar: 12:00-12:59
	20 Mar-31 Mar: 07:00-16:00
	01 Apr-30 Apr: 08:00-16:00
	01 May-19 Jun: 06:00-17:00
	20 Jun-30 Jun: 06:00-17:00
	01 Jul-31 Jul: 07:00- 16:00
	01 Aug-31 Aug: 09:00-16:00
	01 Sep-30 Sep: 08:00-17:00
	01 Oct-31 Oct: 08:00-15:00
	01 Nov-20 Dec: 08:00-14:00
	21 Dec-31 Dec: 12:00-12:59
Schedule 2	01 Jan: No shade curtain
	01 Feb: No shade curtain
	01 Mar: 11:00-16:00
	01 Apr: 11:00-16:00
	01 May: 10:00-16:00
	20 Jun: 08:00-17:00
	01 Jul: 08:00-17:00
	01 Aug: 08:00-16:00
	01 Sep: 09:00-16:00
	01 Oct: 09:00-15:00
	01 Nov: 11:00-14:00
	21 Dec: No shade curtain

A.4 Unit cost estimation for materials used in AGB and CG

Different vendor's website was explored to obtain accurate unit material costs. The unit cost of each material is indicated in Table A-4.

Table 5-4 Unit cost for different materials for vendor's website

Item	Specification	Unit cost	Reference
PE	0.1 mm	\$ 0.4/m ²	Husky plastic sheeting
	0.15 mm	\$ 0.8/m ²	
	0.05 mm	\$ 0.2/m ²	
Polystyrene	40 mm	\$ 15/m ²	Uline.ca
FBG insulation	254 mm	\$ 69/m ²	Knauf insulation
	127 mm	\$ 58/m ²	
	381 mm	\$ 70/m ²	
PC	4 mm	\$ 12/m ²	Duralight Plastics
	10 mm	\$ 23/m ²	
	16 mm	\$ 41/m ²	
	28 mm	\$ 51/m ²	
PVC	1.8 mm	\$ 75/m ²	Global Industrial
	3.18 mm	\$ 87/m ²	
PV glass	6 mm	\$ 138/m ²	Yangtze solar
	19 mm	\$ 184/m ²	
	26 mm	\$ 270/m ²	
GSS	1 mm	\$ 36/m ²	Metals Depot
IMP	150 mm	\$ 84/m ²	Insulation UK
	200 mm	\$ 134/m ²	
	100 mm	\$ 71/m ²	
	75 mm	\$ 67/m ²	
	50 mm	\$ 61/m ²	
	225 mm	\$ 143/m ²	
	306 mm	\$ 156/m ²	
Concrete	-	\$ 86/m ²	Top Concrete
TC	100 mm	\$ 1/m ²	Focus Technology
SC	1.3 mm	\$ 3/m ²	Svensson
HG	4 mm	\$ 1/m ²	Tian Yao Glass Company
	6 mm	\$ 1/m ²	
	10 mm	\$ 1/m ²	
Ventilation vent	910 mm x 430 mm	\$ 295/piece	Planta greenhouses

A.5 Envelope geometry considered under optimization

Profile 1 was considered for the base case with a crop output of 182,172 kilograms of lettuce. Profile 2 and profile 3 were developed to consider different inclinations of the inner and outer glazing and also increase the lettuce crop output to 203,555 kilograms and

decrease the lettuce crop output to 162,393 kilograms. The footprint area remains the same for all the cases, however, the volume of GS was changed, and because of this, the heating and cooling requirements were altered. The profiles from different scenarios are indicated in Figure A-1



Figure 5-1 Represents the cross-sectional details for different profiles of AGB

A.6 References

Ahamed, M. S., Guo, H., Tanino, K., (2019) “Modeling heating demands in a Chinese-style solar greenhouse using the transient building energy simulation model TRNSYS,” *Journal of Building Engineering*, Vol 29, 101114.

Baglivo, C., Mazzeo, D., Panico, S., Bonusa, S., Matera, N., Congedo, P. M., Oliveti, G., (2020) “Complete greenhouse dynamic simulation tool to assess the crop thermal well-being and energy needs,” *Applied Thermal Engineering*, Vol 179, 115698.

Donatelli, M., Bellocchi, G., Carlini, L., (2005) “Sharing knowledge via software components: Models on reference evapotranspiration,” *European Journal of Agronomy*, 24, pp. 186-192.

Dong, S., Ahamed, M. S., Ma, C., Guo, H., (2021) “A time-dependent model for predicting thermal environment of mono-slope solar greenhouses in cold regions,” *Energies* 2021, 14, 5956.

Eden Green Technology, (2023) “Vertical farming crop yield per acre versus traditional farming,” *Sustainability and food security* (Source: [Vertical vs. Traditional Farming: Yield Per Acre Comparison | Eden Green](#))

Pamungkas, A. P., Hatou, K., Morimoto, T., (2014) “Evapotranspiration model analysis of crop water use in plant factory system,” *Environmental Control in Biology*, 52(3), pp. 183-188.

Sandmann, M., Graefe, J., Feller, C., (2013) “Optical methods for the non-destructive estimation of leaf area index in kohlrabi and lettuce,” *Scientia Horticulturae*, Vol 156, pp. 113-120.

Appendix B
PERFORMANCE OF AGB FOR VARIOUS CROPS

The study also examines the performance of AGB across various crops, including lettuce, tomatoes, and strawberries, in Toronto.

B.1 Study of crops under consideration

The heating and cooling requirements of a greenhouse are significantly affected by the presence of plants. Evapotranspiration, which is also affected by weather conditions, varies with changes in location-specific weather patterns (Pamungkas *et. al.*, 2014). This process is further influenced by the type of crop being cultivated, as different crops have distinct LAI and crop coefficients. The crops examined in this study are lettuce, tomatoes, and strawberries, each of which requires different growing methods as indicated in Figure B-1.



Figure 5-2 Represents methods to grow different crops under study (a) Lettuce crops grown in beds (Greener Solutions, 2020) (b) Tomato plants with vines grown in trellises (Essential Home and Garden, 2024) (c) Strawberry crops with runners (Asia Farming, 2024)

As shown in Figure B-1, lettuce can be grown in layers due to its smaller size, allowing growers to maximize the canopy area within the same footprint. Tomatoes, on the other hand, grow vertically with the aid of trellises to support their vines. Strawberries are typically grown in pots or beds, with runners spreading horizontally. The LAI and crop coefficient vary between these crops, along with their optimal temperature ranges as illustrated in Table B-1.

Table 5-5 Crop parameters for different crops

Parameters	Lettuce	Tomato	Strawberry
Temperature Range	20 °C – 25 °C	18 °C – 30 °C	15 °C – 30 °C
Average LAI	4 m ² / m ²	2.55 m ² / m ²	2.5 m ² / m ²
Crop Coefficient	1.1	1.05	0.86

Reference	Sandmann <i>et. al.</i> , (2013); Ahmed <i>et. al.</i> , (2020); Engler and Krarti, (2022)	Kozai <i>et. al.</i> , (2019); Engler and Krarti, (2022); Yang <i>et. al.</i> , (2022)	Amini <i>et. al.</i> , (2022); Engler and Krarti, (2022)
-----------	--	--	--

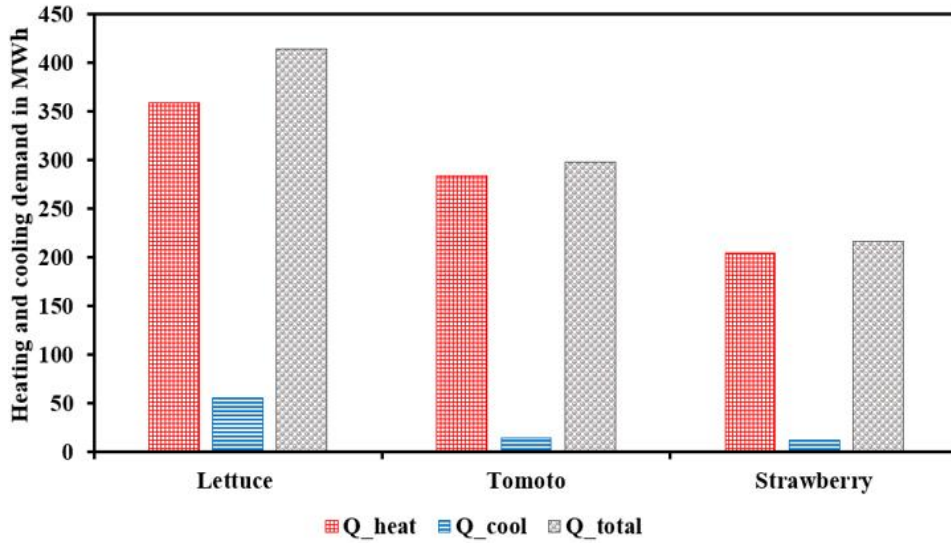
Using the energy modeling guidelines and the AGB model developed in Chapters 3 and 4, energy simulations were conducted. The baseline location was Toronto, Ontario with lettuce crops as the reference case, and variations were analyzed relative to this scenario. It was assumed that the heating was supplied using natural gas and the cost to provide per kWh heat was considered as 5.58 cents (Canada Energy Regulator, 2023), whereas the cooling was supplied using electricity and the cost to provide per kWh cool was considered as 13.03 cents (Energy hub, 2023)

B.2 Results

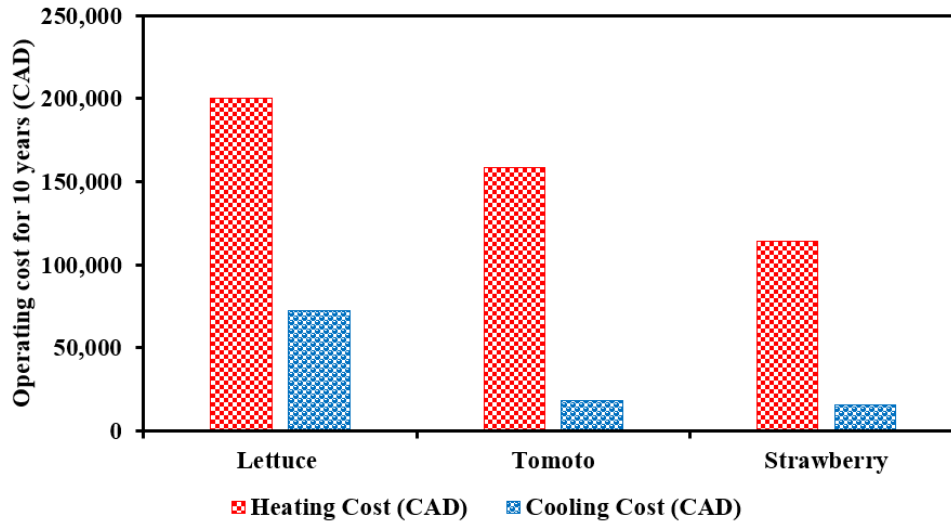
The effect of location and crops on heating and cooling demand is defined below:

B.2.1 Performance of AGB with variation in crops

The heating and cooling requirements varied with changes in crop type, as shown in Figure B-2. Lettuce had higher heating and cooling demands compared to tomatoes and strawberries due to its need for more precise temperature control, specifically between 20 °C to 25°C. In contrast, tomatoes and strawberries could experience temperature variations of 12°C to 15°C, reflecting their different optimal temperature ranges. Among the three, strawberries required the least heating and cooling. Although the weather conditions were consistent for all crops, differences in evapotranspiration due to variations in their LAI and canopy area led to changes in heating and cooling needs. This underscores the importance of accurately modeling plants with their specific LAI, as it significantly impacts energy requirements. Since Toronto was the location considered, the unit prices for natural gas and electricity remained constant across the scenarios. The results indicated that strawberries could be the most economical crop, reducing operating costs by 52% over 10 years compared to lettuce, while tomatoes could reduce costs by 35%.



a)



b)

Figure 5-3 Variation of performance and operating cost for different crops. Heating and cooling demand in MWh (a) Operating cost for 10 years in Canadian Dollars

Greenhouse performance is affected by ambient weather conditions, including temperature, solar radiation availability, and wind. Additionally, these weather conditions influence evapotranspiration rates, which are also impacted by the specific types of crops being grown.

B.3 Reference

Ahmed, H. A., Xin, T. Y., Chang, Y. Q., (2020) “Optimal control of environmental conditions affecting lettuce plant growth in a controlled environment with artificial lighting: A review,” South African Journal of Botany, Vol 130, pp. 75-89.

Amini, A., Karami, F., Sedri, M. H., Khaledi, V., “Determination of water requirement and crop coefficient for strawberry using lysimeter experiment in a semi-arid climate,” H2Open Journal, Vol 5, Issue 4, pp. 642-655.

Asia Farming, (2024) “Strawberry growing information guide,” (Source: [Strawberry Growing Information Guide | Asia Farming](#))

Canada Energy Regulator, (2022) “Data and analysis of Energy commodities,” (Source: [CER – Natural gas bills \(cer-rec.gc.ca\)](#))

Energy hub, (2023) “Electricity prices in Canada 2023,” (Source: [Electricity Prices in Canada 2023 \(energyhub.org\)](#))

Engler, N., Krarti, M., (2022) “Optimal designs for net zero energy-controlled environment agriculture facilities,” Energy and Buildings, Vol 272, 112364.

Essential Home and Garden, (2024) “10 Vegetables that thrive in a greenhouse,” (Source: [10 Vegetables That Thrive In A Greenhouse \(essentialhomeandgarden.com\)](#))

Greener Solutions, (2020) “Lettuce and Herbs,” (Source: [Lettuce and Herbs - Greenhouses, Tunnels & Hydroponic System Suppliers South Africa | Greener Solutions](#))

Kozai, T., Niu, G., Takagaki, M., (2019) “Plant factory: an indoor vertical farming system for efficient quality food production,” Second Edition, Amsterdam, Netherlands: Amsterdam University Press.

Pamungkas, A. P., Hatou, K., Morimoto, T., (2014) “Evapotranspiration model analysis of crop water use in plant factory system,” Environmental Control in Biology, 52(3), pp. 183-188.

Sandmann, M., Graefe, J., Feller, C., (2013) “Optical methods for the non-destructive estimation of leaf area index in kohlrabi and lettuce,” *Scientia Horticulturae*, Vol 156, pp. 113-120.

TRNSYS-18, (2017) “TRaNsient System Simulation program – Weather Data,” Volume 8, Solar Energy Laboratory, University of Wisconsin-Madison

Yang, L., Liu, H., Tang, X., Li, L., (2022) “Tomato Evapotranspiration, Crop Coefficient, and Irrigation Water Use Efficiency in the Winter Period in a Sunken Chinese Solar Greenhouse,” *Water*, Vol. 14, Issue 15.

VITA AUCTORIS

NAME: Gurpreet Khanuja

PLACE OF BIRTH: Jabalpur, Madhya Pradesh, INDIA

YEAR OF BIRTH: 1997

EDUCATION: University Institute of Technology, B.E, Madhya Pradesh, INDIA

University of Windsor, MASc., Windsor, ON, 2024